UNIVERSITY OF TURKISH AERONAUTICAL ASSOCIATION
INSTITUTE OF SCIENCE AND TECHNOLOGY

NUMERICAL INVESTIGATION OF THE THERMAL PERFORMANCE OF A SOLAR WATER HEATING SYSTEM WITH COIL TUBE COLLECTORS

MASTER THESIS

Azhar Shamkhi Jabbar JABBAR

MECHANICAL AND AERONAUTICAL ENGINEERING DEPARTMENT
MASTER THESIS PROGRAM

DECEMBER 2017

UNIVERSITY OF TURKISH AERONAUTICAL ASSOCIATION
INSTITUTE OF SCIENCE AND TECHNOLOGY

NUMERICAL INVESTIGATION OF THE THERMAL PERFORMANCE OF A SOLAR WATER HEATING SYSTEM WITH COIL TUBE COLLECTORS

Master Thesis

Azhar Shamkhi Jabbar JABBAR

ID: 1406080023

IN PARTIAL FULFILLMENT OF THE REQUIREMENT FOR THE DEGREE OF MASTER OF SCIENCE IN MECHANICAL AND AERONAUTICAL ENGINEERING

Supervisor: Assist. Prof. Dr. Mohamed Salem ELMNEFI

بسم الله الرحمن الرحيم

((هوَ الَّذي جَعَلَ الشَّمْسَ ضِيَاءً وَالقَمَرَ
نُوراً وَقَدَّرَهُ مَنَازِلَ لِتَعْلَمُوا عَدَدَ السِنِينَ
وَالحِسَابَ مَا خَلَقَ اللهُ ذلكَ إلاَّ بِالحقِّ
يُفصِّلُ الأياتِ لِقَومٍ يَعْلَمُون))

(يونس ٥)

Azhar Shamkhi Jabbar JABBAR, having student number **1406080023** and enrolled in the Master Program at the Institute of Science and Technology at the University of Turkish Aeronautical Association, after meeting all of the required conditions contained in the related regulations, has successfully accomplished, in front of the jury, the presentation of the thesis prepared with the title of: "**NUMERICAL INVESTIGATION OF THE THERMAL PERFORMANCE OF A SOLAR WATER HEATING SYSTEM WITH COIL TUBE COLLECTORS** ".

Supervisor : **Assist. Prof. Dr. Mohamed Salem ELMNEFI**
University of Turkish Aeronautical Association

Jury Members : **Assoc. Prof. Dr. Nevsan ŞENGIL**
University of Turkish Aeronautical Association

: **Assist. Prof. Dr. Mohamed Salem ELMNEFI**
University of Turkish Aeronautical Association

: **Assist. Prof. Dr. Munir ELFARRA**
Yildirim Beyazit University- Ankara

Thesis Defense Date: 07.12.2017

THE UNIVERSITY OF TURKISH AERONAUTICAL ASSOCIATION
INSTITUTE OF SCIENCE AND TECHNOLOGY

I hereby declare that all information in this study I presented as my Master's Thesis, called "**NUMERICAL INVESTIGATION OF THE THERMAL PERFORMANCE OF A SOLAR WATER HEATING SYSTEM WITH COIL TUBE COLLECTORS"** has been presented in accordance with academic rules and ethical conduct. I also declare and certify on my honor that I have fully cited and referenced all the sources I made used of this present study.

Azhar Jabbar
07.12.2017

ACKNOWLEDGEMENTS

I am grateful to The Almighty ALLAH for helping me to complete this thesis. My Lord mercy and peace be upon our leader Mohammed peace be upon on him, who invites us to science and wisdom, and members of his family and his followers.

I would like to express my deep gratitude for my supervisor, Dr. Mohamed S. Elmnefi, I will forever be beholden to his sincere support and encouragement. His extreme generosity will be remembered always. It is really hard to find words to express my gratitude for his supervision and devotion. Also, I would like to express my deep gratitude for my friend Dr.Esam Mujbel, and I will never forget big help of my brother and my friend Dr.Muwafaq Al-hachami. I thank him for everything he provided throughout my time as their student.

I wish to dedicate this humble work for the spirit my father who died during the study of my master's degree; he wished to see this moment. And to the candle that lit the path of my life. At whom I realize how nostalgia is a killer. For my mother, who built me to be as Im. I would like to pay my life to see her face again, to kiss her blessed hands. Last, but not least, I would like to thank my wife for her understanding and love during the past few years. Her support and encouragement were in the end what made this dissertation possible. Thanks to my daughters Manar, Noor, Qamar and last cluster Mohammed-Sadiq whom always courage me to study. Thanks to my brothers and sisters especially Heithm Alkaabi, Emad Alkaabi, Wisam Alkaabi, Dr.Naer Alkaabi, and Ali Alkaabi, and I don’t forget to thanks all the gorgeous people Eng. Mohammed-Hasan Nassoom, Eng. AbdulSattar Alkhafaji, Assis.Read Alshekry, and Eng. Mohammed Hadi .

To all my friends and my classmates.

To all who gave a hand, I say thank you very much.

07.12. 2017 Azhar Jabbar

LIST OF CONTENTS

LIST OF TABLE

LIST OF FIGURES

ABSTRACT

NUMERICAL INVESTIGATION OF THE THERMAL PERFORMANCE OF A SOLAR WATER HEATİNG SYSTEM WİTH COİL TUBE COLLECTORS

AZHAR SHAMKHI JABBAR

M.Sc., Department of Mechanical Engineering

Thesis supervisor: Assist. Prof. Dr. Mohamed Salem Elmnefi

DEC 2017, 94 Pages

In the present study, a computational analysis was carried out to evaluate the thermal performance of water heater collector due to Iraqi weather (Al-Najaf city).

A water heater collector was simulated using three different materials namely aluminum, copper, and steel with dimensions of 1×2 m².

Simulations have managed using analyses system ANSYS 2015 including an average of outside temperatures, solar radiation and wind speed for the coldest four months (January, February, November, and December) at the year of 2016. A try and error procedure is done using ANSYS until reaching the predicted surface temperature of the collector with an accuracy of 99% at least.

The procedure of simulations included using four different temperatures, radiations, and wind velocities for winter months in Iraq with a water mass flow rate of (0.005, 0.01, 0.015, 0.02, 0.25, and 0.03) kg/s. This procedure has been repeated using aluminum, copper, and steel collectors. For each solution in ANSYS, twelve results are recorded for one hour (every 5 minutes) until collector reaches up to steady state conditions. The results recorded for a minimum, maximum, and average temperature at collector surface. The average temperature for water at an outlet is also recorded. These results helped to study the thermal performance and efficiency for each type of collector.

All ANSYS results had compared with equations results, and they are matched with a maximum error of 1.18%.

The results showed the effect of increasing water mass flow rate, changing water temperature at an inlet, and the effect of environmental conditions. They showed that aluminum and copper had close similar efficiencies where steel has lower efficiency if compared with other two materials. Better thermal conductivity and specific heat capacity for copper make it perform better than aluminum at steady state conditions where aluminum shows better efficiency than copper and steel at a transient time by 4.5% and 6.9% respectively due to the less density, which effects thermal capacity due to volume.

Keywords: Solar energy, Thermal, Flat plate collectors, Weather data assessment, Ansys program.

Özet

Sarmal Boru Kollektörlü Solar Su Isıtıcının Termal Performansının Sayısal Araştırması

AZHAR SHAMKHI JABBAR

Yüksek Lisans, Makine Mühendisliği Bölümü

Tez Danışmanı: Yrd. Doç. Dr. Mohamed Salem Elmnefi

ARALIK-2017, 94 Sayfa

Mevcut çalışmada, Irak hava durumu (El Necef Şehri) için su ısıtıcı kollektörün termal performansını değerlendirme amacıyla sayısal analiz yürütülmüştür.

1x2 m^2 boyutlarında Alüminyum, bakır ve çelik olmak üzere üç farklı materyal kullanılarak su ısıtıcı kollektörü simüle edilmiştir.

Simülasyonlar 2016 yılının en soğuk dört ayı (Ocak, Şubat, Kasım ve Aralık) için ortalama dış sıcaklık, güneş ışınımı ve rüzgar hızını içeren ANSYS 2015 analiz sistemi kullanılarak ele alınmıştır. Kollektörün tahmin edilen yüzey sıcaklığına nihai olarak %99 doğrulukla ulaşılana kadar ANSYS kullanılarak deneme yanılma süreci uygulanmıştır.

Simülasyon süreci Irak'ta kış ayları için dört farklı sıcaklık, ışınım ve rüzgar hızı ile (0.005, 0.01, 0.015, 0.02, 0.25 ve 0.03) olmak üzere su kütle akış hızını içermektedir. Bu süreç alüminyum, bakır ve çelik kollektörler kullanılarak tekrar edilmiştir. ANSYS'de her çözüm için, kollektörler kararlı durum koşullarına ulaşana dek bir saat süre boyunca (her 5 dakika bir) on iki sonuç kaydedilmiştir. Sonuçlar kollektör yüzeyinde minimum, maksimum ve ortalama sıcaklık için kaydedilmiştir. Su için ortalama sıcaklık aynı zamanda çıkış içinde kaydedilmiştir. Bu sonuçlar her tipteki kollektör için termal performans ve verimliliğin analiz edilmesine yardımcı olmuştur.

Bütün ANSYS sonuçları denklem sonuçları ile karşılaştırılmıştır ve sonuçlar maksimum %1.18 hata ile uyumlu olmuştur

Sonuçlar artan su kütle akış hızının, girişte değişen su sıcaklığının ve çevresel koşulların etkilerini göstermiştir. Sonuçlar alüminyum ve bakırın birbirlerine benzer ve yakın verimlilikte olduğunu gösterirken, çelik bu malzemeler ile karşılaştırıldığında daha düşük bir verimlilik sağlamıştır. Bakır için daha iyi termal iletkenlik ve özel ısı kapasitesi kararlılık durumu koşullarında alüminyumdan daha performans göstermiş, bununla birlikte alüminyum hacimden dolayı termal kapasiteyi etkileyen daha düşük yoğunluğu sayesinde sırası ile % 4.5 ve % 6.9 olmak üzere geçici sürede bakır ve çelikten daha iyi verimlilik göstermiştir.

Anahtar Kelimeler: Güneş enerjisi, Termal, Düz plakalı kollektör, Hava veri değerlendirmesi, Ansys programı.

NOMENCLATURES

TM	Max temperature (˚C)
T	Avg temperature (˚C)
$WS_{\_avg}$	Avg wind Speed (m/s)
L	Local latitude
N	Number of day of the year
i	Number of day of the month
A_c	Area collector (m²)
Q_T	Total heat supplied to collector (W)
I	Intensity of solar radiation, in W/m²
Q_u	Useful energy gain from collector (W)
Q_{loss}	The energy losses from the collector (W)
U_L	Overall heat loss coefficient based on collector area Ac (W/m².K)
T_p	Average temperature of the absorbing surface (˚C)
T_a	Ambient temperature (˚C)
$h_{c,p-g}$	Convection heat transfer coefficient between plate and glass (W/m².K)
R_L	Overall thermal resistance (m ².K/W)
U_t	Top heat loss coefficient (W/m².K)
U_b	Bottom heat loss coefficient (W/m².K)
U_e	Edges heat loss coefficient (W/m².K)
$h_{r,p-g}$	Radiation heat transfer coefficient (W/m².K)
N_g	Number of glass covers
h_w	Wind heat transfer coefficient (W/m².K)
V	Wind velocity (m/s)
L	Length of collector(m)=2
t_b	Thickness of back insulation (m). =0.05
k_b	Conductivity of bottom insulation (W/m-K).=0.12
$h_{c,b-a}$	Convection heat loss coefficient from bottom to ambient (W/m².K).
t_e	Thickness of edge insulation (m).
k_e	Conductivity of edge insulation (W/m-K).=0.12
$h_{c,e-a}$	Convection heat loss coefficient from edge to ambient (W/m². K).
T_{wo}	Water outlet Temp. (˚C)
T_{win}	Water inlet Temp. (˚C)
$\dot{m}$	Mass flow rate of fluid (kg/s)
c_p	Specific heat at constant pressure (J/kg-˚C)
Re	Reynolds number
Nu	Nusselt Number

GREEK

δ	The declination angle (degrees)
η	Collector thermal efficiency
ε_g	Emissivity of glass covers=0.88
ε_p	Absorber plate emittance=0.05
σ	Stefan -Boltzmann constant, = 5.67×10^{-8} ($W/m^2.K^4$)
β	Collector slope (degrees)=35
ρ	Density (kg/m^3)
μ	Viscosity (kg/m-s)

ABBREVIATIONS

FPCs	Flat-plate collectors
SWHs	Solar water heating system
CFD	Computational Fluid Dynamics
DNI	Direct Normal Irradiation
SDHW	Solar Domestic Hot Water
CPCs	Stationary compound parabolic collectors
ETCs	Evacuated tube collectors
DHW	Domestic hot water
ANSYS	Analysis system
SRt	Total Solar Radiation
AST	Apparent solar time
LST	Local standard time
SL	Standard longitude
LL	Local longitude
DS	Daylight saving
ET	Equation of time

CHAPTER ONE

INTRODUCTION

1.1 Background

Originally, the energy forms in the world that human being know them are solar in basic. Coal, Oil, wood, and natural gas were formed by photosynthetic processes accompanied with complex chemical reactions in the way of decaying vegetation was exposed to very high temperatures and pressures for a long period of time. Also the energy of the tide and wind has a solar basis because they are produced when variances in temperature are happened in numerous regions of the earth. Solar energy falls down on the earth's surface at a rate of (120) petawatts (1 petawatt = 10^{15} watt). This means that the solar energy received from the sun in one day can cover the whole world's demand for more than (20) years. Scientists have been able to calculate the potential for both renewable energy source based on today's technology. The advance in future technology will lead to higher potential for each type of the energy source. Because the worldwide demand on energy is expected to continue increasing at 5% each year. The solar energy is the best choice that can fulfill such a steadily and huge increasing demand [1][2].

Solar energy may be either used directly as heat photovoltaic power and solar thermal heating or used indirectly through hydro, biomass and wind,so as shown in Figure 1.1 [3].

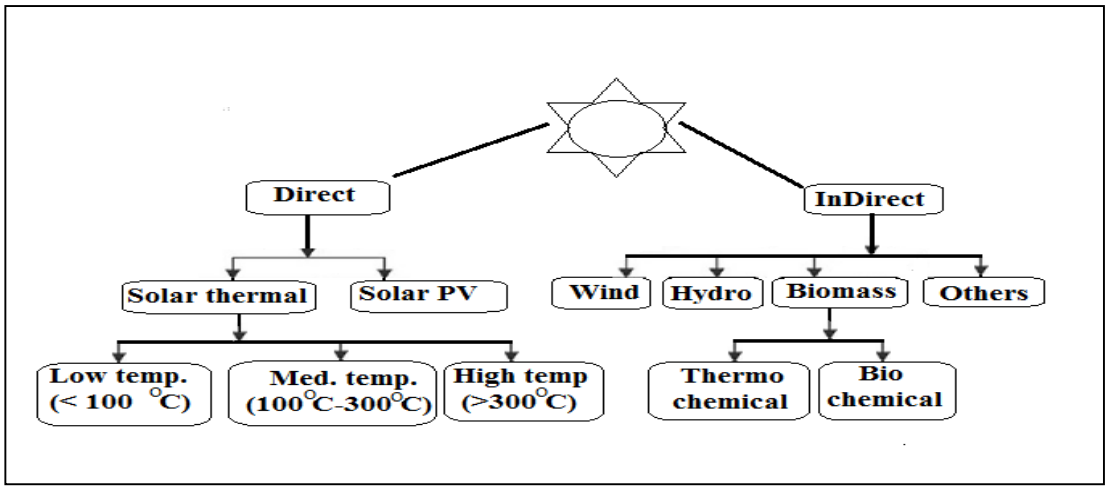

Figure (1.1): Traditional classification of renewable energy

The solar thermal energy has an increasing importance among other powers required for heating building's water and domestic hot water. Thermal solar systems can cover a considerable portion of this energy requirement; with the increasing use of thermal insulation in buildings and the resulting reduction in heating energy requirements [4].

Solar energy can be used by three technological processes [5]: chemical, electrical and thermal (Figure1.2). Chemical process, through photosynthesis, maintains life on earth by producing food and converting CO_2 to O_2. Electrical process, using photovoltaic converters, provides power for spacecraft and is used in many terrestrial applications. Thermal process can be used to provide much of the thermal energy required for solar water heating and building heating. Another form of converted solar radiation is mechanical energy as wind and water steams [5][6].

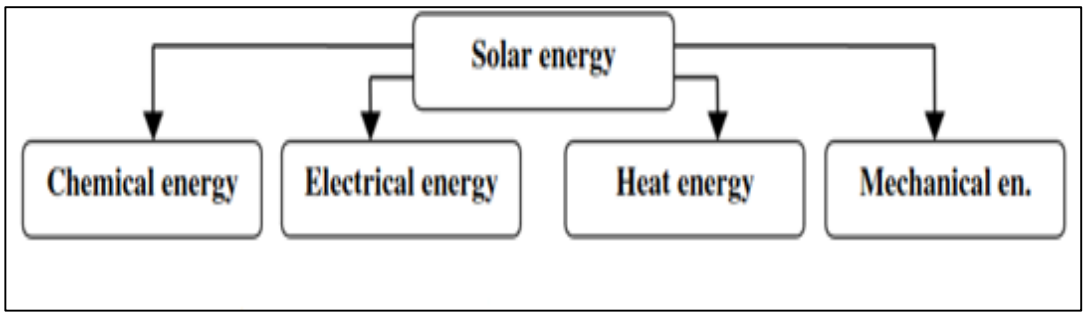

Figure (1.2): Conversion of solar radiation to other energy forms

1.2 Solar Energy in Iraq

In Iraq, the Iraqi government facility all requirements and apply for development, renewable energy research to reduce the energy that have gotten from other kinds, for example (gas turbine power plant , diesel power plant and steam turbine power plant). The renewable energy is economical and the more important it is environmentally friendly and low pollution, the alternative energy is that the favorite among these various solutions and for many reasons, namely:

- Iraq atmosphere has a large numbers of sunny hours during twelve months (year).
- The winter season has a high percentage of sunny days when it compares with rainy days and cloudy day.
- The solar systems are easy to install.

All these reasons above lead to the result that the solar energy is the best choice for alternative energy source Iraq [7].

Iraq suffers from electricity shortages, and many challenges will have to be overcome to meet future increases in electrical demands. This investigation found that solar, wind and biomass energy are not being utilized sufficiently at present, but these energies could play an important role in the future of Iraq's renewable energy. Additionally, the potential of offshore-wind energy in the Gulf (near Basrah in the southern part of Iraq) needs to be investigated. The Iraqi government's attempts to utilize renewable energy have been discussed [8].

In Iraq, the study of solar energy began after the 1973 energy crisis. Many studies were undertaken to determine equations for the representation of solar intensity in Baghdad. During that time in Iraq, numerous theoretical and practical studies were commenced to study domestic water heaters and coolers that used solar energy and build theoretical models that represented solar water heaters [9].

1.3 Geographical nature of Iraq

The Iraq location is within the high solar zone. This location is the best when it compares with European countries, which requires not to lose this opportunity, and to take advantage of this feature which is not found in those countries which they doing their best take benefit of the sun's energy to highest of levels.

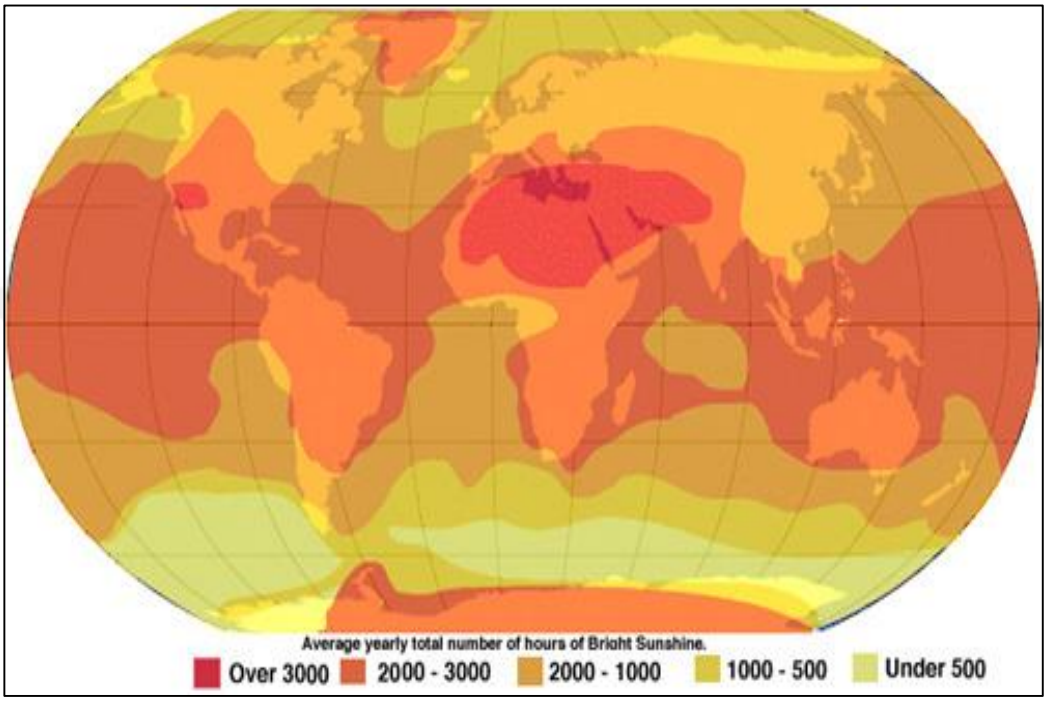

Figure (1.3): Iraq position in area of over than 3000 yearly number of hours of bright sunshine

The solar radiation energy is reaching values between (6.5 - 7) kWh / m² from periods of sunshine ranging from 2800 to 3300 hours per year that ensuring access to large amounts of energy compared to Canada and Russia. For example, which does not exceed the number of sunny hours about 1000 hours a year and although it is used to generate solar energy. The vast desert areas in western Iraq is a strategic place to generate solar energy and at low cost and modest effort to end the power crisis plaguing the country. see Figure (1.3) [6].

1.4 Basic Designs

Today there are many significant directions for solar technology development. As an example, photovoltaic systems directly convert the solar energy into electrical

energy whereas focused solar power systems first convert the solar energy into thermal energy then convert it into electrical energy through a thermal engine [2].

Due to the nature of solar energy, two units are needed to have a functional solar energy generator. These two units are a collector and a storage unit. The collector collects the radiation that falls on that and converts it to different types of energy (heat, electricity). While the storage unit is needed due to the unsteady of solar energy, as throughout cloudy days the quantity of energy made by the collector are going to be quite little. The storage unit will hold the energy made throughout the periods of most radiation and release it once it's required or the productivity drops.

Ways of grouping and storing solar energy vary depending on the utilization of the solar generator. In general, there are three kinds of collectors (flat -plate collectors) , focusing collectors, and passive collectors) [10].

1.5 Statement of the problem

One of the main issue is providing hot water in the winter. At present, most commercial and industrial applications for hot water in Iraq benefit mainly from the use of electric boilers. Unfortunately, the lack of production and poor electrical power delivery as a result of sabotage and wars, high energy costs, environmental affairs, depleted nature of the current primary energy sources use to make electric heaters less attractive, because the new price will be 120 ID/kWh Iraqi's dinar per kilowatt hours, it equals about 0.96 $/kWh of electricity consumption in residential buildings [11]. So that electricity prices increases together with increased consumption. In addition, the demand for electricity is overgrowing; therefore, in periods of cold weather sometime morning and evening, when demand for hot water is higher, and often the consumption of electricity is more than its production, resulting in some cases to power outages, especially in developing countries, like in Iraq.

1.6 Thesis Objective

The main aim of the research is to study the work of flat plate collectors and make compare the three types of materials used (copper, aluminum, steel) under the climatic conditions of Najaf in Iraq and during the winter at variable mass flow rate.

And calculate the efficiency of each of the three types by using simulation Computational Fluid Dynamics (CFD) packages by Ansys program.

1.7 Methodology

- Choose Al- Najaf city in Iraq in the west desert to conduct the research.
- Pick out a solar water heating systems type (flat plate collectors).
- Choose three types of materials to make three solar collectors (copper, aluminum, and steel).
- Working on the cold months of the winter (November, December, January and February).
- Take data form Meteorological Department for Najaf City for those four months and extract the intensity of solar radiation, temperature and wind speed rates.
- Make simulation of those data for flat plate solar collectors through the software program (Ansys 15 program).
- Find the efficiency of each types for flat plate solar collectors and validation the results.

1.8 Organization of the Thesis

- Chapter 1 "Introduction" This chapter offers a brief overview of solar energy and explain solar energy in Iraq with a discussion of the aims and methodology, a graphic impersonation of the methodology and a presentation of the structure of this thesis.
- Chapter 2 "Literature reviews" The literature reviews provide an overview of water heater system type flat plat collector classification of solar thermal collectors, and future solar energy in Iraq.
- Chapter 3 "Theoretical Background" focuses on the theory behind the research; Mathematical calculations (day length, radiation intensity, collector energy losses (top loss, bottom loss and edge losses)), and presenting the methodology of simulation for solar thermal analysis to a flat plate collector by Ansys 15 program.

- Chapter 4 " Results and Discussion " showing the simulation results for verification procedure, the effect of solar radiation, fluid inlet temperature for different mass flow rate and different materials (copper ,Aluminum, steel) on the thermal efficiency to flat plate collector and validation of results from Ansys program.
- Chapter 5 " Conclusions and Recommendations " This chapter concludes the research and presents the final recommendations.

CHAPTER TWO

LITERATURE REVIEW

2.1 Introduction

In this chapter we discuss the literature reviews related to solar energy in Iraq and water heater of solar type-flat plate collector, the flat plate collector efficiency and solar thermal what includes the components for example flat plate collector and absorber plate.

Almost 90% of Iraqis are connected to the electricity grid, with over 80% of grid-supplied electricity coming from hydrocarbon-fueled power plants, nearly 75% of what is crude-oil, heavy fuel oil or gas oil [12]. A small amount, less than 20%, comes from hydropower. In Iraq, the demand for power increase (through a growth of population and increased electricity in homes requirements and offices), but the reliability of supply is insufficient and reduced loads are a common daily experience for Iraqis [12].

The Republic of Iraq location is in southwestern Asia, in the northeast of the Arabian Peninsula. It is bordered by Turkey, Iran, Kuwait, Saudi Arabia, Jordan, and Syria. Iraq lies between latitudes 29º05´–37º22´ N and longitudes 38º45´–48º45´E, and it has an area of 435,052 km² [13]. The location of Iraq in the region latitude (20º-40º) North-South called Sun-Belt area. Available insolation data uses a map of Direct Normal Irradiation (DNI), temperature and wind velocity. Figure (2.1) shows the solar map of Iraq.

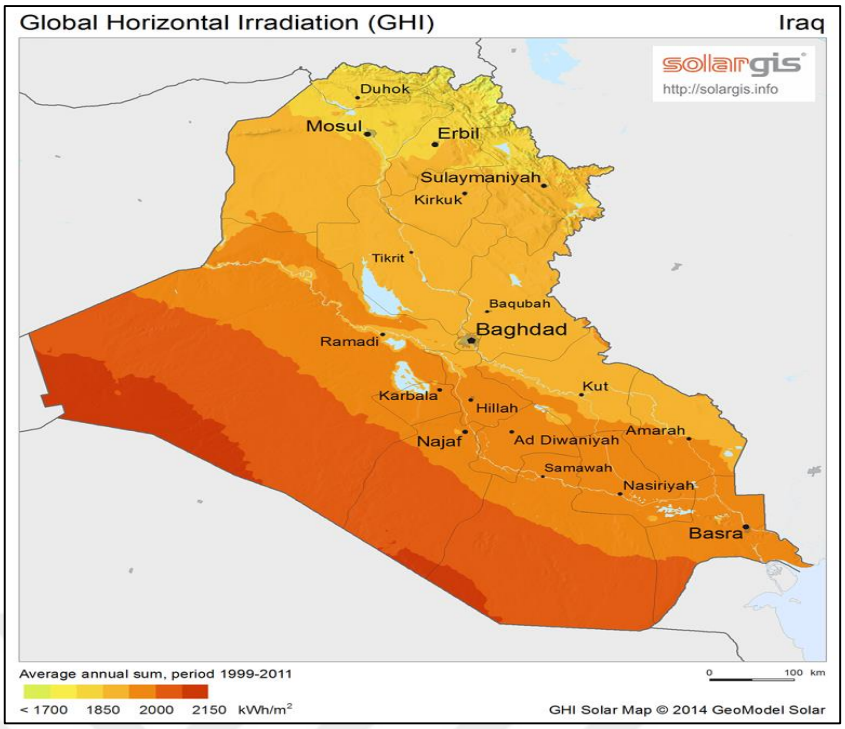

Figure (2.1): Solar map of Iraq [14].

2.2 Solar Water Heating

Solar energy can be used as a form of heat, for example, solar water heating and use electricity, such as solar photovoltaic. The systems of solar water heating are commonly referring to the industry as the systems of Solar Domestic Hot Water (SDHW) systems, and it is a technology that is not entirely new. In 1891, Clarence Kemp patented the old design of metal tanks exposed to the sun by adding a metal panel to the tank, shown below in Figure(2.2), in order to increase the solar tank efficiency [15].

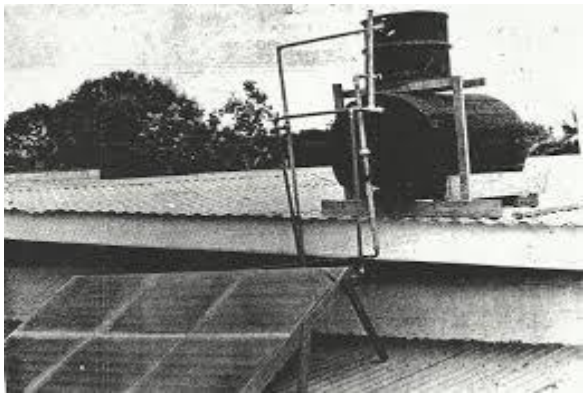

Figure (2.2): A prototype Solar Water Collector [15].

In 1909 a California engineer named William J. Bailey began selling a system named the "Day and Night" solar water heater. It consisted of a solar collector and a separate storage tank mounted above the collector [16].

In the 1960s in Japan a simple solar water heater was created consisting of a basin with its top covered by glass; where more than 100,000 collectors of this type were in use.

2.3 Solar Energy Collector

- Solar energy collectors are a special type of heat exchangers that transform radiation of solar energy to internal energy of the transport medium.
- The main part of any solar system is that the solar collector.
- This can be a device that absorbs the incoming radiation of solar, converts it into heat, and transfers this heat to a fluid (usually air, water, or oil) flowing through the collector.
- The solar energy collected is carried from the circulating fluid either directly to the hot water or maybe drawn for use at nighttime or on cloudy days.
- There are essentially (two) kind of solar collectors: non-concentrating or stationary and concentrating.
- A non-concentrating collector has the similar area for intercepting and absorbing solar radiation, whereas a sun-tracking concentrating solar collector typically has concave reflecting surfaces to intercept and focus the sun's beam radiation to a smaller receiving area, thereby increasing the radiation flux.
- Concentrating collectors are suitable for high-temperature applications.
- Solar collectors also can be distinguished by the type of heat transfer liquid used (water, non-freezing liquid, air, or heat transfer oil) and whether or not they are covered or uncovered [17].

2.4 Collectors' Classification

There are a variety of various design styles for collectors, but generally, they are either stationary or concentrating.

- The stationary type includes:

Solar energy collectors are essentially distinguished by their motion stationary, single- axis following, and two-axis following and also in the operating temperature. These collectors are permanently fixed in position and don't track the sun. Three major types of collectors fall into this category:

1. Flat-plate collectors (FPCs).
2. Stationary compound parabolic collectors (CPCs).
3. Evacuated tube collectors (ETCs).

- The Concentrating type includes:
  1. Parabolic and cylindrical trough collectors.
  2. Parabolic dish reflector.
  3. Heliostat field collector [18].

2.5 Flat Plate Collectors (FPCs).

It has been chosen flat plate collector to the investigation of this study. Flat plate collector could be a basic and simple heat absorber which absorbs heat from the sun radiation. Flat plate collector as called now was developed by Hottel and Whillier in the 1950s, it is the most common for residential water-heating and space heating installations [19].

- A typical flat-plate solar collector as shown in the following Figure (2.3).
- When solar radiation passes through a transparent cover and impinges on the blackened absorber surface of high absorptivity, a large portion of this energy is absorbed by the plate and transferred to the transport medium in the fluid tubes, to be carried away for storage or use.
- The underside of the absorber plate and the two sides are well insulated to reduce conduction losses.

Figure (2.3): typical flat-plate collector.

- The liquid tubes can be welded to the absorbing plate or they can be an integral part of the plate.
- The liquid tubes are connected at both ends by large-diameter header tubes.
- The header and riser collector is the typical design for flat-plate collectors.
- The transparent cover is used to reduce convection losses from the absorber plate through the restraint of the stagnant air layer between the absorber plate and the glass. It also reduces radiation losses from the collector because the glass is transparent to the shortwave radiation received from the sun, however, it's nearly opaque to long wave thermal radiation emitted by the absorber plate (greenhouse effect). Furthermore, it reduces heat radiation from the absorbent into the atmosphere during a similar way as a greenhouse will. However, the glass additionally reflects a small a part of the sunlight, that doesn't, then reach the absorbent at all. Figure 2.4 shows the processes occurring at a flat-plate collector [20].
- The advantages of flat-plate collectors are that they are inexpensive to manufacture, they collect each beam and diffuse radiation, and they're permanently fixed in position, so no following of the sun is needed.

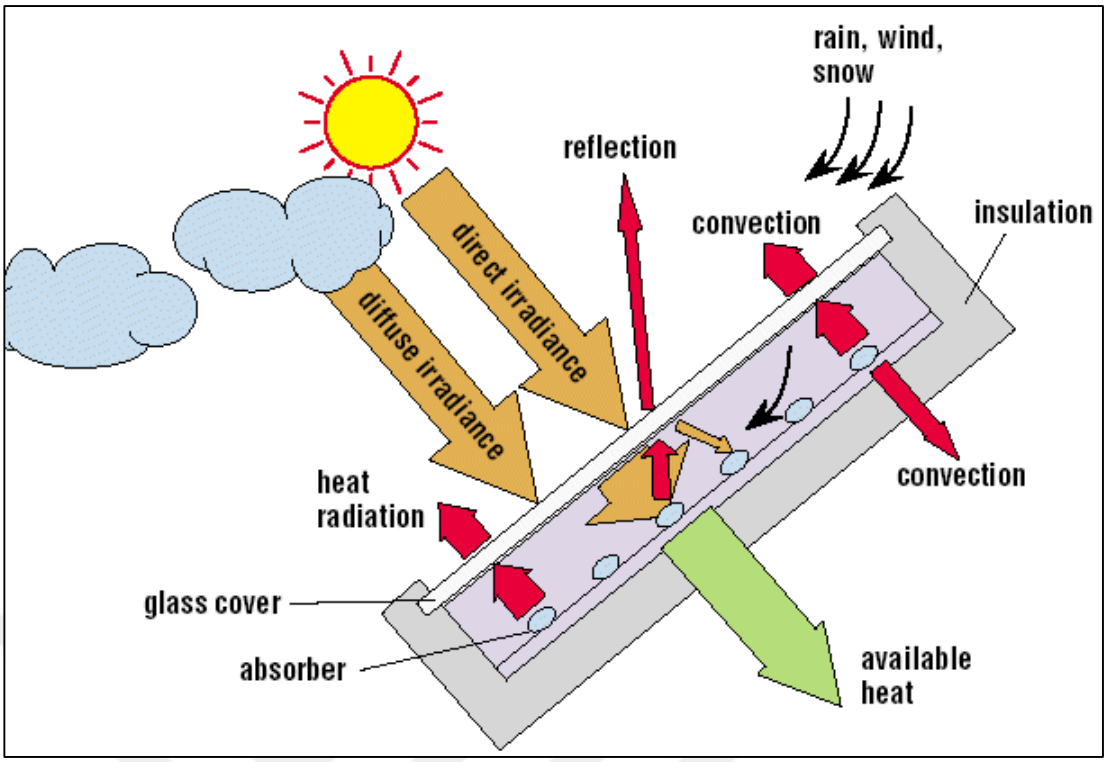

Figure (2.4): Processes occurring at a flat-plate collector**.**

Flat plate collectors are of two type:

- Liquid heating type.
- Air heating type.

The most obvious difference between the two is the mode of heat transfer between the absorber plate and also the heated fluid. Within the best type of liquid plate collector, that typically makes use of a fin-tube construction, heat absorbed is transferred to the tubes by conduction. In a conventional flat-plate air heater there is a duct (passage) between the absorbing plate and rear plate. Thus the difference being within the heat transfer exchanger design.

2.6 Components of a Flat Plate Collector.

The main parts of a flat-plate collector, as shown in Figure (2.5) are the following:-

- **Cover** one or more sheets of glass or other radiation-transmitting material.
- **Heat removal fluid passageways** Tubes, fins, or passages that conduct or direct the heat transfer fluid from the inlet to the outlet.

- **Absorber plate flat** corrugated, or grooved plates, to that the tubes, fins, or passages are attached. A typical attachment method is that the embedded fixing shown within the detail of Figure 2.4. The plate is usually coated with a high-absorptance, low-emittance layer.
- **Headers or manifolds** Pipes and ducts to admit and discharge the fluid.
- **Insulation** Accustomed minimizes the heat loss from the bottom and sides of the collector.
- **Container** A water-proof box surrounds the foregoing components and keeps them free from dust and moisture [21].

Flat -plate collectors have been built in a wide variety of designs and from many different materials. They have been used to heat fluids such as water plus antifreeze additive, or air. Their major purpose is to gather the maximum amount.

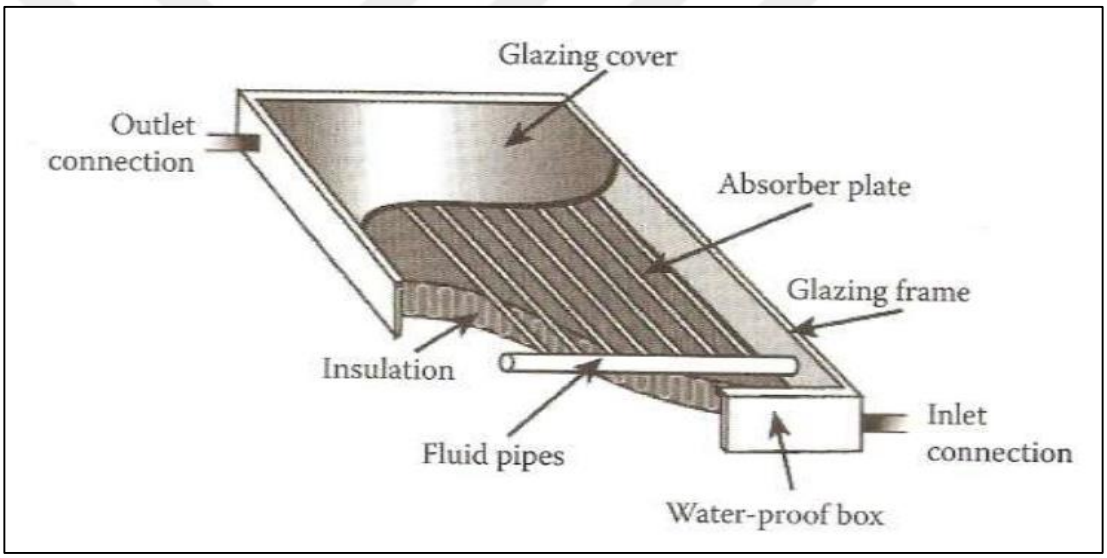

Figure (2.5): Basic component in flat plate collector

The collector will reach temperatures up to 200°C when no liquid flows through it and so all the materials used should be ready to resist such heat. The absorbent is usually manufactured from metallic materials like copper, steel or aluminum. The collector housing is often manufactured from plastic, metal or wood, and also the glass front cover should be sealed so heat doesn't escape, and also the collector itself is protected from dirt, insects or humidity [20].

2.7 Glazing Material

The aim of a glazing material is to transmit the shorter wavelength solar radiation and block, the longer wavelength radiating from the absorber plate and reduce the heat loss by convection from the highest of the absorbent. Glazing additionally acts as the cover on the top of the collector casing [20]. The commercially available window glass can have normal incidence transmittance of about 0.87 to 0.90. Transparent plastic is additionally usually used as glazing material in FPC. This plastic poses high short wave transmittance, but because most of the plastic properties that cannot stand the ultra-violet radiation for a long period of time, transparent plastic is unpopular as glazing material in the flat plate collector. Table 2.1 shows transmittance for varied glazing material when the direct solar radiation is perpendicular to the glazing material. Crystal clear glass and window glass have a highest transmittance of solar radiation. The ability of the glass makes it appropriate as a heat trap in the collector. Thus, window glass is appropriate as a result, it's wide utilized in local flat plate collector [22].

Table 2.1: Transmittance of various glazing material

Material	Transmittance (τ)
• Crystal glass	0.91
• Window glass	0.85
• Acrylate, Plexiglass	0.84
• Polycarbonate	0.84
• Polyester	0.84
• Polyamide	0.80

2.8 Tubing

There are two types of tubing configuration sometime found in flat plate collector specifically parallel configuration and serpentine configuration.

2.8.1 Parallel configuration

Most flat plate collector has small parallel tubes connected to a larger main carrier pipes as shown in Figure (2.5)fi. These small parallel tubes are called riser tubes because this is where the working fluids would rise in order to harvest the heat from the sun. The parallel tube is intended to move working fluid from the bottom of the flat plate collector to the top of the flat plate collector.

The fluids pressure is higher at the base of the collector and least at the top. If the top and bottom pipes are large, the pressure difference is moderated and the rate of flow in each of the parallel pipes is a lot of uniform. Unfortunately, the flow rate is minimal at the center where most of the heat is concentrated. Other problems associated with this configuration are the cost and leaking problems. One small leak can cause catastrophic mess in experimentation and calculation [23].

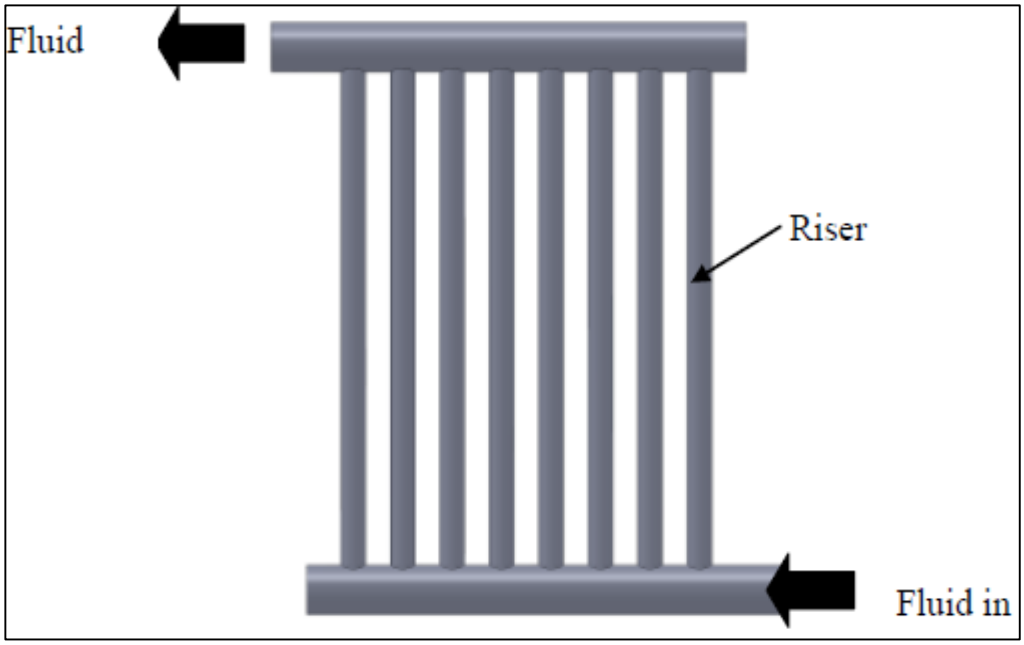

Figure (2.6): Parallel flow configuration.

2.8.2 Serpentine configuration

The serpentine flow in Figure (2.7) below consists of one long continuous versatile tube thus there's no problem with uniform rate of flow. The working fluids flow continuously from bottom to the highest of the collector. This ends up in steady heat transfer from the heat absorbent to the working fluid. Since the rate of flow for the fluid through the serpentine tube is uniform the heat collection method is uniform. The size of this flexible tubing is an important consideration. The size used for tubing is (0.025 m) of diameter. Thus, serpentine configuration is used in this investigation attributable to uniform fluid flow ensuing uniform heat transfer from absorbent plate to working fluid. What is more, serpentine configuration is simpler to construct compare to parallel that have a lot of welding joints. The probability of leaking in parallel configuration is high compare to serpentine configuration. copper, aluminum, steel tubes are utilized within this project [24].

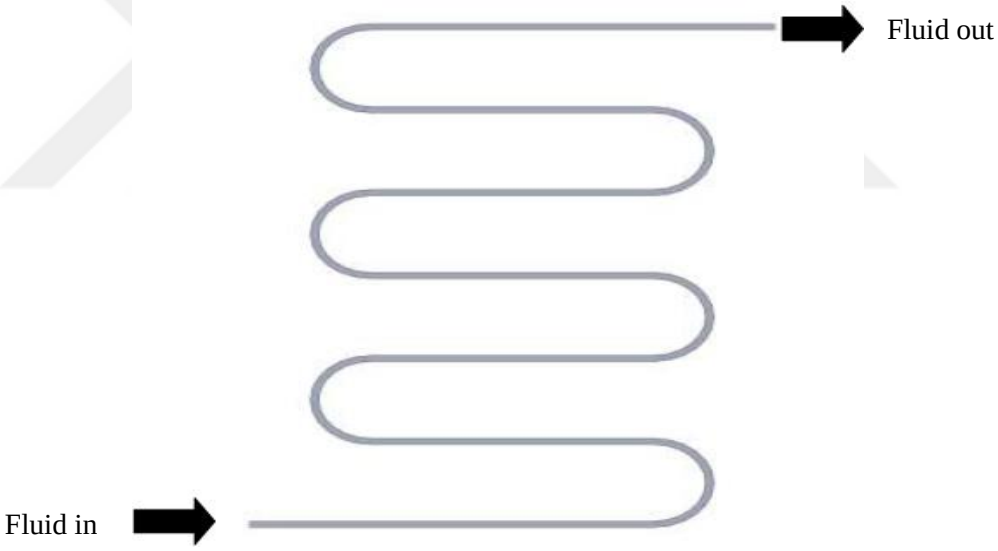

Figure (2.7): Serpentine flow configuration

2.9 Solar collector absorber:

This is a part of the water solar collector that receives the solar radiation, so it's called the absorber. It consists of pipes and metal sheets which are welded together or pipes made from same sheet plate. The absorber surface usually coated with a black selective coating or any dark color, because the lighter colors tend to reflect rather than

absorb [25] , to get high absorption for shortwave solar radiation and low emissivity for longwave thermal radiation [26]. Specific coatings on the absorber surface assist the collector in reducing re-emission of the amount of radiation that can lose the absorber [25]. The absorber is mostly made from aluminum, plastics, steel, or copper. The high thermal conductivity of copper makes it the preferred solution, despite it is high price. The main task of the absorber is absorbing solar energy and transferring the collected heat to the heat transporting fluid that flows through pipes in an absorber [26]. One interesting phenomenon is that on dark nights, a black color absorber surface become colder than the ambient air or other light color materials surrounding it, this can waste the heat when the pumps incidentally left switched on [25]. The absorber piping configurations include:

- Panel absorbent is that the absorbent plate with straight vertical pipes and horizontal headers;
- Strip absorbent is that the absorbent plate forming a vertical pipeline;
- Serpentine absorbent or serpentine riser with serpentine coils coated to a flat metal plate;
- Absorbent with a single surface flow channel with two metal sheets welded, as a sandwich structure;
- Vertical harp-type absorbent, with vertical parallel pipes and horizontal headers, connected to a flat metal sheet;
- Horizontal harp-type absorbent, with horizontal parallel pipes and vertical headers, connected to a flat metal sheet [26].

2.10 Collector insulation:

The Insulation on collector behind and to the side of the absorbent pipes to reduce conduction losses. Commonly, this insulation consists of 1-6 cm of high-temperature fiberglass batting or semi-rigid board or maybe mineral wool. Styrofoam and urethane foams are sometime not used as result of they will deform at high temperatures or provide off gases that can be toxic. The insulation must be separated from the absorbent plate by 0.5 to 0.75 cm and they have a reflective foil facing the absorber plate. If fiberglass insulation is employed, it mustn’t be typical construction grade that contains phenolic binders which will "outgas" at the stagnation temperature

of the collector. In all cases, insulations should be not flammable, so they should have a low thermal expansion coefficient, not melt or outgas at collector stagnation [27].

2.11 Flat plate problem statement:

In the application of DHW (Domestic hot water) and solar space heating, the flat-plate collectors are the most commonly employed solar collector. An insulated metal box with a glass or plastic cover, also it called the glazing. The dark-colored absorber plate is a typical flat-plate collector, which is shown in Figure (2.3). These collectors make hot the liquid or air at temperatures less than 80˚C [24]. Flat-plate collectors are used for hydraulic space-heating installations as well as domestic water heating. Figure (2.8) shows a schematic drawing of the energy losses through a collector. There is 80% of the solar energy absorbed in the collector plate. The radiant energy reflects and heat loss in the collector surface is around 10–35% [28].

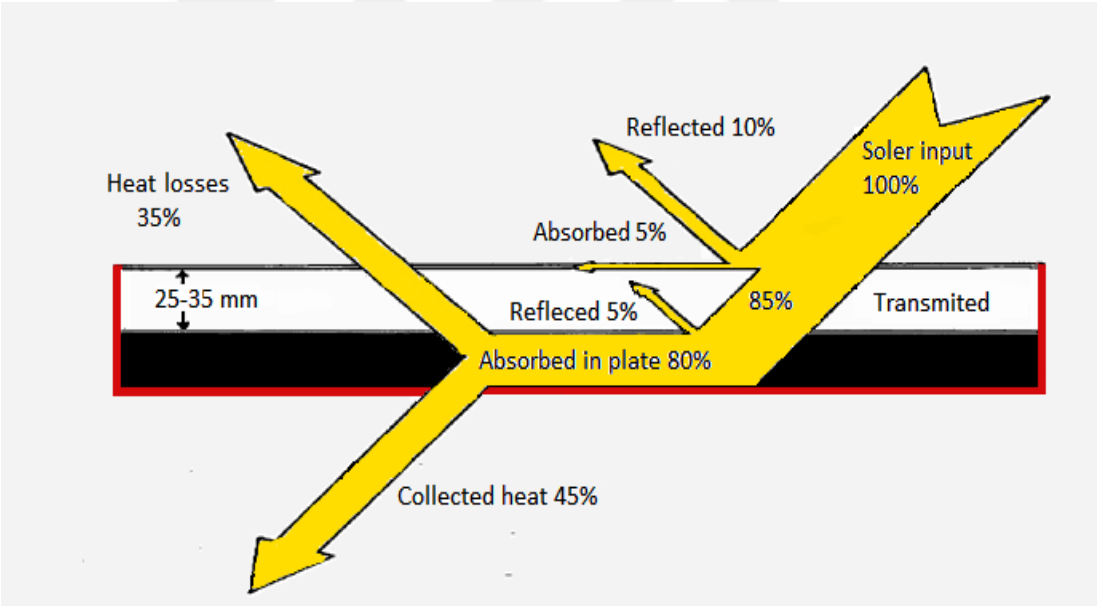

Figure (2.8): Heat flow through a Flat Plate solar collector[29].

CHAPTER THREE

THEORY

3.1 Theoretical Background

The main purpose of the collector is to absorb the sun's energy and transfer this energy efficiently to the liquid flowing in it. There are a great variety of flat plate collectors, one of these named Serpentine that have chosen in this thesis.

This chapter deals with the theory behind the modes of work of flat plate collector through the different materials of absorb and the various mass flow rates in an environment of Iraq. Another critical issue that investigated in this chapter solar radiation calculations and the length of the day for AL-Najaf city in Iraq, in addition to the predictions of losses of flat plate collector by ANSYS software program.

3.2 Software

One of the most famous program software that deal with heat transfer is the ANSYS program. ANSYS, an abbreviation for ANALYSIS SYSTEM is a programmatic based on the method of finite elements, invented by Dr. John Swanson. The workbench of ANSYS Fluid Flow (CFX) environment is an intuitive up-front finite part analysis tool that is used in conjunction with CAD systems and/or Design Modeler. ANSYS work table may be a software system environment for performing structural, thermal, and electromagnetic analyses [30].

3.2.1 Types of Cells

The following common sorts of cells occur in several of the analysis and element systems accessible in ANSYS work bench. Other cell sorts could also be accessible in certain systems see Figure (3.1).

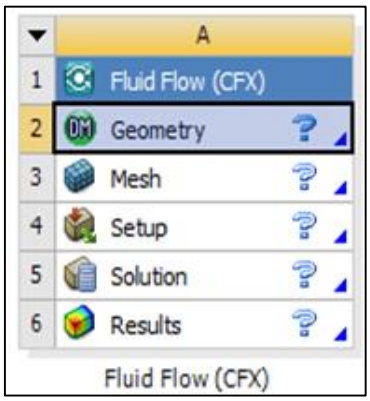

Figure(3.1): Cells of workbench

- **Geometry:-**

First process in the ANSYS program is a design the workbench by Geometry. Sketch the body and put dimensions by depend the axises see Figure (3.2).

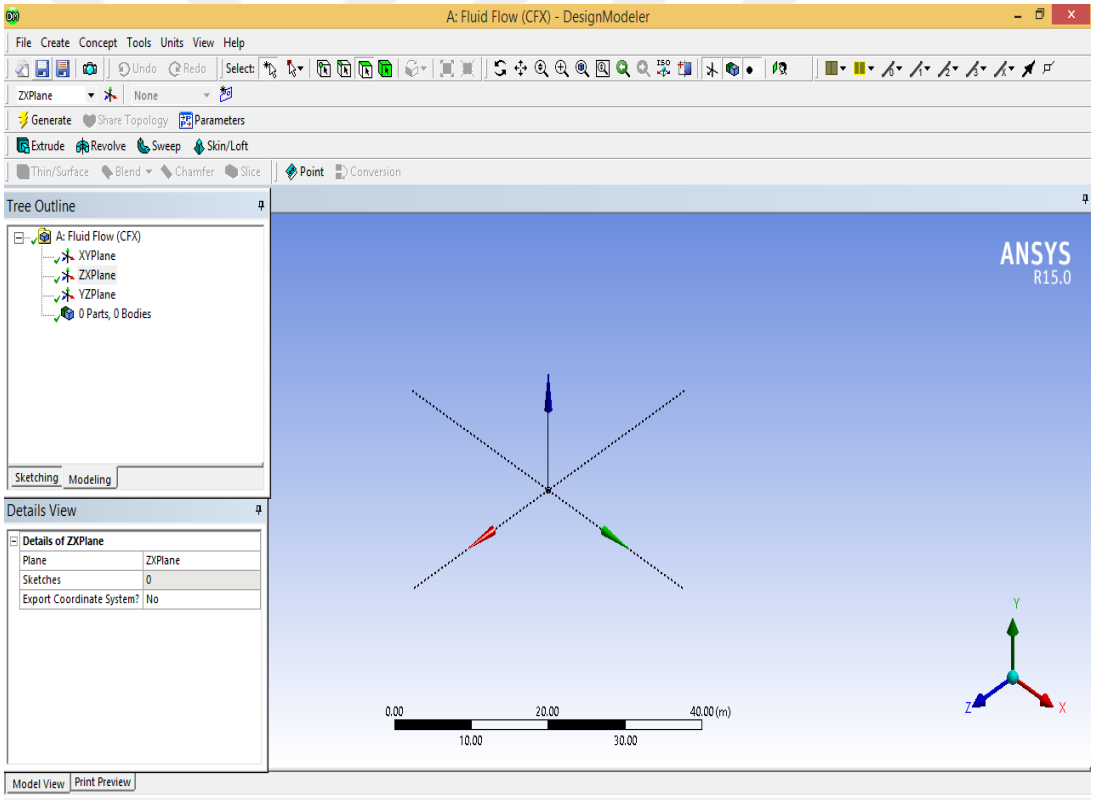

Figure (3.2): Geometry window

- **Mesh:-**

The goal of meshing within the workbench of ANSYS program give strong, simple to use meshing tools which will modify the mesh generation method. These tools have the advantage of being extremely automated along with having a moderate to high degree of user management by divided the body to nodes and parts see Figure (3.3).

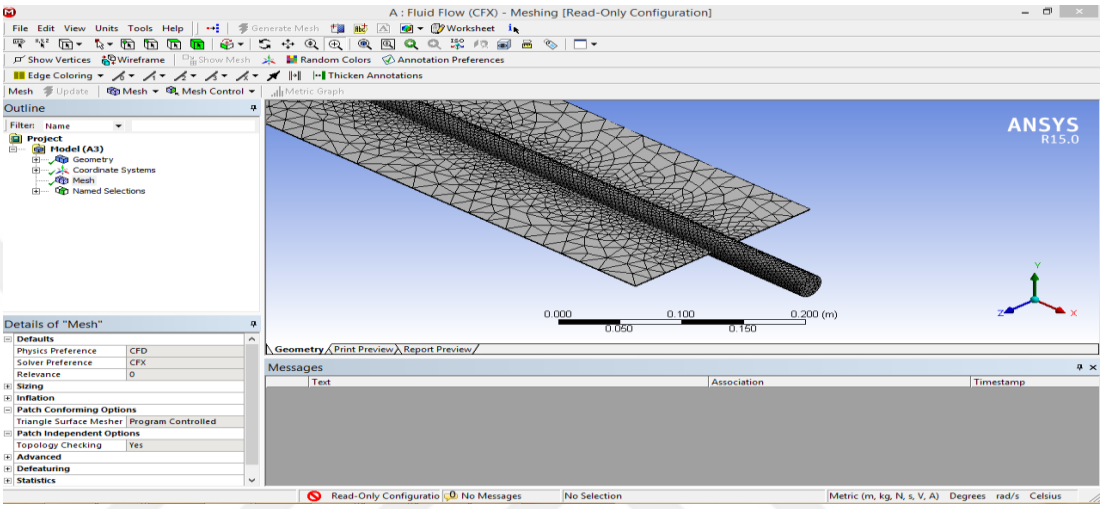

Figure (3.3): Mesh window

- **Setup:-**

Setting bondery condiations on the workbench for the purpose of simulating the required test work see Figure (3.4).

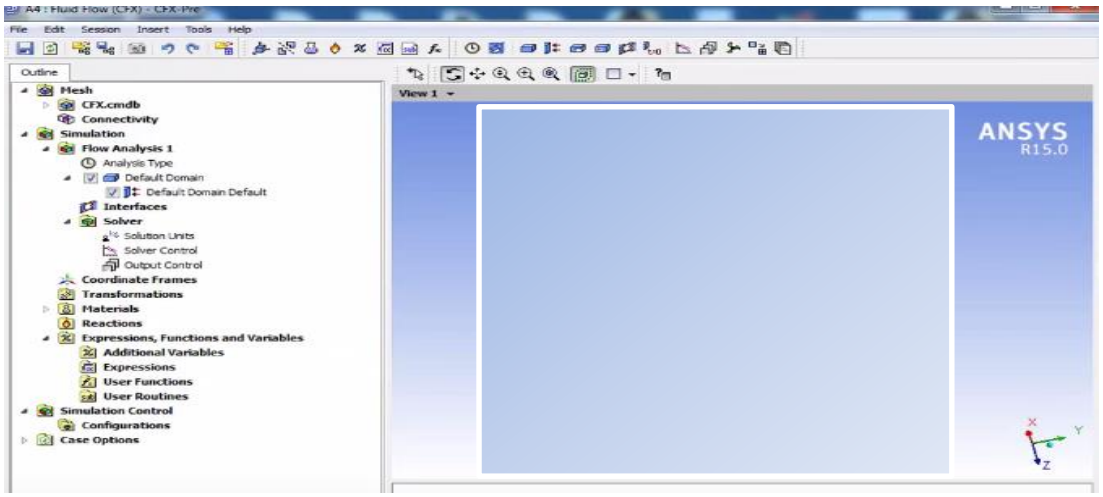

Figure (3.4): Setup window

- **Solution :-**

There is a folder with a big fat punctuation mark on the highest of the Solutions branch in ANSYS Mechanical. it's known as “Solution info.” Most users click on that after their run is completed and perhaps look into the output from the ANSYS Mechanical solve see Figure (3.5).

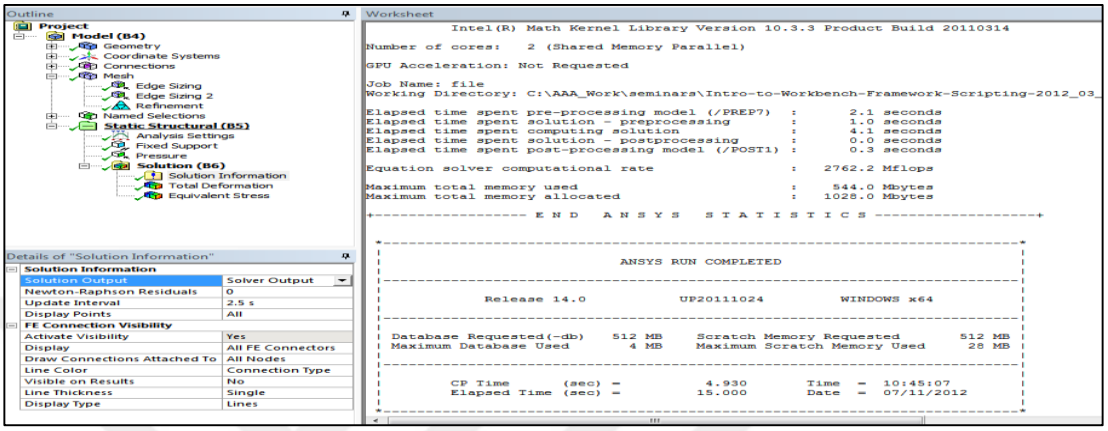

Figure(3.5): Solution window

- **Results**

The results are displayed after the solution is completed see Figure (3.6).

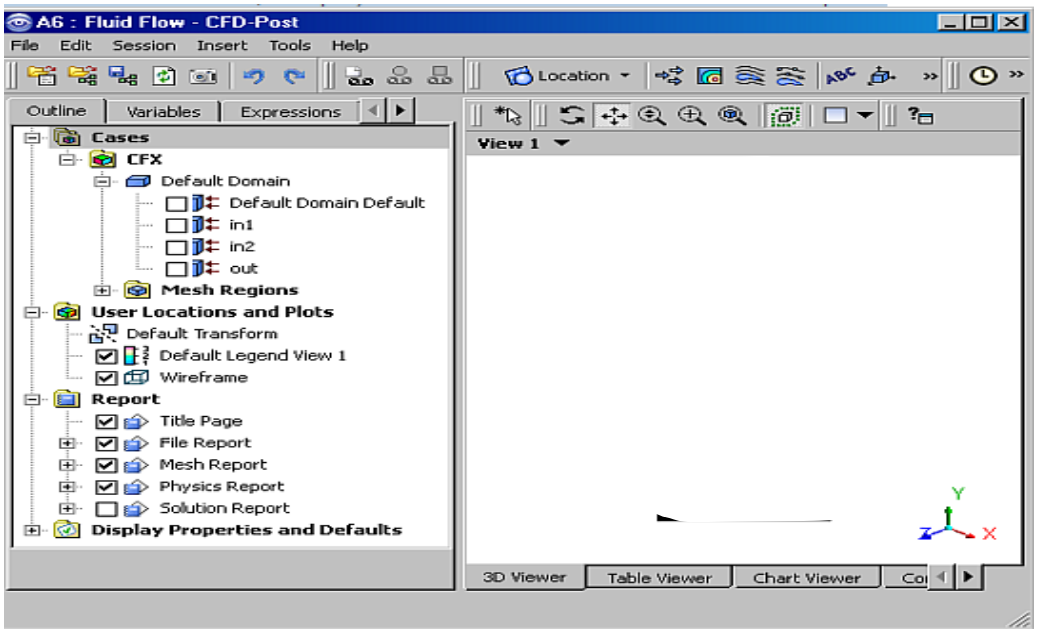

Figure (3.6): Results window

3.3 Location Selection

The Iraqi city of Najaf has been chosen for experiments on this thesis for two reasons:-

1. Coordinates of Al- Najaf city are (Latitude: 32.11° N, Longitude: 44.36° E) [31].It has a good location ,borders Saudi Arabia in the Iraqi Desert in Belt area see Figures (3.7 A,B) [32][33].
2. This city was chosen by the Ministry of Electricity for the purpose of building an electric generating station by using solar energy PV (photovoltaic)

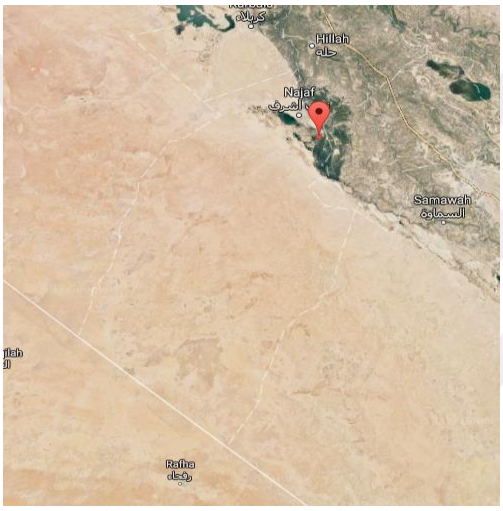

Figure (3.7 A) Satellite Image of An Najaf

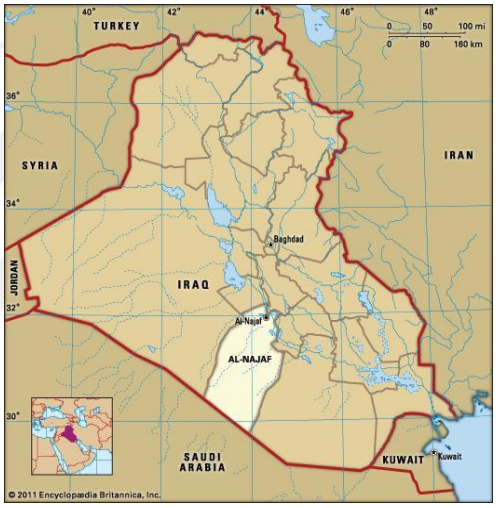

Figure (3.7 B) Iraq's map

3.4 Data Sources of Solar Irradiance

The data of solar radiation, wind velocity, and environmental temperature are used from the records of Iraqi Meteorological Organization and Seismology- Republic of Iraq Ministry of Agriculture -Najaf Governorate – Abbasiyah station-2016 [34].Colder months was selected of the year to Najaf city it's the months (11,12,1,2) (November , December, January, February) see Table 3.1 and see APPENDIX A1,A2,A3.

Table 3.1: Available data of Najaf city [33].

Najaf Governorate - January 2016									
Date	TM C°	Tm C°	T C°	HM %	Hm %	SRt Mj/m2/m	WS_avg m/s	WS_max m/s	$Et_{\circ}$ _avg mm/day
1/1/2016	13.47	7.83	11.03	99.98	78.77	2.65	1.88	8.67	0.70
1/2/2016	12.39	5.09	8.91	99.98	41.63	13.71	1.81	7.46	1.60
1/3/2016	13.35	2.62	7.41	99.98	43.33	12.84	1.09	7.85	1.30
1/4/2016	17.64	5.83	10.40	94.72	34.78	13.31	1.57	6.11	1.90
1/5/2016	17.97	3.30	10.88	99.98	40.91	10.14	1.36	7.15	1.60
1/6/2016	19.55	5.55	12.47	99.98	50.39	12.51	0.70	3.80	1.40
1/7/2016	19.46	8.41	13.61	99.97	55.83	11.82	1.61	7.34	1.70
1/8/2016	19.36	11.27	14.75	99.96	61.26	11.12	2.51	10.87	1.80
1/9/2016	18.84	8.33	13.67	99.96	38.02	10.35	2.07	9.69	2.10
1/10/2016	17.09	5.22	10.20	99.97	33.53	14.04	1.54	6.18	1.90
1/11/2016	17.62	3.03	9.54	99.98	36.68	13.95	1.12	5.44	1.70
1/12/2016	17.73	4.54	10.14	99.98	41.73	11.35	1.17	5.97	1.60
1/13/2016	17.80	5.39	10.68	99.98	44.44	13.66	1.42	6.21	1.80
1/14/2016	20.12	2.56	11.34	100.00	36.74	13.90	0.94	4.57	1.70
1/15/2016	20.45	5.84	12.85	99.41	49.37	13.34	1.41	4.30	1.90
1/16/2016	19.23	4.75	11.38	97.55	40.28	13.94	1.39	5.30	1.90
1/17/2016	18.01	3.65	9.91	95.68	31.18	14.53	1.37	6.29	2.00
1/18/2016	22.69	4.57	14.18	99.97	32.39	10.38	2.68	9.91	3.00
1/19/2016	18.40	8.20	14.38	80.51	26.51	11.94	2.83	10.81	3.00
1/20/2016	19.41	6.13	12.26	92.95	31.41	12.87	1.29	4.56	2.00
1/21/2016	19.24	4.56	11.40	99.98	35.60	12.87	0.92	4.41	1.70
1/22/2016	16.31	7.86	12.03	99.96	55.51	3.93	1.27	5.10	1.20
1/23/2016	21.69	10.77	15.13	99.97	42.69	6.37	1.73	8.44	2.00
1/24/2016	18.76	7.14	12.50	99.98	41.79	12.27	1.68	7.61	2.00
1/25/2016	17.05	6.89	11.40	87.81	38.63	13.39	1.91	7.39	2.20
1/26/2016	15.33	6.64	10.29	75.63	35.46	14.51	2.13	7.16	2.40
1/27/2016	10.72	0.19	5.80	77.19	20.73	10.26	1.96	8.36	2.00
1/28/2016	9.76	1.23	5.24	77.55	25.50	14.59	2.81	10.00	2.30
1/29/2016	11.65	-1.66	4.38	64.23	14.79	15.05	2.02	7.27	2.40
1/30/2016	14.39	-1.27	6.41	65.25	22.37	15.31	1.74	6.84	2.30
1/31/2016	16.64	1.61	8.20	73.26	25.28	14.26	1.32	6.17	2.20

Where

TM =Max Temperature
Tm =Min Temperature
T =Avg Temperature
HM =Max Humidity
Hm =Min Humidity
SRt =Total Solar Radiation
WS_avg =Avg Wind Speed
WS_max =Max Wind Speed
$Et_{\circ}$_avg =Avg Evapotranspiration

For one year (2016) the Total Solar Radiation of every month shown in the Figure (3.8).

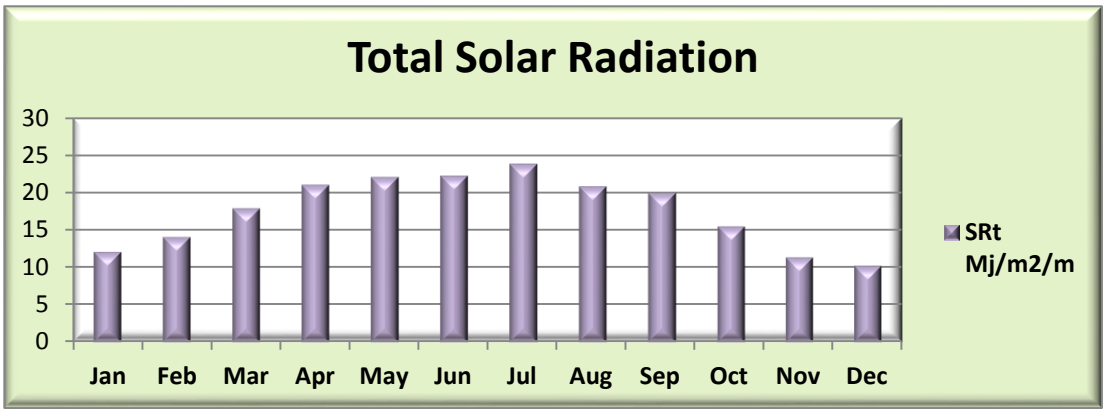

Figure (3.8): Total Solar Radiation of Al Najaf **[34]**.

From the table, the data results of the total solar radiation have gotten with unit (MJ/m²/m) for these have been used these equations under below. Unit conversion, it must be converted from (MJ/m²/m) to (w/m²) after that it can be used in Ansys model. Here in the equations:-

$$\text{Total Solar Radiation (SRT) } (W/m^2) = \frac{(SRT(MJ/m^2/m)\times 1000000)}{(\text{daylength}\times 3600)} \qquad (3.1)$$

$$\text{day length} = \frac{2}{15}\times \cos^{-1}\left[\ (-\tan(L)\times\tan(\delta)\ )\right] \qquad (3.2)$$

$$\delta = 23.45\times \sin\left[\frac{360(284+N)}{365}\right] \qquad (3.3)$$

Where

L= local latitude city by degrees, defined as the angle between a line from the center of the earth to the site of interest and the equatorial plane. Values north of the equator are positive and those south are negative.

* (L) from AL NAJAF city = (32.11 °N) latitude [31].

δ=The declination in degrees for any day of the year (N) can be calculated approximately by the equation [35].

N= Number of day at the beginning of the year from January see Table (3.2)

Table 3.2: Day Number

Month	Number of days (N)
January	i
February	31+i
March	59+i
April	90+i
May	120+i
June	151+i
July	181+i
August	212+i
September	243+i
October	273+i
November	304+i
December	334+i

Where i =number of days of the any month.

The day length has been found the values for one year in Al- Najaf city is confined between minimum No. hours (9.894012 h) in 20/12/2016 in winter solstice and maximum No. of hours (14.10599 h) in 20/6/2016 in summer solstice [36].See Figure (3.9 A).

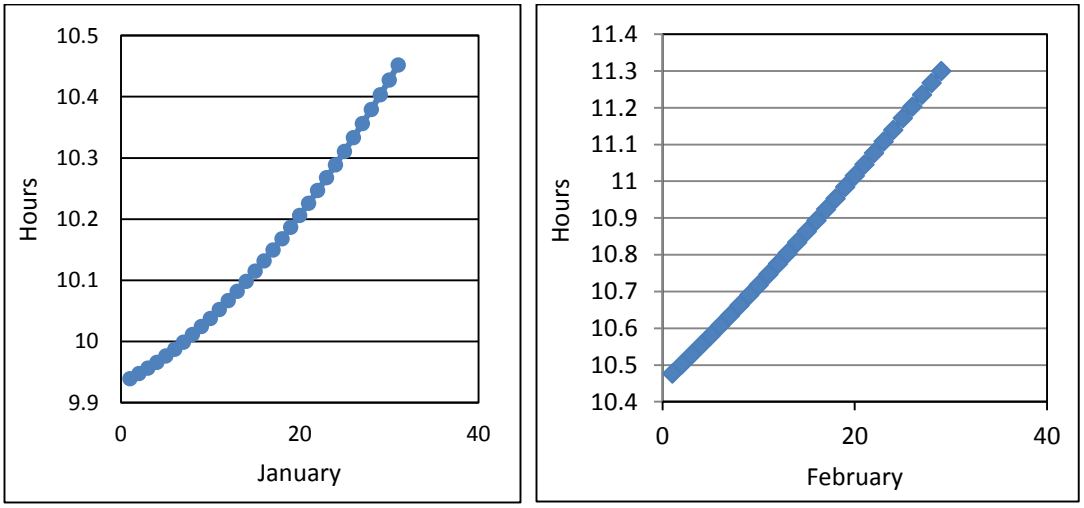

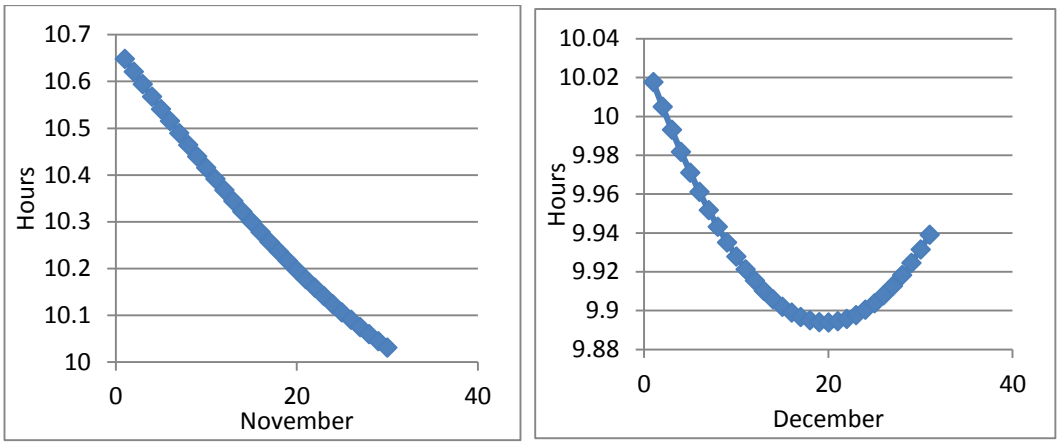

Figure (3.9A): Day length of January, February, November and December

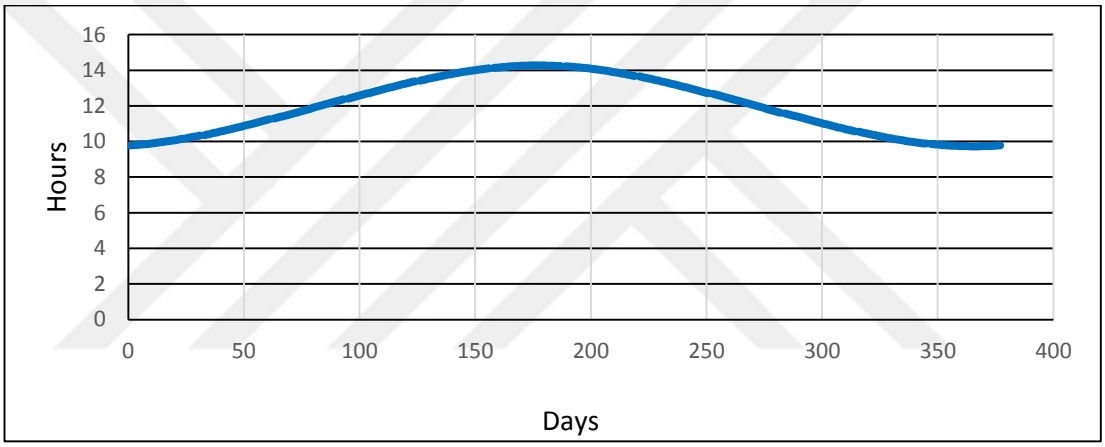

Figure (3.9 B) Day length of one year of Al Najaf city.

Meteorological data are illustrated from continuous collecting over winter of the year 2016 The SRT for Al-Najaf city. From data information of this city for months (January, February, November, December) after converting SRT from ($MJ/m^2/m$) units to (W/m^2) units explained in following by Figure (3.10) A,B,C,D and tables in APPENDIX B1,2,3,4 respectively:-

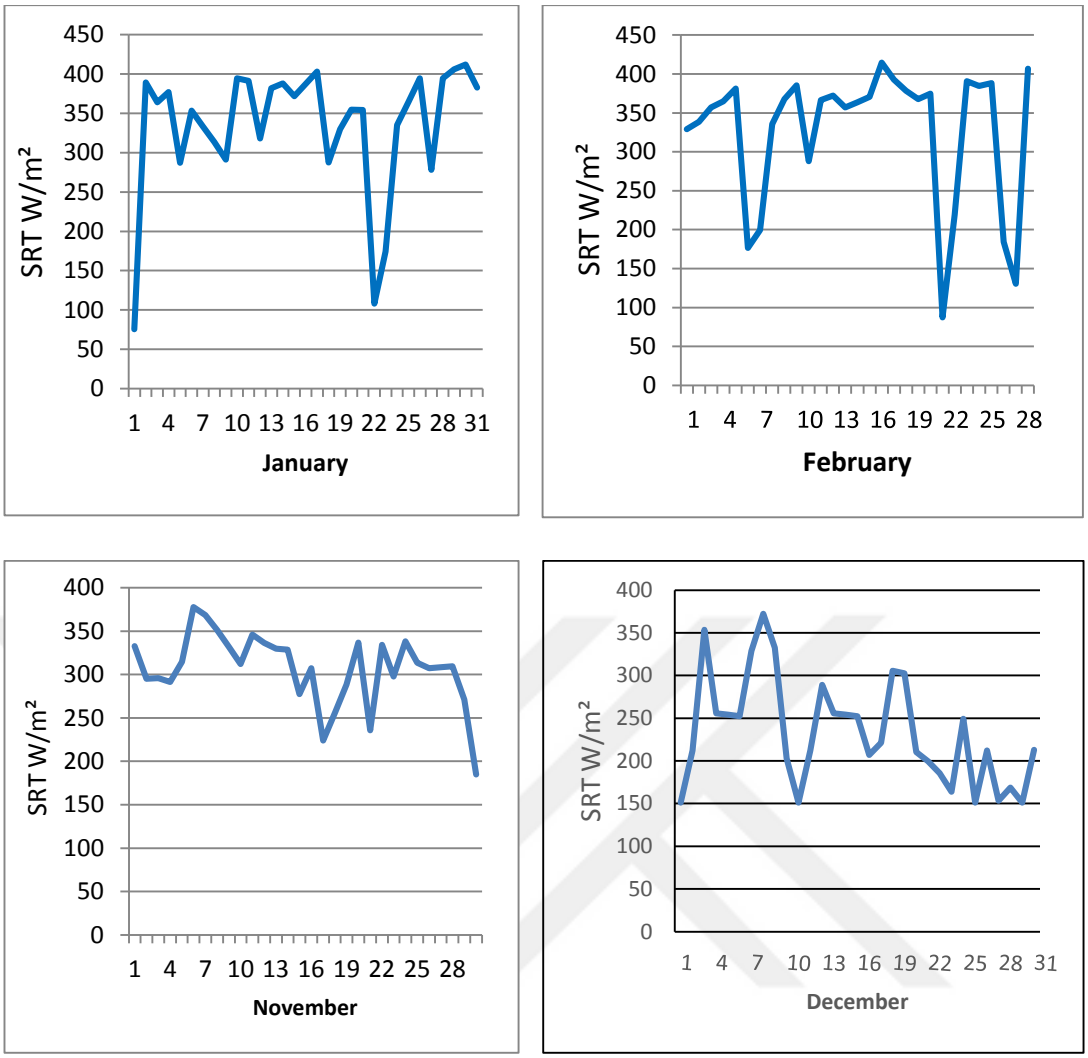

Figure (3.10): SRT of January, February, November and December.

3.5 Estimate of the solar time

Solar time is the timing for each site and not necessarily be identical to the time clock. For each point, (longitude) solar time is different from any other point (or a line the length of time). It is known as the solar time: "Virtual time based on the angular momentum that we see the sun in the sky, and observation through the site." Solar back to a place known as the "The moment of crossing the sun during the midday circle." It is the same as the moment of the sunbeam in the level of the meridian of this site, and this moment is at 12 p.m. by the solar time. To determine the solar time for a site, it is needed to know the manner in which it is the timing system. In principle, the noontime moving permanently as a result of the continuous rotation of the earth, even in the same country, the noontime moves westward over time. Time to become

applicable is the same as the solar time it is necessary that each timing point be disputed by longitude incurred by itself, but that would not be practical.

This means that the local time will be fixed for each of the different areas. In fact, this installation of the timing within each region to facilitate the everyday within each region or a patch of ground. In addition, what was the Earth's rotation by one degree of latitude needed for 4 minutes , it should be to determine the correct time for each local time point in the area where this point is located. The amount of correction will depend on the difference between the longitude of the point and line of standard length or reference fir the area where this point is located, the apparent solar time (AST) of a site can be calculated from the following relationship:

$$AST = LST + ET \pm 4 \times (SL - LL) - DS \quad (3.4)$$

Where:

LST = local standard time.

ET = equation of time.

SL = standard longitude.

LL = local longitude.

DS = daylight saving (it is either 0 or 60 min).

- If a location is east of Greenwich, the sign of equation (3.4) is a negative **(-)**, and if it is west, the sign is a Positive point **(+)**.
- The term **DS** depends on whether day-light saving time is in operation (usually from end of March to end of October).

Can be corrected by the time the relationship of the following equation account:

$$ET = 9.87 \times \sin(2B) - 7.53 \times \cos(B) - 1.5 \times \sin(B) \quad (3.5)$$

Where B is calculated from the following relationship:

$$B = \left(\frac{360}{364}\right)(N - 84) \quad (3.6)$$

all above calculation are used to determine the amount of solar radiations, the best angle of collector, day length, solar time,....etc. while we are studying water heater collector which is used at winter season, we have to know that some clouds can affect

all these calculations. All weather data are recorded from Iraqi Meteorological Organization and Seismology- Najaf Governorate – Abbasiyah station-2016. Because of the radiation fluctuation due to time either because of continuously change of incident angle or due to weather conditions changes, collector cannot reach to steady state conditions.

3.6 Thermal analysis of flat-plate collectors:

Normally flat plate collector, designed inside a box with one or two flat glass facing sun. The basic parameter to consider is the collector thermal efficiency (η). This is defined as the ratio of the useful energy delivered to the energy incident on the collector aperture. The incident solar flux consists of direct and diffuse radiation. While flat-plate collectors can collect both solar radiation types, concentrating collectors can utilize direct radiation only if the concentration ratio is greater than 10 [37]. Next calculations are used at collector to determine heat gain, losses, efficiency ...etc.

Thus it is necessary to define step by step the singular heat flow equations in order to find the governing equations of the collector system If **I** is the intensity of solar radiation, in W/m², incident on the aperture plane of the solar collector having a collector surface area of $\mathbf{A_c}$ m², then the amount of solar radiation received by the collector is[38][39]:

$$Q_T = I \times A_c \quad (3.7)$$

$$Q_u = Q_T - Q_{loss} \quad (3.8)$$

Depends on design losses equation can be written:

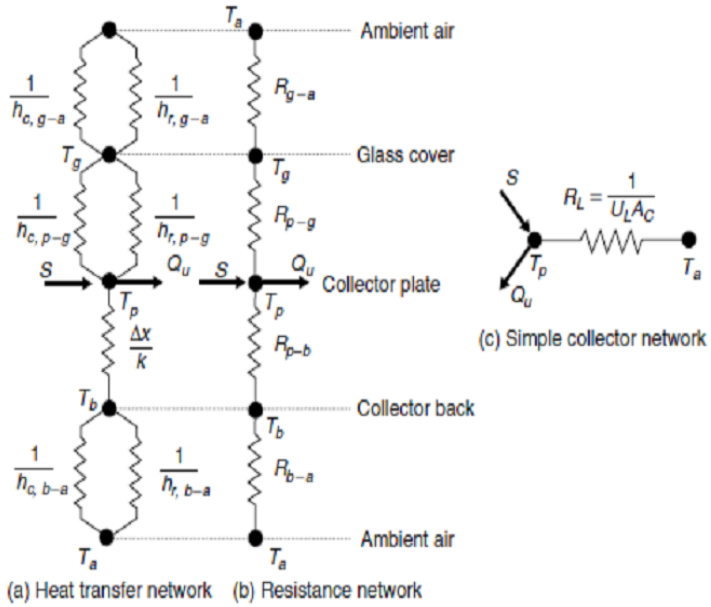

Figure (3.11): Heat transfer and resistance network for collector plate with one glass only.

$$Q_{loss} = \frac{T_p - T_a}{R_L} = U_L\ A_c\ (T_p - T_a) \qquad (3.9)$$

Where

U_L = overall heat loss coefficient based on collector area A_c ($W/m^2.K$)

T_p = plate temperature ($C°$).

A_c =area collector (m^2).

T_a = ambient temperature.

* Through the data of the city of Najaf , we find the average temperature for each month of the year 2016, see Table(3.3).

Table3.3: average wind velocity for year 2016

Month	Temperature °C
Jan	10.73
Feb	14.43
Mar	19.1
Apr	24.88
May	30.04
June	34.07
July	36.15
Aug	35.69
Sep	30.59
Oct	25.24
Nov	16.06
Dec	10.56

Overall losses include losses from three parts,

$$U_L = U_t + U_b + U_e \tag{3.10}$$

Where subscripts t, b, and refer to top, bottom, and edges

Heat losses from the upper face of the plate is coming from convection and radiation;

$$Q_t = A_c\, h_{c,p\text{-}g}\, (T_p - T_a) + \frac{A_c\left(T_p^4 - T_a^4\right)}{\left(1/\varepsilon_p\right) + \left(1/\varepsilon_g\right) - 1} \tag{3.11}$$

$h_{c,p-g}$ = convection heat transfer coefficient between plate and glass ($W/m^2.K$)

ε is infrared emissivity of absorber plate and glass p, g for respectively.

The second term of losses due to radiation is neglected in ANSYS analyses due to ANSYS limitations.

To linearize radiation term;

$$h_{r,p\text{-}g} = \frac{\sigma\left(T_p + T_g\right)\left(T_p^2 + T_g^2\right)}{\left(1/\varepsilon_p\right) + \left(1/\varepsilon_g\right) - 1} \tag{3.12}$$

$$Q_t = A_c\,(h_{c,p\text{-}g} + h_{r,p\text{-}g})(T_p - T_a) = \frac{(T_p - T_a)}{R_{p\text{-}g}} \tag{3.13}$$

where

$$R_{p\text{-}g} = \frac{1}{A_c(h_{c,p\text{-}g} + h_{r,p\text{-}g})} \tag{3.14}$$

The same procedure can be done between glass and ambient;

$$h_{r,p\text{-}a} = \varepsilon_g \sigma\left(T_p + T_g\right) \times \left(T_p^2 + T_g^2\right) \tag{3.15}$$

$$R_{g\text{-}a} = \frac{1}{A_c(h_{c,g\text{-}a} + h_{r,g\text{-}a})} \tag{3.16}$$

While R_{p-g} and R_{g-a} are in series, so $R_t = R_{p-g} + R_{g-a}$

$$Q_t = \frac{(T_p - T_a)}{R_t} = U_t\,A_c\,(T_p - T_a) \tag{3.17}$$

Solutions by iterations are required for the calculation of the top heat loss coefficient, U_t, since the air properties are functions of operating temperature. Because the iterations required are tedious and time consuming, straight forward evaluation of U_t is given by the following empirical equation with sufficient accuracy for design purposes [1][40]:

$$U_t = \frac{1}{\dfrac{N_g}{\dfrac{C}{T_p}\left[\dfrac{T_p - T_a}{N_g + f}\right]^{0.33}} + \dfrac{1}{h_w}} + \frac{\sigma\left(T_p + T_g\right)\left(T_p^2 + T_g^2\right)}{\dfrac{1}{\varepsilon_p + 0.05N_g\left(1 - \varepsilon_p\right)} + \dfrac{2N_g + f - 1}{\varepsilon_g} - N_g} \tag{3.18}$$

$$f = (1 - 0.04h_w + 0.0005h_w^2)(1 + 0.091N_g) \tag{3.19}$$

$$C = 365.9(1 - 0.00883\beta + 0.0001298\beta^2) \quad (3.20)$$

$$hw = \frac{8.6 \times V^{0.6}}{L^{0.4}} \quad (3.21)$$

Where V is wind velocity (m/s) and L is the length of collector.

* Through the data of the city of Najaf , we find the average wind velocity for each month of year 2016, see table (3.4).

Table 3.4 Monthly average wind speed

Month	Average Wind Speed m/s
Jan	1.653
Feb	1.819
Mar	2.115
Apr	1.744
May	2.37
June	2.27
July	2.354
Aug	1.605
Sep	1.846
Oct	1.273
Nov	1.67
Dec	1.368

U_b refers to back of plate heat transfer cofficient. back heat loss cofficient typically in the range of 0.3-0.6 ($W/m^2.K$) due to the limitation of condution resistance of insulations behind collector plate.

$$U_b = \frac{1}{\frac{t_b}{k_b} + \frac{1}{h_{c,b-a}}} \quad (3.22)$$

Where

t_b = thickness of back insulation (m).

k_b = conductivity of back insulation (W/m.K).

$h_{c,b-a}$ = convection heat loss coeffi cient from back to ambient (W/m^2 .K).

Smilarly for edges:

$$U_e = \frac{1}{\frac{t_e}{k_e} + \frac{1}{h_{c,e-a}}} \quad (3.23)$$

Where

t_e = thickness of edge insulation (m).

k_e = conductivity of edge insulation (W/m.K).

$h_{c,e-a}$ = convection heat loss coeffi cient from edge to ambient (W/m^2.K).

Typically, edge heat loss cofficient value in the range of 1.5-2 (W/m^2.K).

In this project, while ANSYS simulation is applied, the following assumptions and specifications are assumed as followed:

- Collector slope (tilt angle) assumed β=35 degree
- ε_g=0.88, ε_p=0.05, N_g=1 at equations ((3.18), and (3.19))
- At equation ((3.21)), V= 1.65, 1.82, 1.669, and 1.368 m/s for the months of January, February, November, and December respectively while collector lengh is 2 m.
- T_p at intial time equal ambient temperature (T_a) which is 10.73, 14.43, 16.06, and 10.56 at months of January, February, November, and December respectively. T_{win} have the same value of T_a always.
- To start calculate using itiration technique at equation ((3.18)), T_p assume firstly equal 350 k.
- t_b and t_e in equations (3.22) and (3.23) are assumed 0.05m
- The material of insulation is assumed plywood. The plywood thermal conductivity(k_b , k_e)=0.12 [41].
- $h_{c,b-a}$ and $h_{c,e-a}$ in eqations ((3.22), and (3.23)) are assumed 0.6 and 2 (W/m^2.K) respectively.

3.7 Flow Chart

To solve problem using equations and ANSYS program, the following flow chart will be applied for each case:-

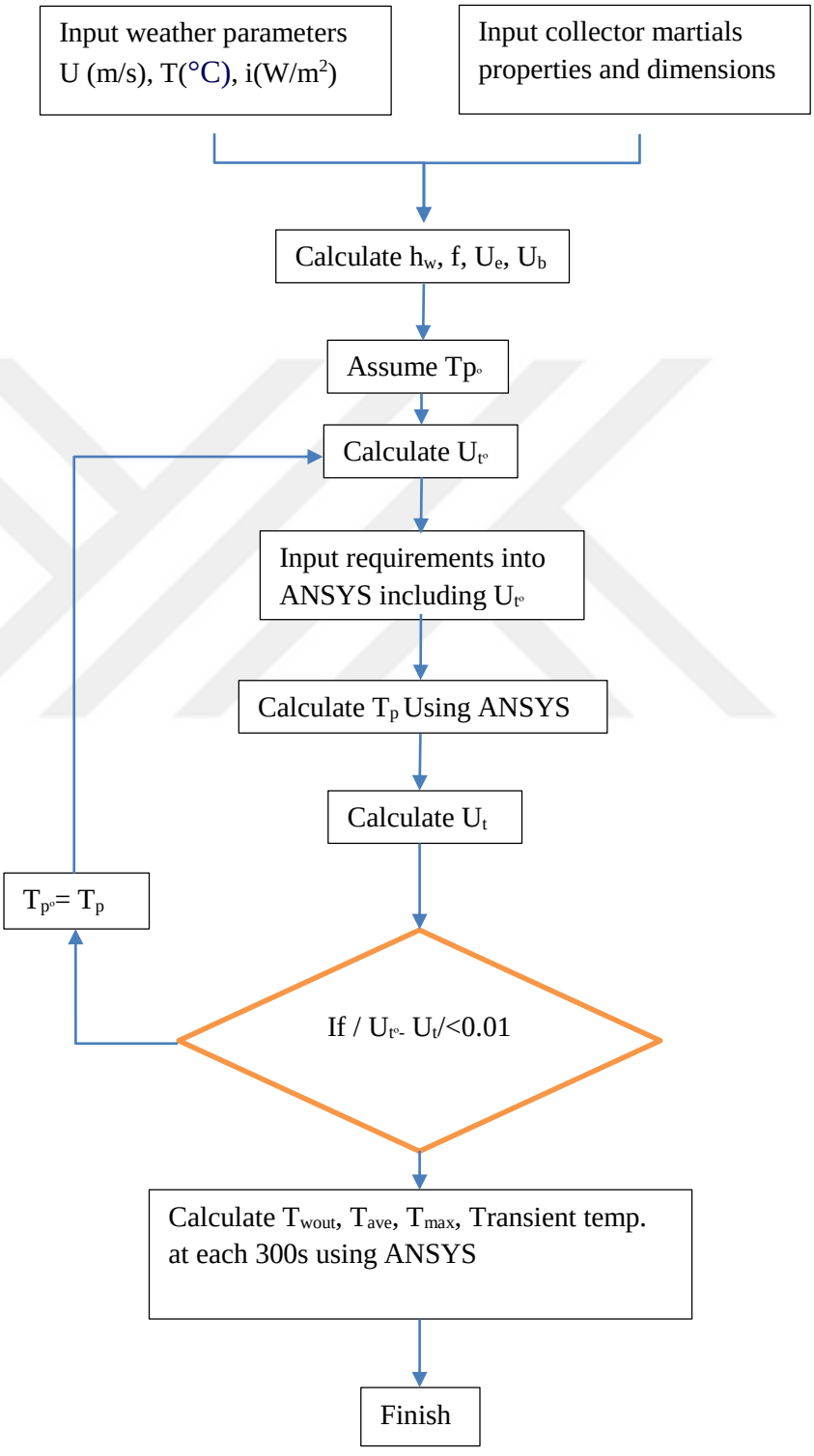

CHAPTER FOUR

RESULTS AND DISCUSSION

4.1 Introduction

All inputs used in ANSYS are recorded at Al-NAJAF/IRAQ. Average of outside temperatures, solar radiation and wind speed for the coldest four months (January, February, November, and December) at 2016 are used in this simulation using CFX analyses systems of ANSYS 2015 as shown in table below.

Table 4-1: Average weather conditions at Al-Najaf city/Iraq.

Month	Temperature °C	Wind Speed m/s	Solar radiation W/m^2	SRt $MJ/m^2/m$
Jan	10.73	1.653	335.42	12.102
Feb	14.43	1.819	360.813	14.06
Mar	19.1	2.115	420.74	17.918
Apr	24.88	1.744	453.75	21.06
May	30.04	2.37	443.99	22.057
June	34.07	2.27	434.78	22.268
July	36.15	2.354	472.71	23.847
Aug	35.69	1.605	435.82	20.812
Sep	30.59	1.846	453.016	19.966
Oct	25.24	1.273	383.585	15.497
Nov	16.06	1.67	306.675	11.34
Dec	10.56	1.368	233.024	8.206

Refers to maximum Refers to

Where SRt is Total Solar Radiation

Table shows that higher solar radiations and temperature are found at month of February and November while the less are found at December.

Because of the daily fluctuation of solar radiation Figure (4.1), which may be caused by clouds of any other weather conditions like dust, humidity… etc., monthly average of solar radiation has been used in calculations as in Figure (4.2) and this will give more stability and better idea for all months.

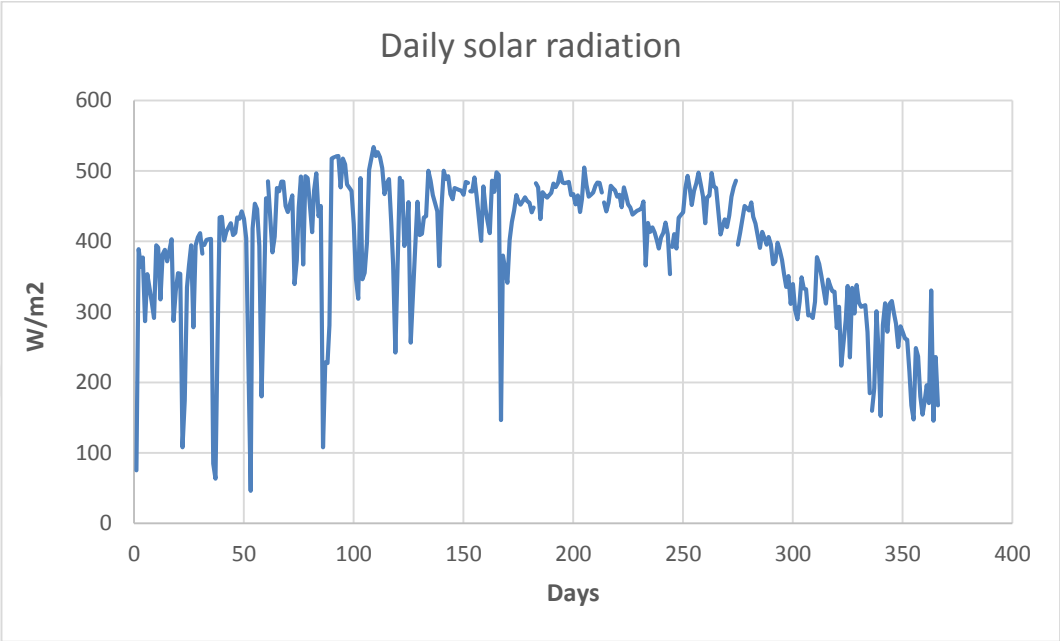

Figure (4.1): daily solar radiation fluctuation.

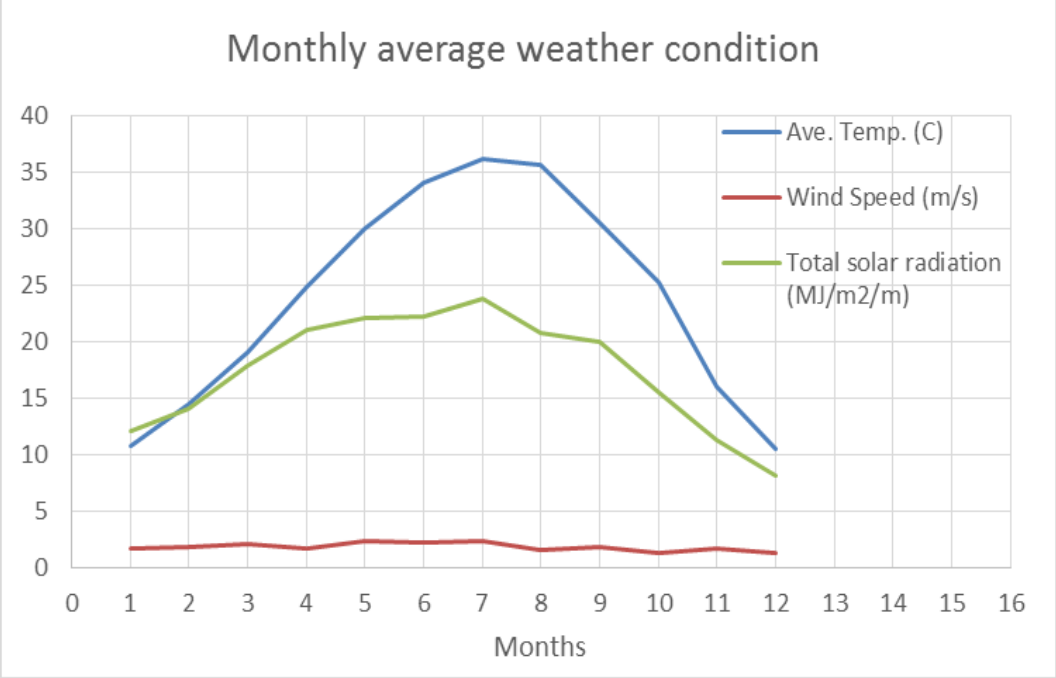

Figure (4.2): monthly weather condition.

4.2 ANSYS Model

4.2.1 Design Modeler

ANSYS version 15.0 is used for these analyses where a solar collector with dimension of 2×1 m^2 and pipe of outer diameter (0.025) m is used for water with one inlet and one outlet. All material used with thickness of (0.001) m for both plate of collector and pipe Figure (4.3).

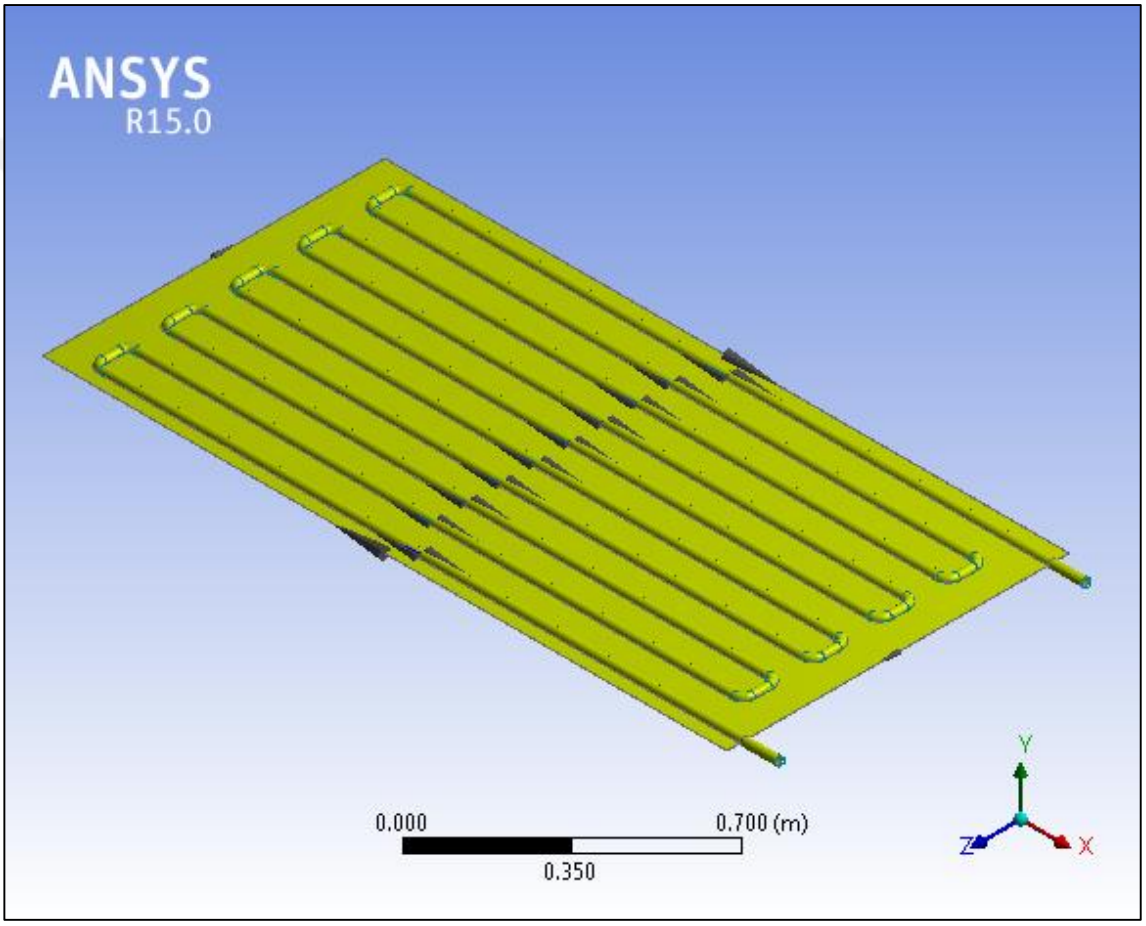

Figure (4.3): Main collector shape drawn in Design Modeler.

Pipe shape is designed to cover all collector surface as possible with the shown design where (0.05) m is left from both sides along the pipe and length of collector and (0.01) m is left from both top and bottom. (0.010) m also is the gap between each two pipes.

Solid volume is measure using ANSYS as (0.0029674) m^3 where pipes can hold (0.0079338) m^3 of water.

Top surface area is measured as 2.249 m^2 which includes flat plate surface area and the area of upper half of pipe which is subjected to solar radiation. Area for the sides of collector is found to be 0.00595 m^2.

4.2.2 Mesh

Model has to be divided into small elements to get solution using finite volume. Dividing the model is done using ANSYS-Mesh as shown in Figure (4.4)

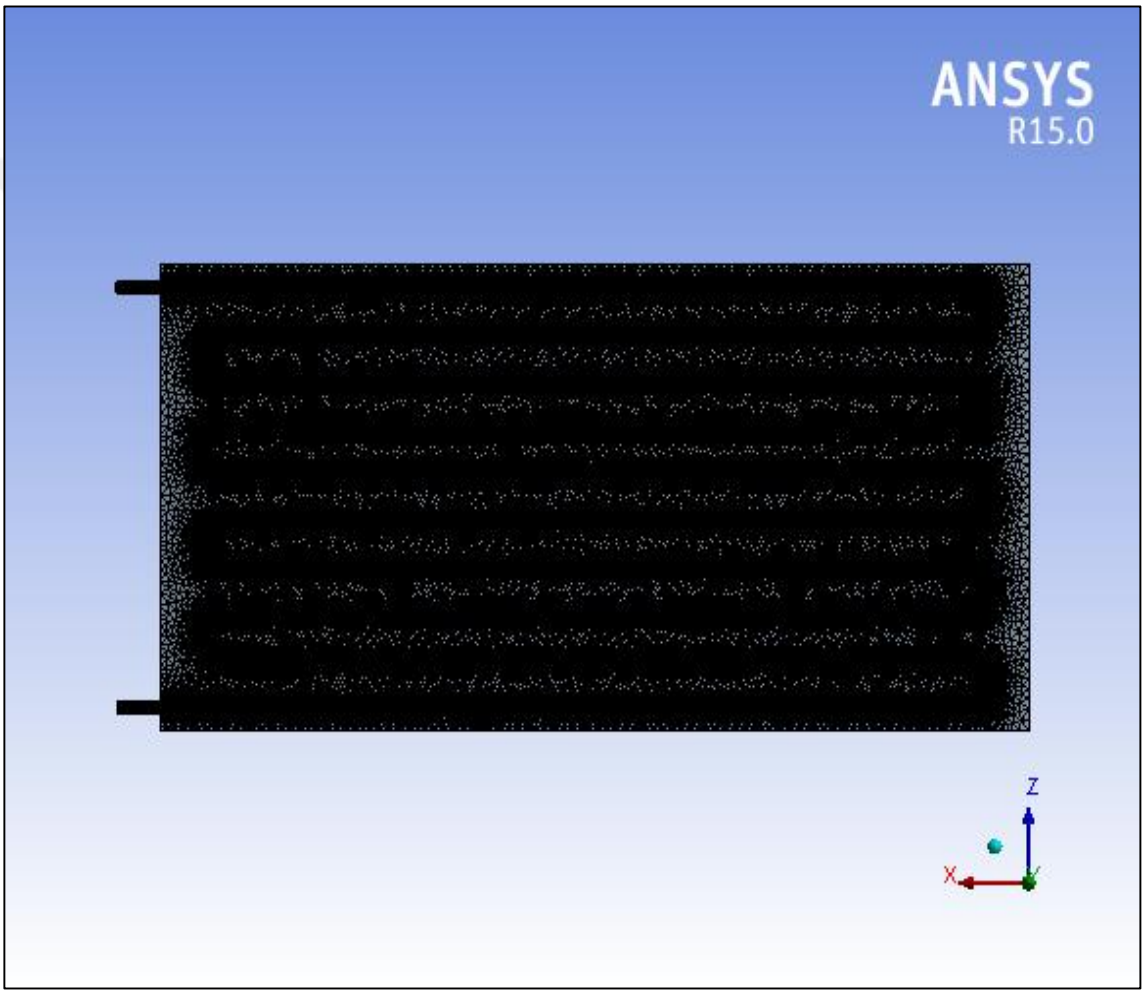

Figure (4.4) Mesh of solar collector.

To get better view, a small part at outlet is zoomed as shown in Figure (4.5).

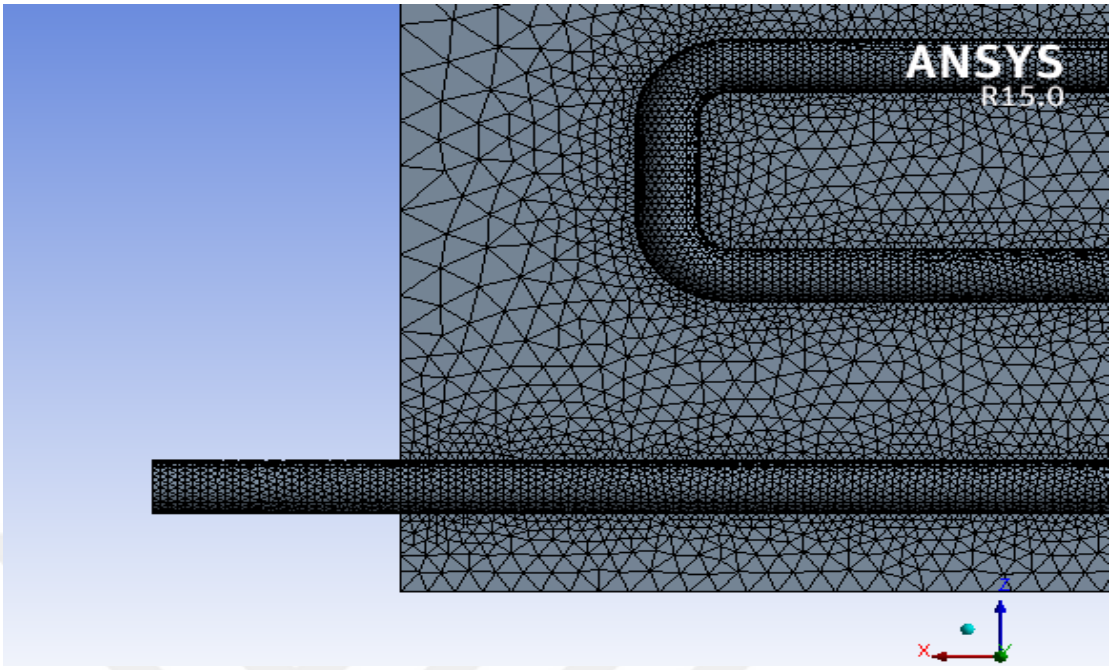

Figure (4.5): Small part of the mesh.

Physics preference of CFD is used in the shown mesh. Statistics show that (656782) nodes in this model and (1284810) elements also. CFD gives the ability of dealing with fluids and heat transfer.

When the number of elements and nodes are 1839679 and 1061743 respectively, the water outlet temperature is kept same value almost that as shown in table below.

Table 4.2: compare between two values of meshing.

Meshing	No. of elements	No. of nodes	Max. temperature (k)
Mesh 1	1284810	656782	313.0
Mesh 2	1839679	1061743	312.9

4.2.3 CFX-Pre

This window is responsible for dealing with all parameters related with materials type, initial conditions, and boundary conditions .etc.

Three materials (Aluminum, Copper, and Steel) are used in these analyses with six-water mass flow rate (0.005, 0.01, 0.015, 0.02, 0.025, and 0.03) kg/s. above conditions are repeated for four months which are (January, February, November, and

December). Outlet temperatures at these months are used as an inlet water temperature and as initial condition for collector plate. Solar radiation is subjected to the upper face of collector with convection for upper, lower, and side surfaces. Losses due to radiation is neglected due to the difficulties of adding it to same upper surface area.

Transient condition are used many time until reach up to the steady state conditions. Total time of one hours is found to be suitable to reach up to the steady state condition for all three types of materials and so it is divided into (12) steps by the mean of (5) minutes for each step.

Engineering date for ANSYS shows the properties for all materials which are saved in ANSYS library.

The following table shows Aluminum, Copper, and Steel properties.

Table 4-3: materials properties in ANSYS library.

material	Density(ρ) (kg/m^3)	Thermal conductivity(K) (W/m. °C)	Specific heat(c_p) (J/kg. °C)	Volumetric specific heat(c_v) (J/m^3. °C)	Total mass of collector(m) (kg)
Aluminum	2689	237.5	951	2557239	7.98
Copper	8933	400	385	3439205	26.51
Steel	7850	60.5	434	3406900	23.29

A general connection type used to connect interfaces between water and solid material to insure fully heat transfer flow without and contact resistance.

4.3 Solving procedure

Three types of material, six water mass flow rates are solved using ANSYS for four months. A solar collector is assumed to be tilted at 35 degree to the south direction for be fully faced for solar rays.

The main difficulty, which face losses calculation in solar collector, is the temperature assumption of collector plate where it is unknown and it has to be found

using trial and error method. This method will lead after many attempts to find approximate temperature for collector plate, which is ununiformed. Trial and error method is led in this project using ANSYS where plate temperature is assumed (it affects directly the value of top loss coefficient ($W/m^2.K$)) which is required in ANSYS for boundary conditions. ANSYS will solve to find plate collector temperature and that will be compared with assumed one and so on until get matched results. Average temperatures for all nodes at collector upper face is calculated by ANSYS to represent plate temperature. Water temperature at outlet, maximum temperature at plate surface, and minimum temperature at plate surface are calculated also using ANSYS.

To validate solutions, the average plate results and water temperature at outlet are compared with the following equations results.

$$Q_u = Q_T - Q_{loss} \quad (4.1)$$

$$Q_T = I \times A_c \quad (4.2)$$

$$Q_u = \dot{m} c_p (T_{wo} - T_{win}) \quad (4.3)$$

$$Q_{loss} = U_t A_t (T_p - T_a) + U_b A_b (T_b - T_a) + U_e A_e (T_e - T_a) \quad (4.4)$$

$$e = \frac{(\text{calculated results} - \text{ANSYS results})}{(\text{calculated resutls})} \times 100\% \quad (4.5)$$

A_e =Area for the sides of collector = (0.00595) m^2.

$A_c = A_t = A_b$ = Area collector is measured as (2.249) m^2

From equation (4.3), water temperature at outlet is found where plate temperature is found from equation (4.4).The total comparison for four months and six different water mass flow rates show average error of 0.29%, 0.4%, and 1.18% for the difference temperature between outlet and inlet results and 0.014%, 0.017%, and 0.045% for water temperature at outlet respectively for Copper, Aluminum, and Steel.

Comparison between calculated results using equations and results using ANSYS validate results due to the values of errors listed in table 4-4.

Table 4-4: Error in temperature calculated using equations and ANSYS.

Mass flow rate kg/s	Month	Copper		Aluminum		Steel	
		Error in ΔT	Error in Tout	Error in ΔT	Error in Tout	Error in ΔT	Error in Tout
0.005	Jan.	0.1230	0.0353	0.4898	0.0286	1.0421	0.0992
	Feb.	0.0717	0.0220	0.4104	0.0538	0.9371	0.0823
	Nov.	0.0693	0.0132	0.4504	0.0279	0.8878	0.0765
	Dec.	0.0874	0.0081	0.4144	0.0129	0.8784	0.0716
0.01	Jan.	0.1984	0.0189	0.2596	0.0189	1.4850	0.0856
	Feb.	0.4303	0.0339	0.5982	0.0337	1.2434	0.0673
	Nov.	0.4992	0.0158	0.5765	0.0163	1.3166	0.0557
	Dec.	0.4236	0.0017	0.4979	0.0012	1.5918	0.0501
0.015	Jan.	0.7770	0.0215	0.6885	0.0215	0.4617	0.0124
	Feb.	0.7665	0.0438	0.4140	0.0227	1.2446	0.0327
	Nov.	0.2236	0.0021	0.4170	0.0021	1.1917	0.0487
	Dec.	0.2541	0.0149	0.3205	0.0136	1.1688	0.0330
0.02	Jan.	0.2198	0.0206	0.4053	0.0206	1.7269	0.0548
	Feb.	0.2967	0.0013	0.3971	0.0035	1.2224	0.0456
	Nov.	0.2665	0.0179	0.3932	0.0179	1.0987	0.0345
	Dec.	0.2283	0.0120	0.0354	0.0143	0.9569	0.0095
0.025	Jan.	0.4213	0.0072	0.6074	0.0415	1.8956	0.0415
	Feb.	0.2663	0.0057	0.3600	0.0036	1.1697	0.0223
	Nov.	0.2216	0.0119	0.3262	0.0108	1.0306	0.0313
	Dec.	0.2307	0.0027	0.2790	0.0014	1.0258	0.0267
0.03	Jan.	0.2064	0.0274	0.3946	0.0274	1.6778	0.0620
	Feb.	0.2702	0.0030	0.3387	0.0010	1.1274	0.0225
	Nov.	0.1890	0.0021	0.2898	0.0009	1.0157	0.0255
	Dec.	0.2053	0.0079	0.3044	0.0069	0.9696	0.0015
Average		0.2894	0.0146	0.4029	0.0168	1.1819	0.0455

4.4 Collector behavior at transient time

In real condition, solar collector never reach to steady state condition due to many continuously changed condition like solar rays intensity, incident angle, wind velocity, environment temperature, ...etc.

Collector has been analyzed at different times, it is noticed that collector reached to steady state condition at about one hours (to reach up to steady state conditions, all effected factors are assumed stable), and Figures (4.6) show temperature distribution at collector surface.

At initial conditions, collector material and water at inlet are at same temperature as the ambient conditions.

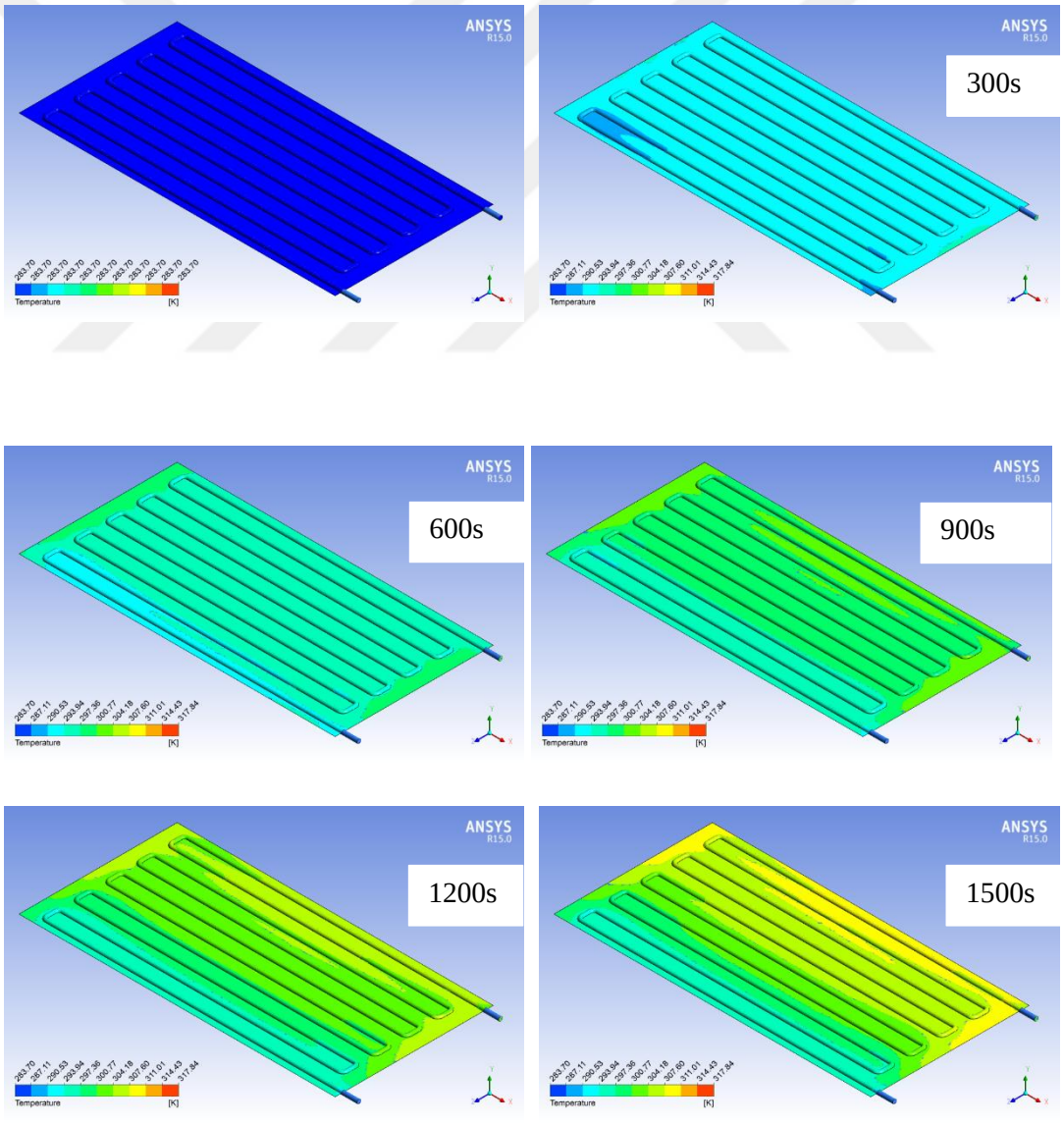

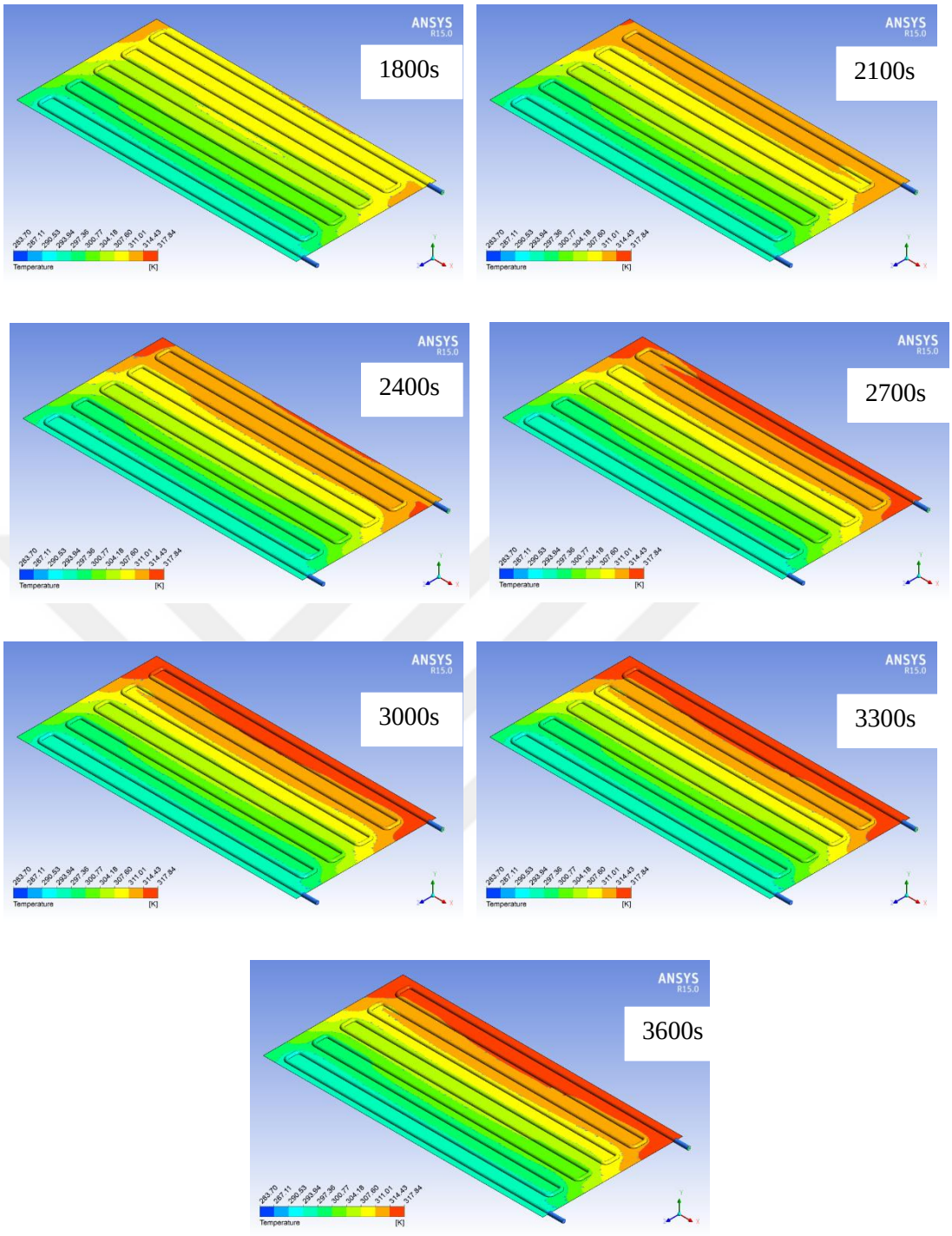

Figures (4.6): Global temperature distributions for a Copper collector where water mass flow rate is 0.005 kg/s at January.

The behavior of temperature distribution in figures above show that the side of water inlet kept at low temperature and the hottest area at the side of water outlet. More heat is concentrated at corners where the far area from water flow and at the top or bottom of collector. The general behavior for Aluminum and Steel collector is same with small different due to materials features.

Figures 4.7, 4.8, and 4.9 show temperature distribution on collector surface for copper, aluminum, and steel after one hour where water mass flow is 0.01, 0.02, and 0.03 kg/s to compare material behavior.

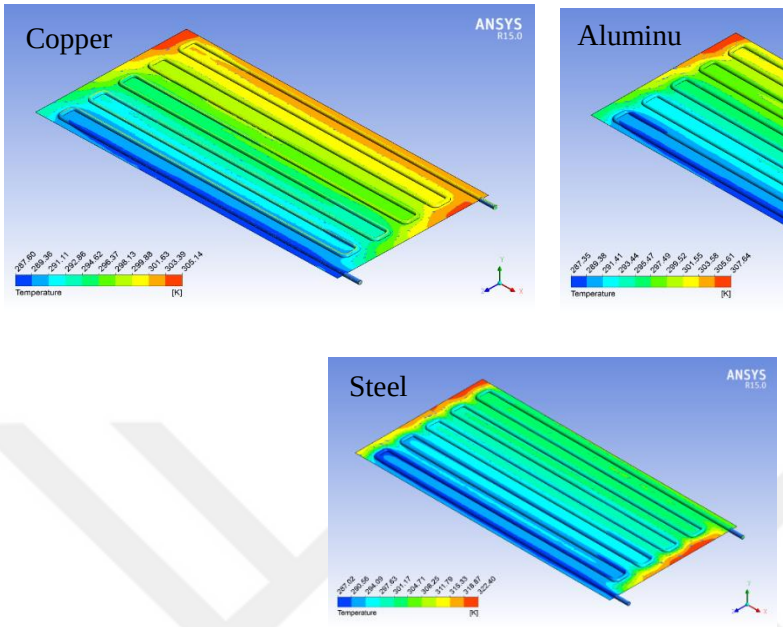

Figure (4.7): Temperature distribution on collector surface where water mass flow rate is 0.01 kg/s.

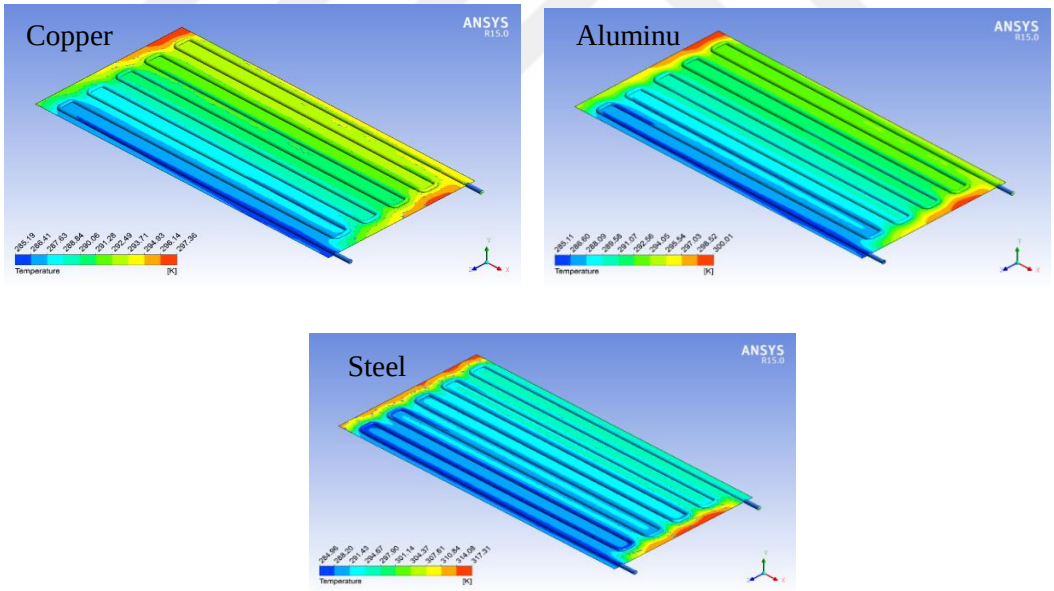

Figure (4.8): Temperature distribution on collector surface where water mass flow rate is 0.02 kg/s.

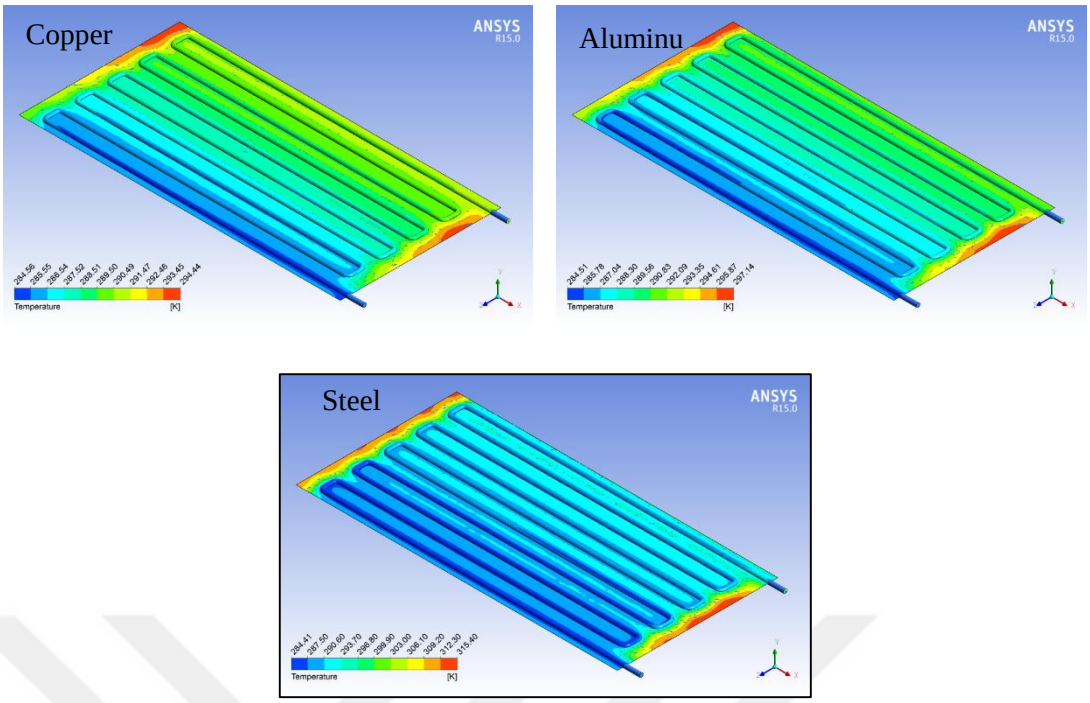

Figure (4.9) Temperature distribution on collector surface where water mass flow rate is 0.03 kg/s.

Due to thermal conductivity difference for the three materials, the less thermal conductivity needs more time to transfer heat from material to water and so will have highest maximum temperature as shown in figures below.

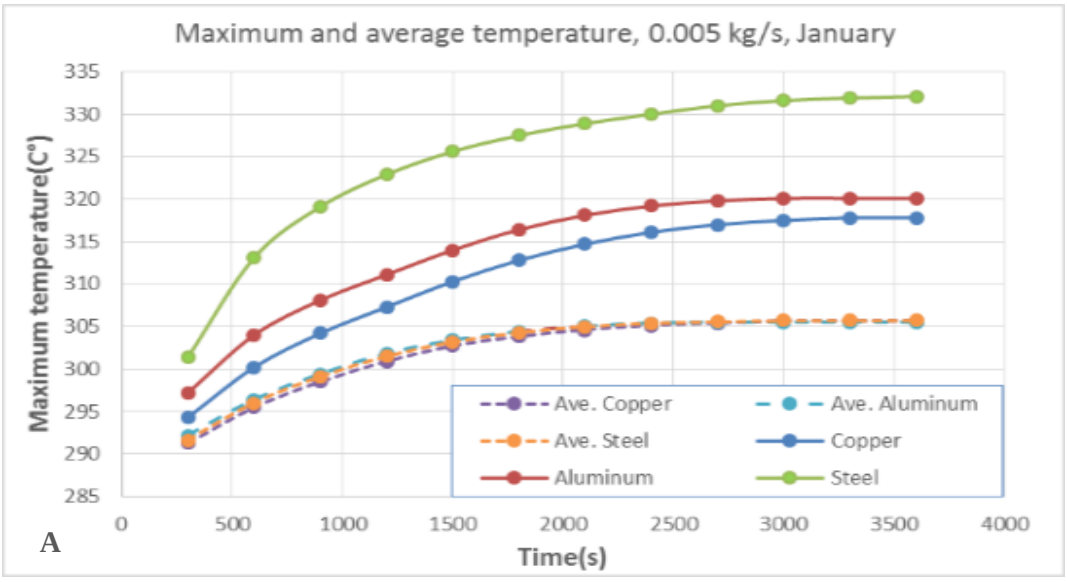

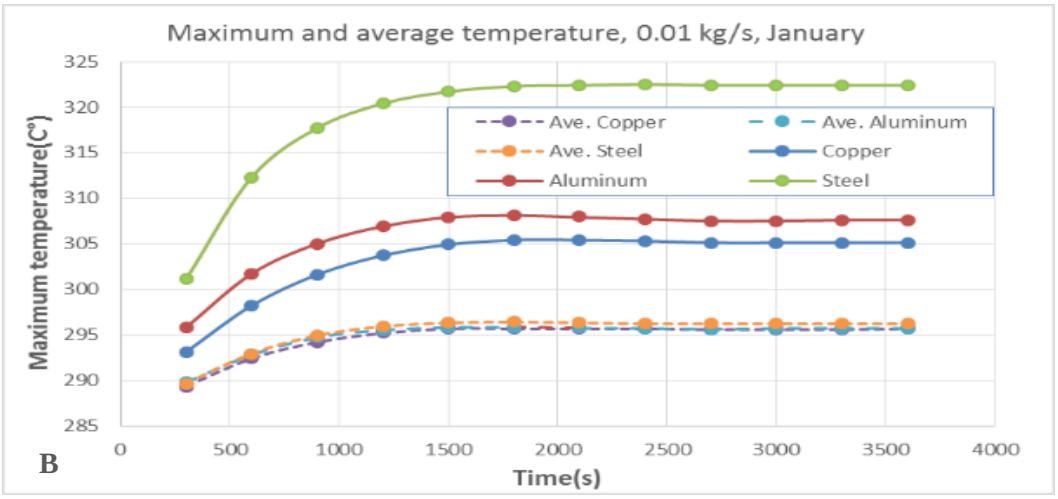
Maximum and average temperature, 0.01 kg/s, January
Maximum temperature(C°)
Time(s)
Ave. Copper
Ave. Aluminum
Ave. Steel
Copper
Aluminum
Steel

B

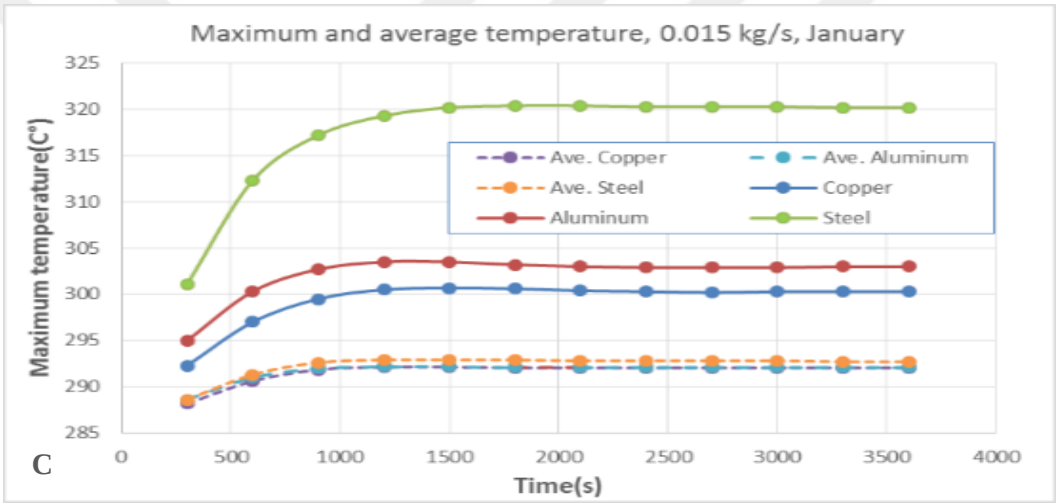
Maximum and average temperature, 0.015 kg/s, January
Maximum temperature(C°)
Time(s)
Ave. Copper
Ave. Aluminum
Ave. Steel
Copper
Aluminum
Steel

C

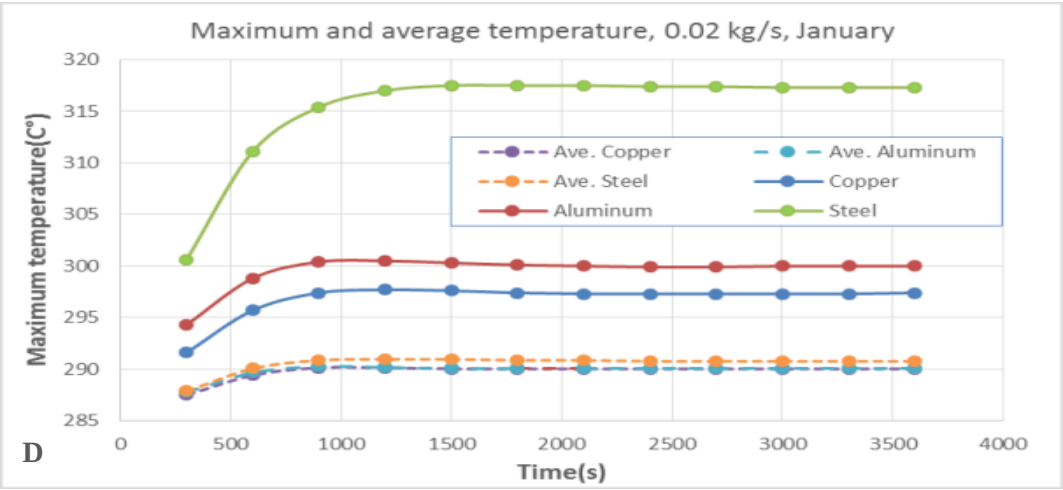
Maximum and average temperature, 0.02 kg/s, January
Maximum temperature(C°)
Time(s)
Ave. Copper
Ave. Aluminum
Ave. Steel
Copper
Aluminum
Steel

D

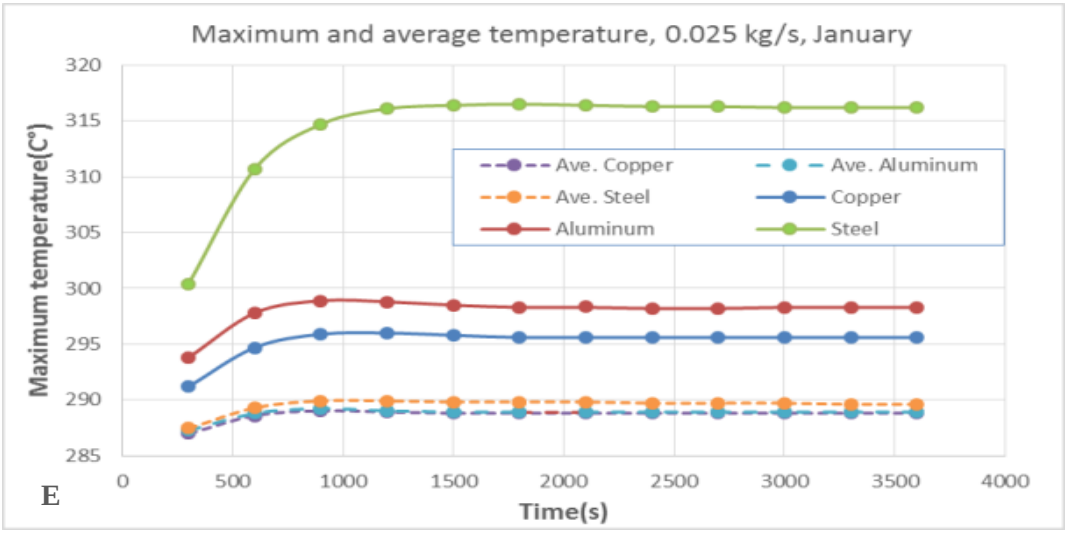

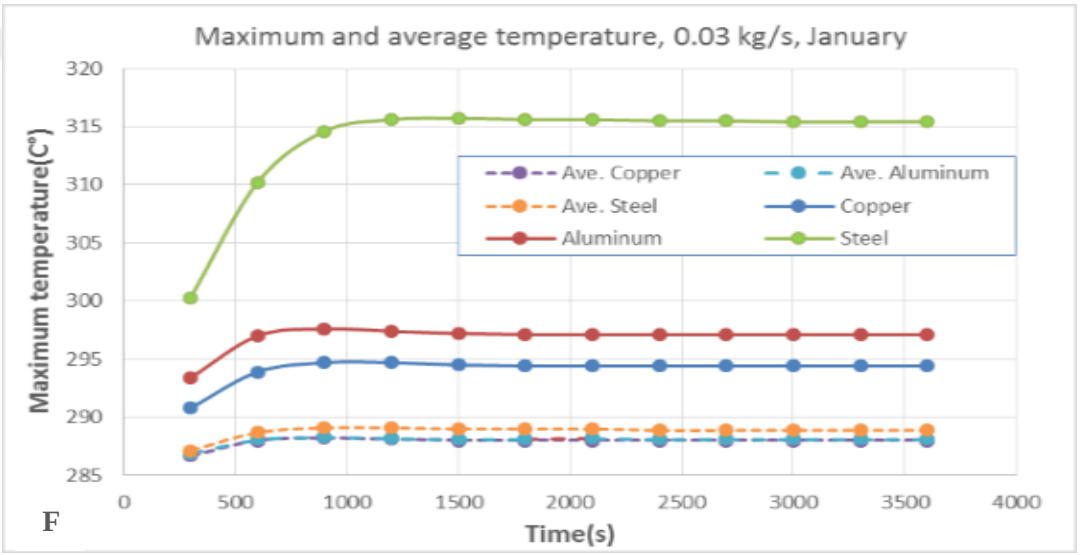

Figure (4.10 A-F): Maximum and average temperature for different materials in January. (The behavior is same for other months).

Tables below list maximum and average temperature at collector surface for different materials using different water mass flow rate at time of 3600 (s) which may represent steady state conditions.

Table 4-5 Maximum temperature at collector surface for different materials and different water mass flow rate.

mass flow rate (kg/s)			0.005	0.01	0.015	0.02	0.025	0.03
Material	month	Time (s)	$T_{p\max}$ (K)					
Copper	Jan.	3600	317.8	305.1	300.3	297.4	295.6	294.4
	Feb.	3600	324	310.4	305	302.1	300.2	298.9
	Nov.	3600	320.3	308.7	304.1	301.5	300	298.9
	Dec.	3600	307.6	298.6	295	293.1	291.9	291
Aluminum	Jan.	3600	320.1	307.6	303	300	298.3	297.1
	Feb.	3600	326.4	313.1	307.8	304.9	303.1	301.8
	Nov.	3600	322.4	311	306.5	304	302.4	301.3
	Dec.	3600	309.2	300.4	296.9	294.9	293.8	292.9
Steel	Jan.	3600	332.1	322.4	320.2	317.3	316.2	315.4
	Feb.	3600	339.1	328.9	325.3	323.3	322.1	321.2
	Nov.	3600	333.4	324.5	321.4	319.8	318.8	318.1
	Dec.	3600	317.9	310.7	308.4	307.2	306.3	305.7

Table 4-6: average temperature at collector surface for different materials and different water mass flow rate.

mass flow rate (kg/s)			0.005	0.01	0.015	0.02	0.025	0.03
Material	month	Time (s)	T_{pavr} (K)					
Copper	Jan.	3600	305.6	295.7	292	290	288.8	288
	Feb.	3600	310.9	300.3	296.3	294.2	292.9	292.1
	Nov.	3600	309.2	300	296.6	294.8	293.7	293
	Dec.	3600	299	291.9	289.3	287.9	287.1	286.6
Aluminum	Jan.	3600	305.5	295.7	292.1	290.1	288.9	288.1
	Feb.	3600	310.8	300.3	296.3	294.3	293	292.2
	Nov.	3600	309	300	296.6	294.9	293.8	293.1
	Dec.	3600	298.9	291.9	289.3	288	287.2	286.6
Steel	Jan.	3600	305.7	296.2	292.7	290.8	289.6	288.9
	Feb.	3600	311	300.9	297	295	293.8	293
	Nov.	3600	309.2	300.5	297.2	295.5	294.5	293.8
	Dec.	3600	299	292.3	289.8	288.5	287.7	287.2

Figure (4.10 A-F) and table 4-4 show that highest maximum temperature at steel collector while the lowest one is for copper. The main reason for these results is that

thermal conductivity for each material helps to spread heat from any part of collector toward water moving inside pipes. The highest value of thermal conductivity spreads heat better while the less one need more the transfer heat from far parts toward water. Figure (4.10 A-F) and table 4-5 show that average temperature at collector surface are too close for copper and aluminum while steel is higher.

The main target from solar collector is to increase water temperature. In solar heaters, if it is found that one collector is not enough to rise water temperature to the target, two or more collectors can be fixed as parallel or series. Figures below show the temperature distribution for water at outlet pipe of collector. Wherever T_{out} is used, it means average of water temperature at outlet.

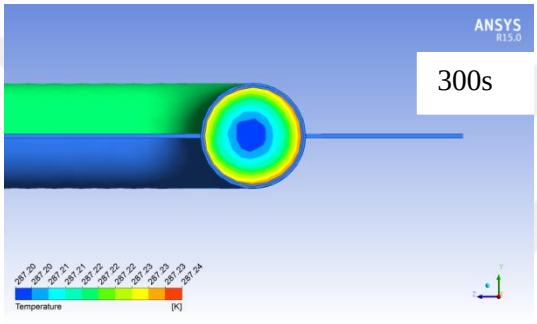

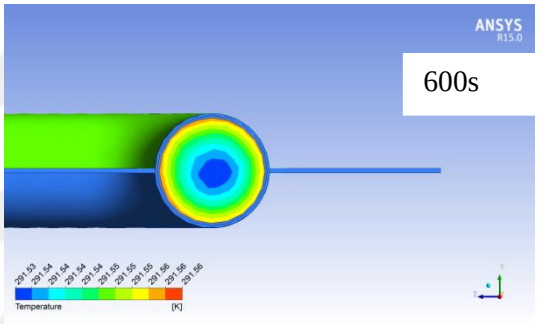

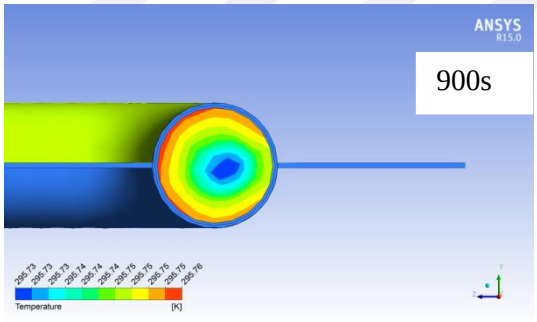

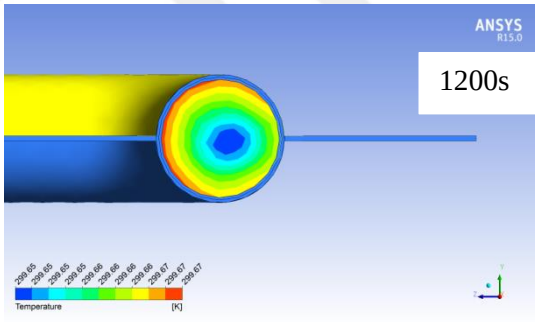

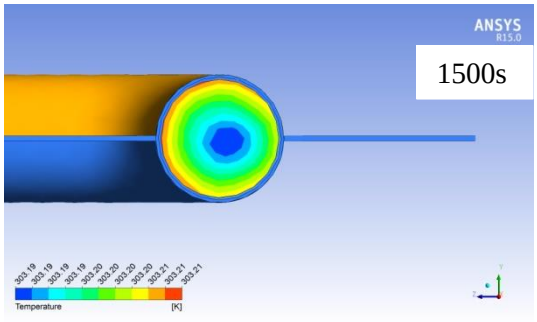

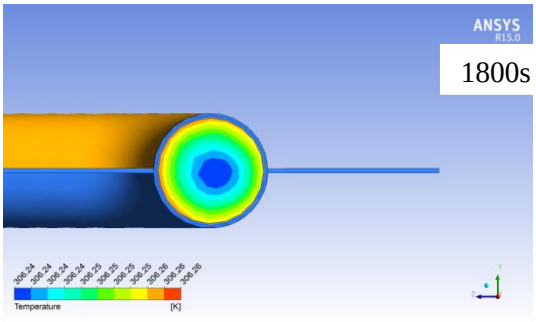

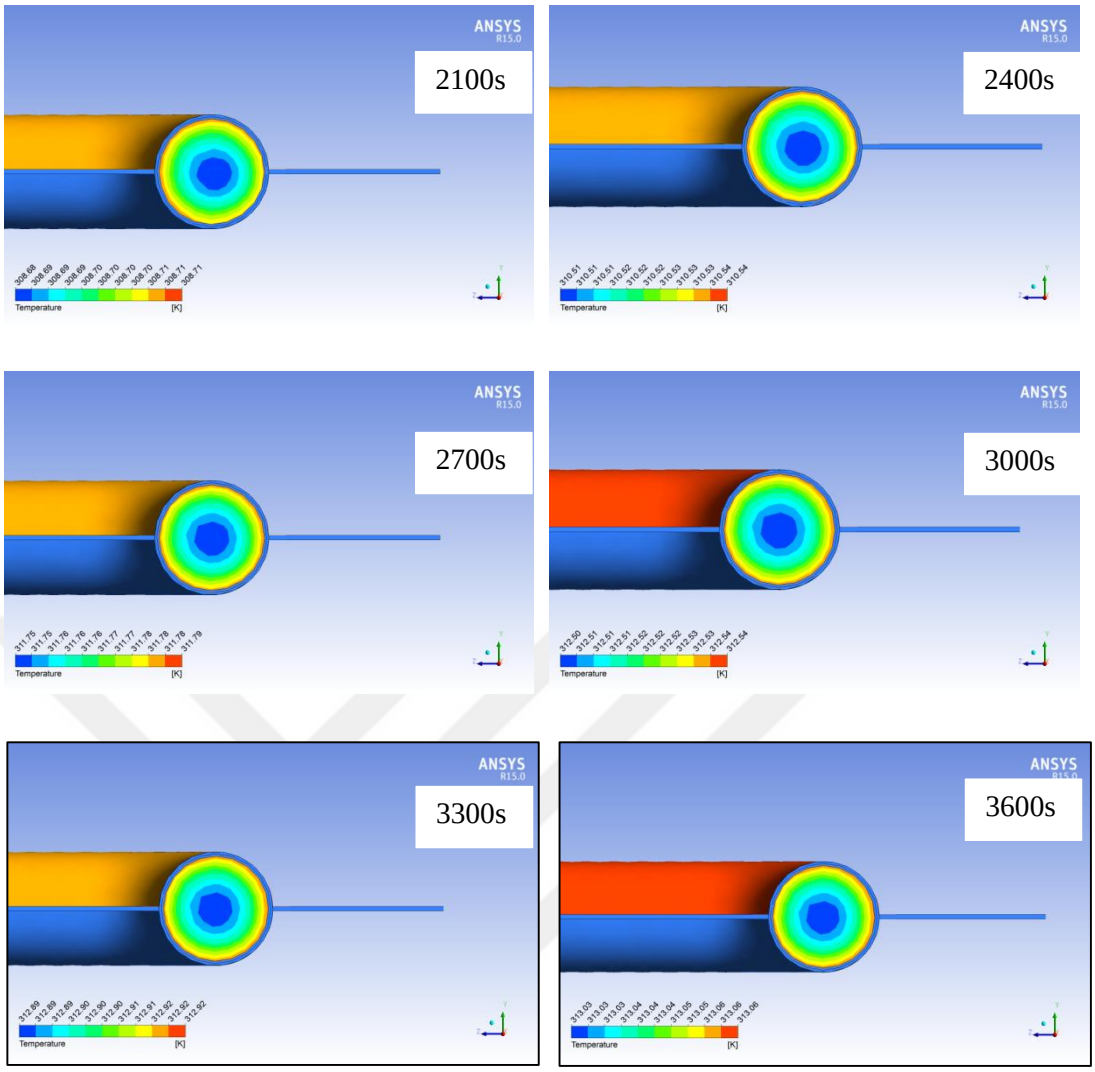

Figure (4.11) Behavior of temperature distribution at water outlet at different time where water mass flow rate is 0.005 kg/s at January using copper collector.

Above figures, show that heat is concentrated at boundaries of pipes near hot material where coldest part of water at center.

Effect of material properties expanded to the temperature distribution at cross section of water at outlet as shown in figures below which compare temperature distribution at water outlet for aluminum and steel materials.

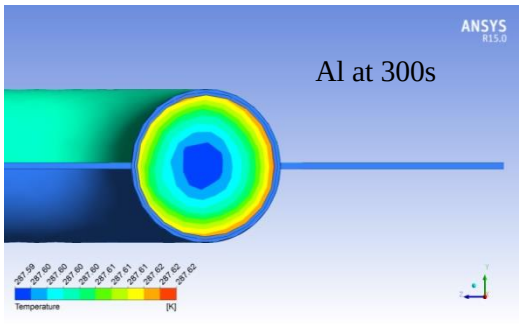
ANSYS
R15.0
Al at 300s
Temperature
[K]

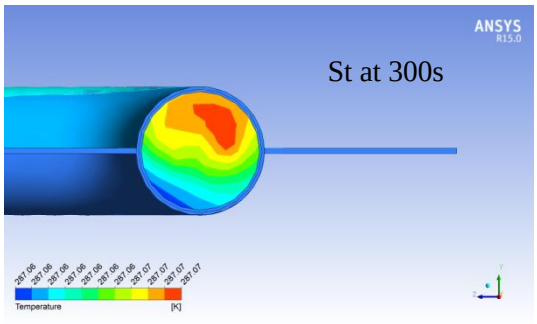
ANSYS
R15.0
St at 300s
Temperature
[K]

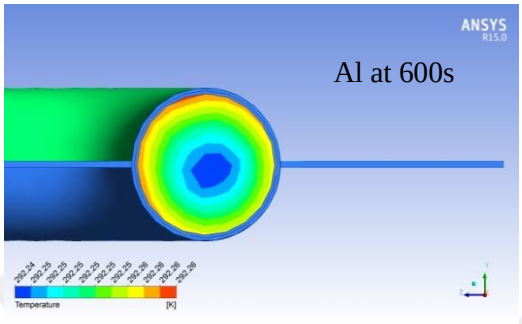
ANSYS
R15.0
Al at 600s
Temperature
[K]

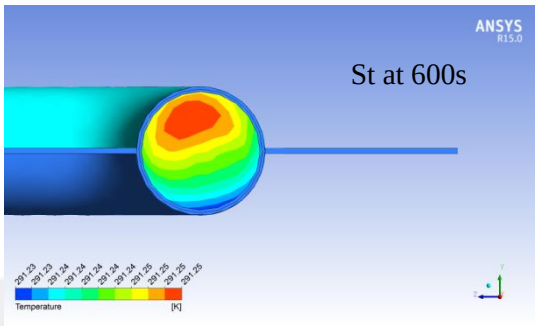
ANSYS
R15.0
St at 600s
Temperature
[K]

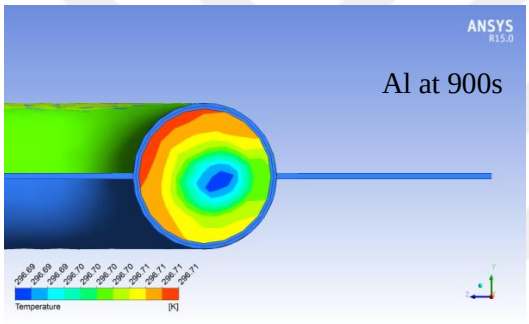
ANSYS
R15.0
Al at 900s
Temperature
[K]

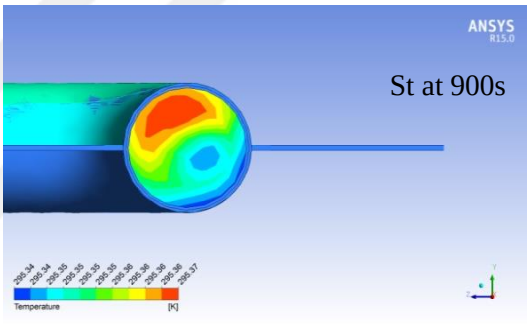
ANSYS
R15.0
St at 900s
Temperature
[K]

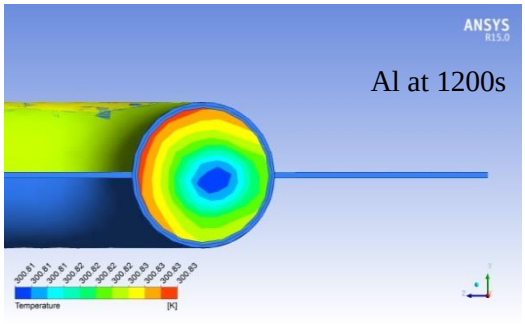
ANSYS
R15.0
Al at 1200s
Temperature
[K]

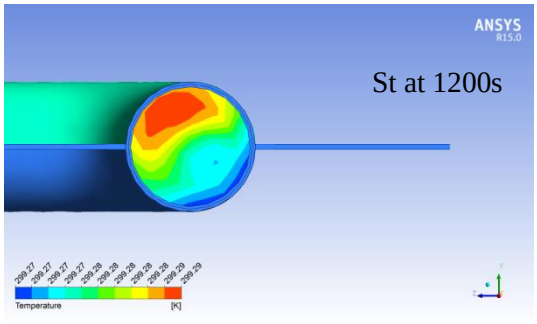
ANSYS
R15.0
St at 1200s
Temperature
[K]

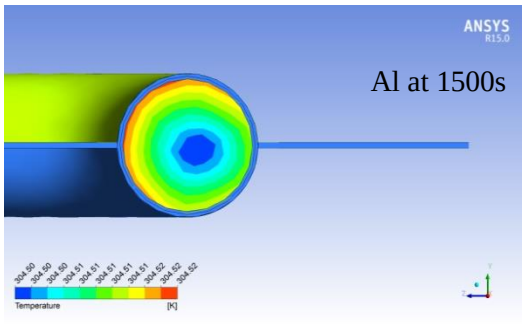
ANSYS
R15.0
Al at 1500s
Temperature
[K]

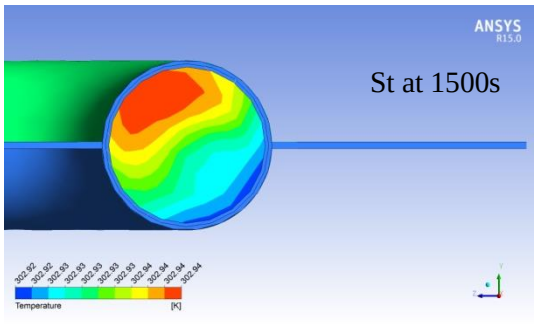
ANSYS
R15.0
St at 1500s
Temperature
[K]

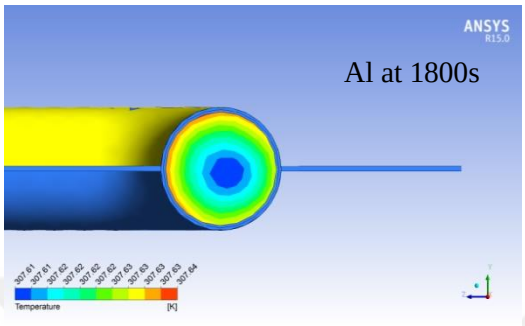
ANSYS
R15.0
Al at 1800s
Temperature
[K]

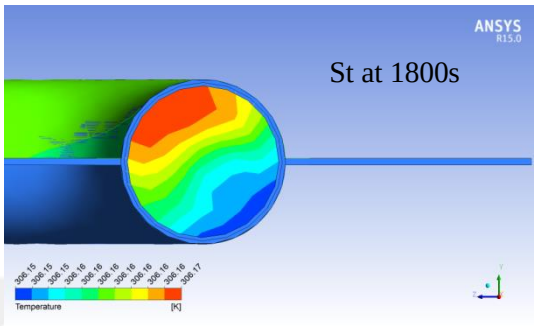
ANSYS
R15.0
St at 1800s
Temperature
[K]

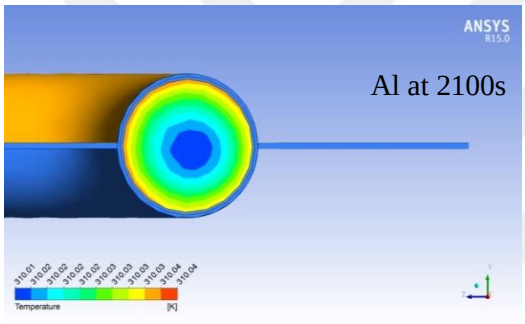
ANSYS
R15.0
Al at 2100s
Temperature
[K]

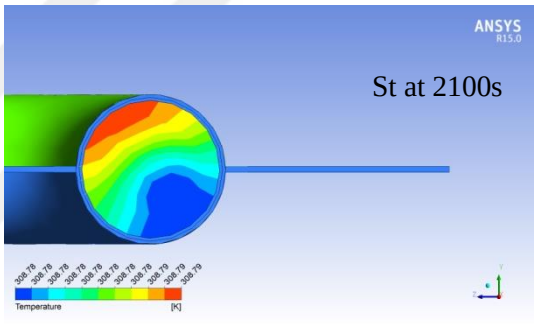
ANSYS
R15.0
St at 2100s
Temperature
[K]

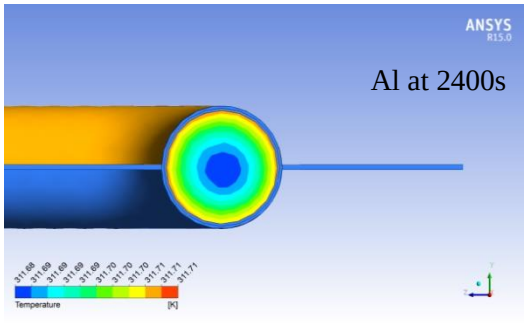
ANSYS
R15.0
Al at 2400s
Temperature
[K]

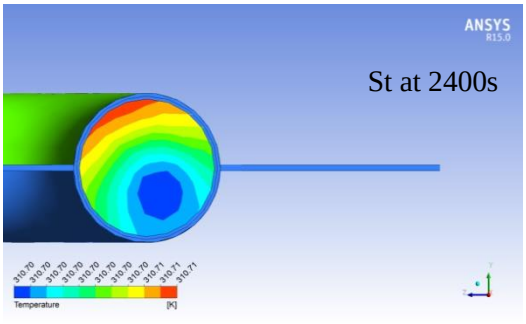
ANSYS
R15.0
St at 2400s
Temperature
[K]

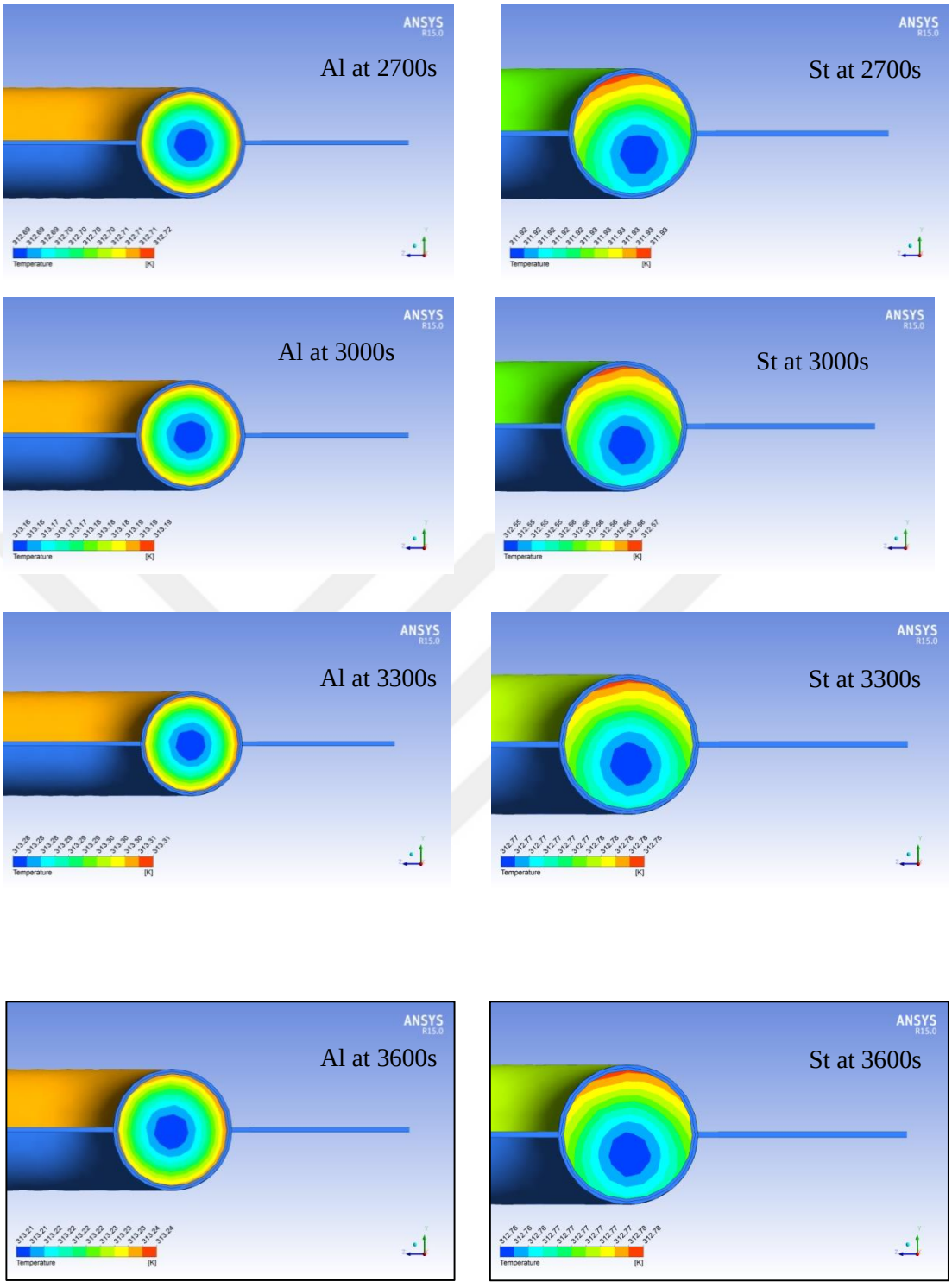

Figure (4.12): Behavior of temperature distribution at water outlet at different time where water mass flow rate is 0.005 kg/s at January using aluminum and steel collector.

Because of the low thermal conductivity for steel, it is clear that heat is transfer to water from one side where solar radiation is subjected while high thermal conductivity for copper and aluminum transfer heat to all sides and so cold water is concentrated at center of pipe.

Efficiency of collector can be found as:

$$\eta = \frac{Q_T}{Q_u} \tag{4.6}$$

Where

$$Q_u = \dot{m} c_p (T_{wo} - T_{win}) \tag{4.7}$$

$$Q_T = I \times A_c \tag{4.8}$$

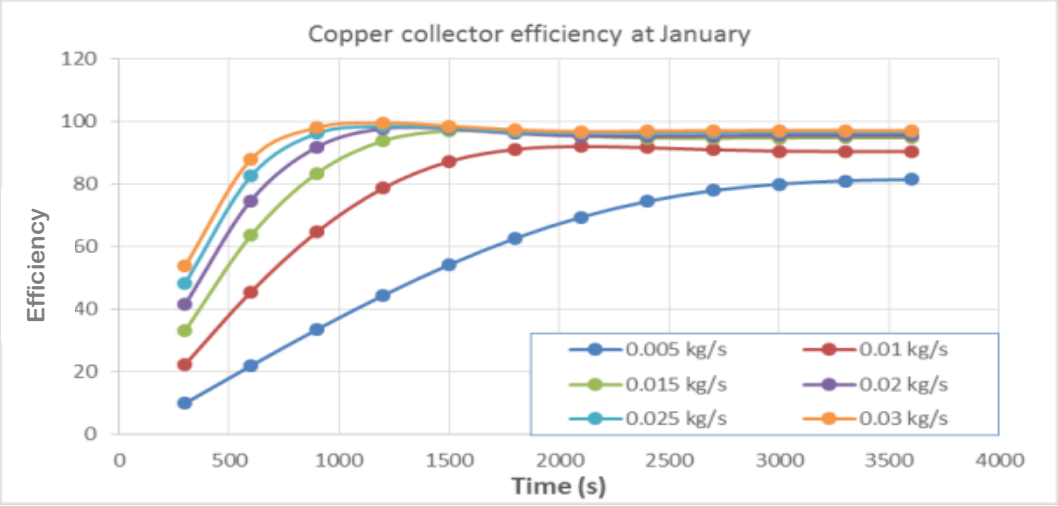

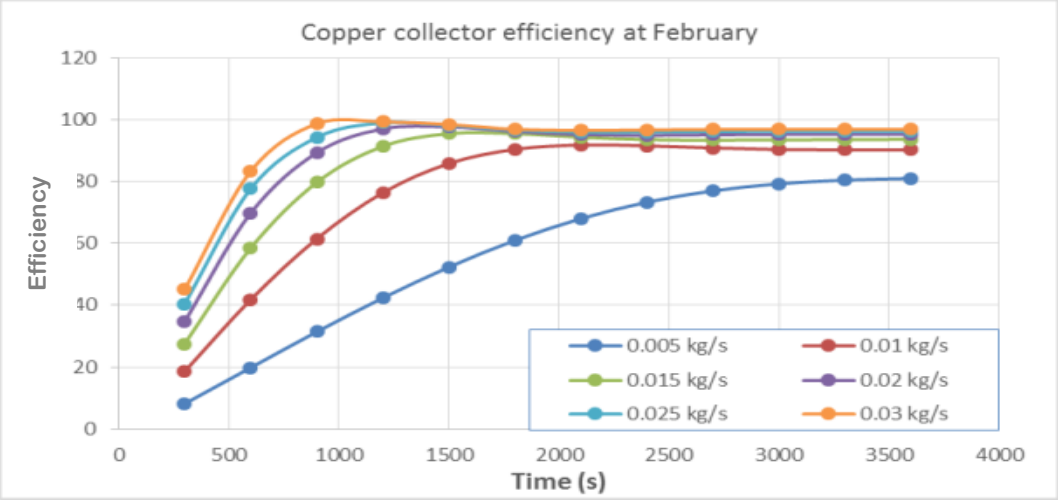

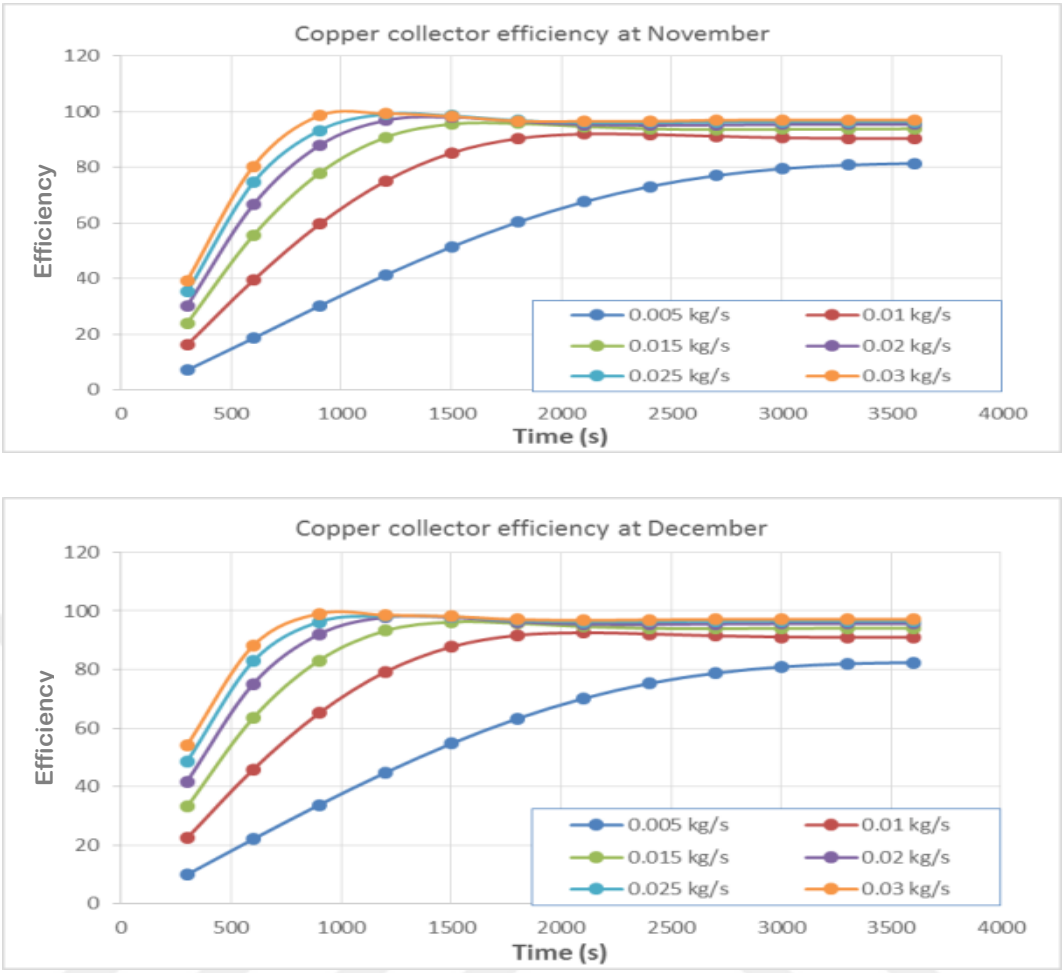

Figure (4.13): Copper collector efficiency at transient time.

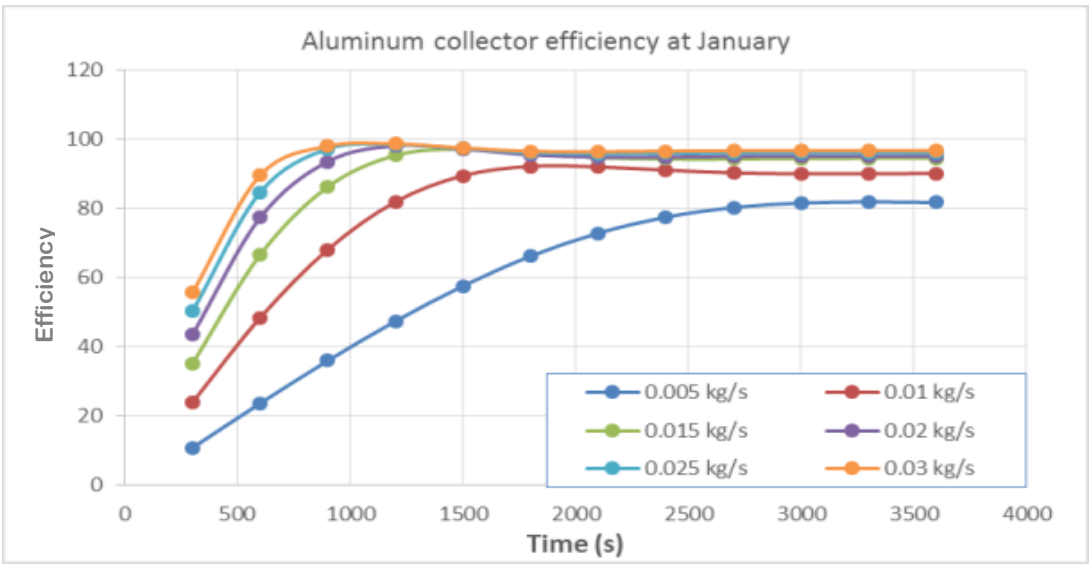

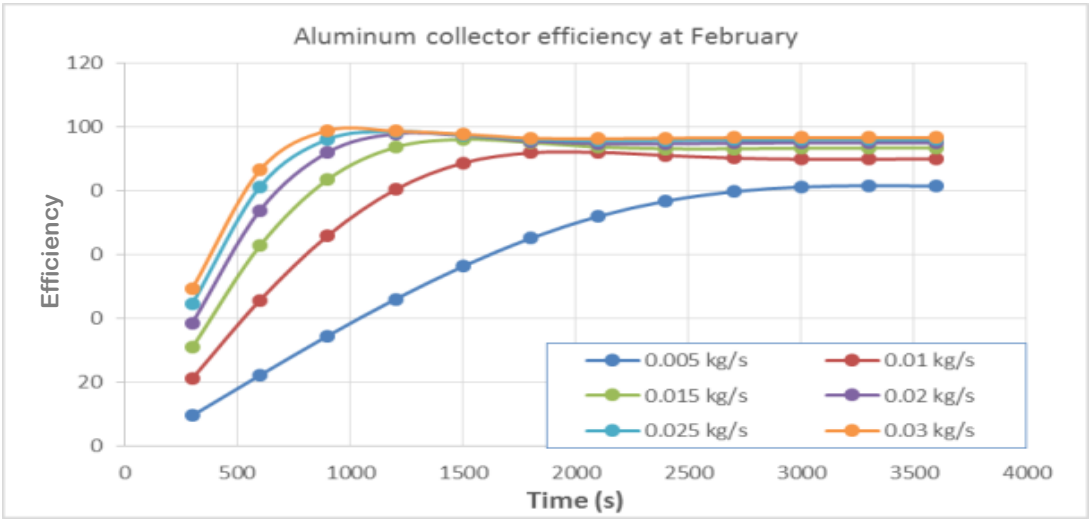

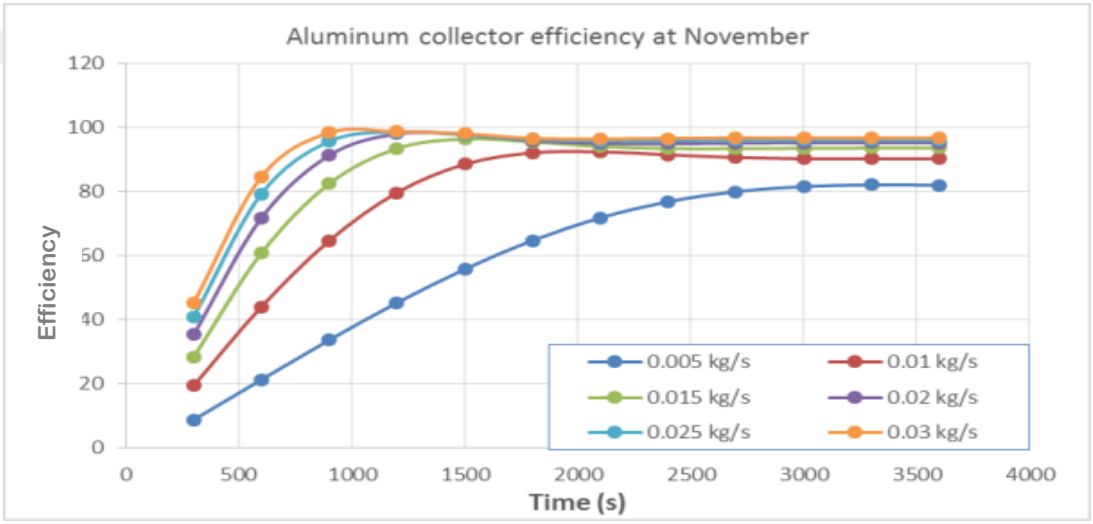

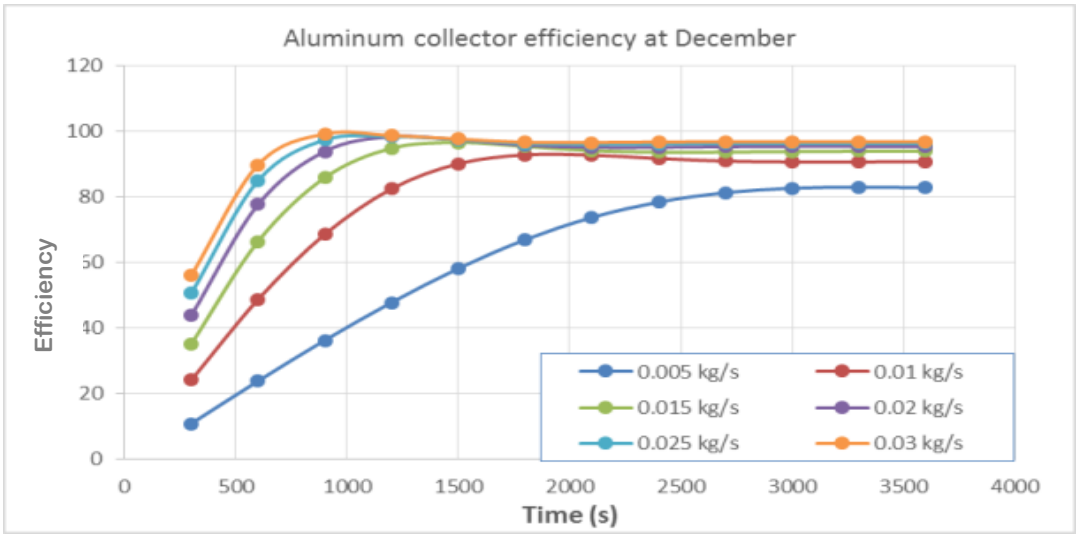

Figure (4.14): Aluminum collector efficiency at transient time.

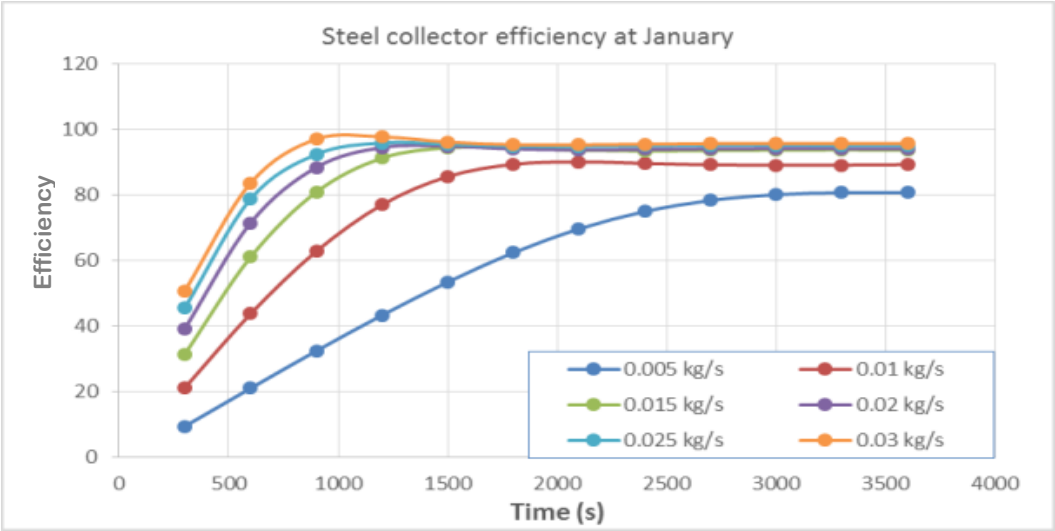
Steel collector efficiency at January
Efficiency
Time (s)
0.005 kg/s
0.01 kg/s
0.015 kg/s
0.02 kg/s
0.025 kg/s
0.03 kg/s

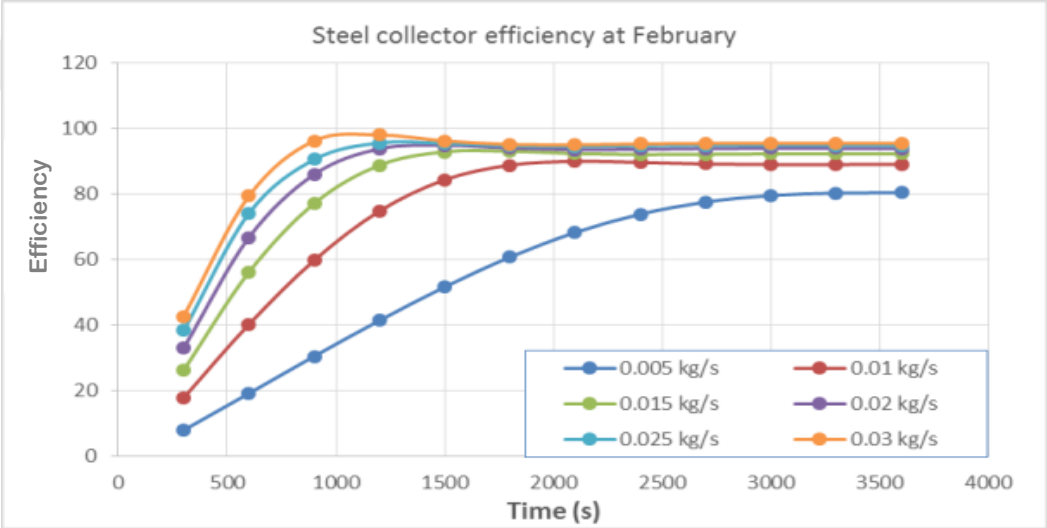
Steel collector efficiency at February
Efficiency
Time (s)
0.005 kg/s
0.01 kg/s
0.015 kg/s
0.02 kg/s
0.025 kg/s
0.03 kg/s

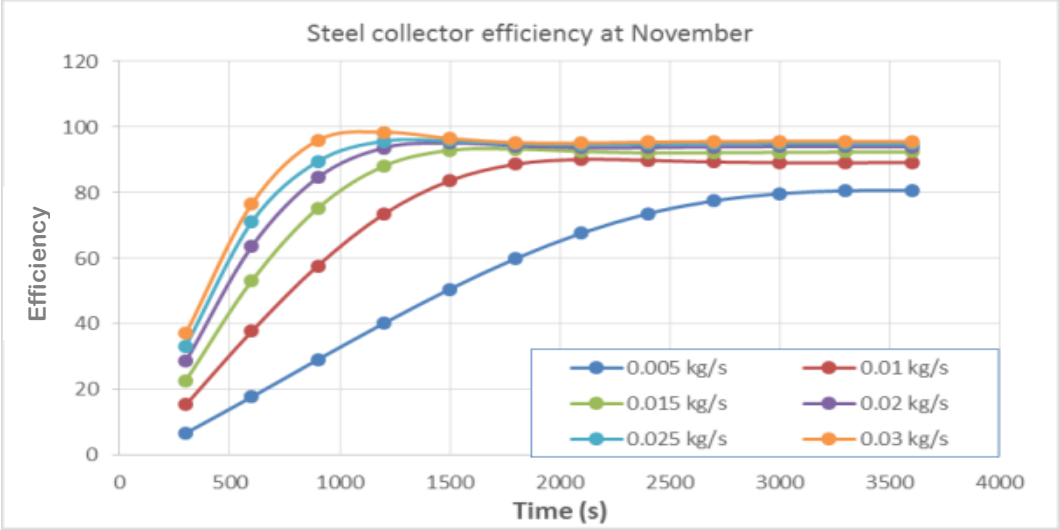
Steel collector efficiency at November
Efficiency
Time (s)
0.005 kg/s
0.01 kg/s
0.015 kg/s
0.02 kg/s
0.025 kg/s
0.03 kg/s

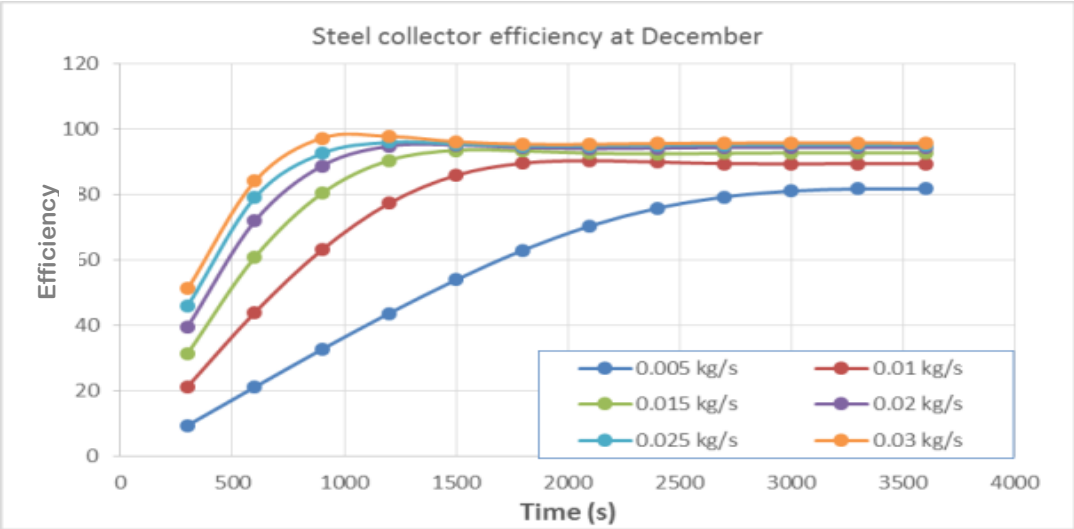

Figure (4.15): Steel collector efficiency at transient time.

Better idea can be got by taking average for each set of efficiencies (the average is taken for six different water mass flow rates) due to time as listed in tables for each material.

Table 4-7: Average efficiency for six water mass flow rates using copper collector.

Average efficiency for six water mass flow rates using copper collector				
Time	Jan.	Feb.	Nov.	Dec.
300	34.6%	29.1%	25.4%	35.0%
600	62.6%	58.5%	55.8%	62.9%
900	77.8%	75.8%	74.6%	78.2%
1200	85.3%	84.2%	83.7%	85.3%
1500	88.7%	88.0%	87.9%	88.8%
1800	90.0%	89.4%	89.4%	90.1%
2100	90.8%	90.3%	90.4%	91.0%
2400	91.4%	91.0%	91.1%	91.7%
2700	92.0%	91.5%	91.7%	92.2%
3000	92.3%	91.9%	92.1%	92.6%
3300	92.5%	92.1%	92.3%	92.8%
3600	92.5%	92.2%	92.4%	92.8%

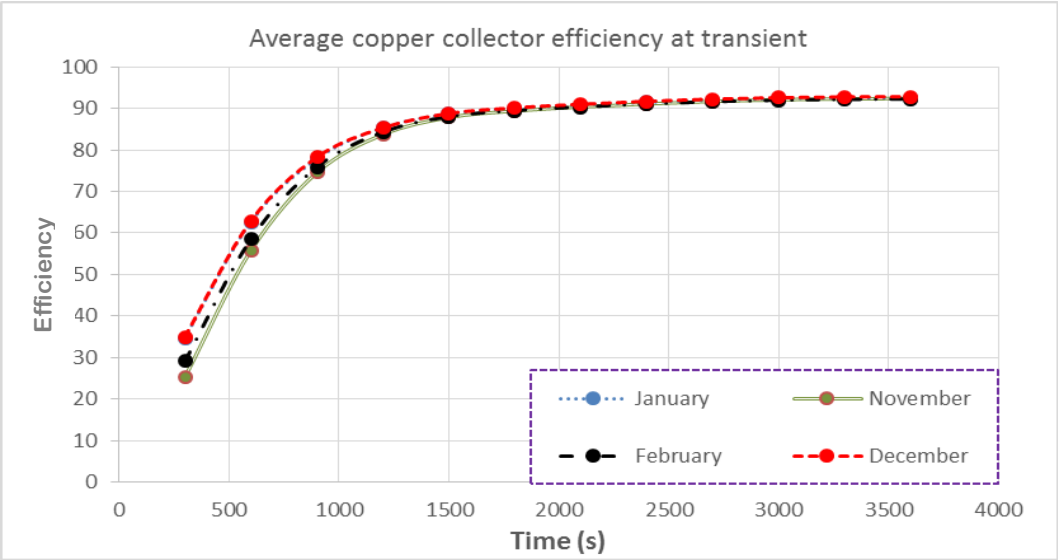

Figure (4.16): Average efficiency for six water mass flow rates using copper collector.

Table 4-7 and figure 4.16 clears that copper collector efficiency increasing with time until reaching up to steady state condition.

Same behavior proved by tables 4-8 and 4-9 which are drawn in figures 4.17 and 4.18 for aluminum and steel collectors respectively.

Table 4-8: Average efficiency for six water mass flow rates using aluminum collector.

Average efficiency for six water mass flow rates using aluminum collector				
Time	Jan.	Feb.	Nov.	Dec.
300	36.6%	32.4%	29.6%	36.8%
600	65.1%	62.1%	60.3%	65.3%
900	79.9%	78.5%	77.7%	80.3%
1200	86.7%	85.9%	85.7%	86.9%
1500	89.5%	89.0%	89.1%	89.7%
1800	90.5%	90.1%	90.3%	90.8%
2100	91.2%	90.8%	91.0%	91.5%
2400	91.8%	91.4%	91.6%	92.1%
2700	92.2%	91.8%	92.1%	92.5%
3000	92.5%	92.1%	92.3%	92.8%
3300	92.5%	92.2%	92.4%	92.8%
3600	92.5%	92.1%	92.4%	92.8%

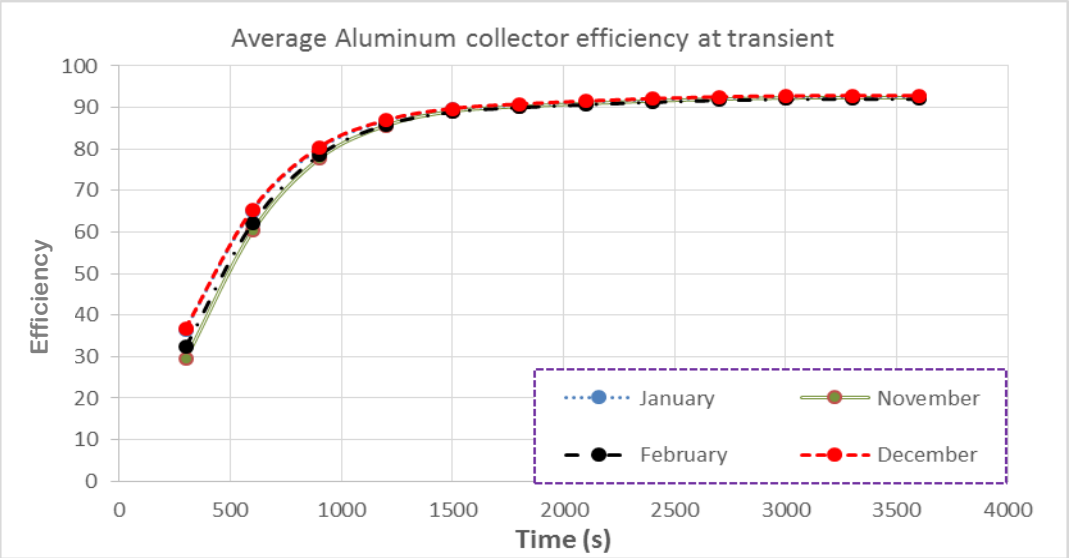

Figure (4.17): Average efficiency for six water mass flow rates using aluminum collector.

Table 4-9: Average efficiency for six water mass flow rates using steel collector.

Average efficiency for six water mass flow rate using steel collector				
Time	Jan.	Feb.	Nov.	Dec.
300	32.8%	27.6%	24.0%	33.2%
600	59.9%	55.8%	53.4%	60.2%
900	75.5%	73.2%	72.1%	75.8%
1200	83.2%	81.9%	81.6%	83.3%
1500	86.5%	85.8%	85.8%	86.7%
1800	88.3%	87.6%	87.7%	88.4%
2100	89.4%	88.8%	89.0%	89.6%
2400	90.3%	89.7%	89.9%	90.5%
2700	90.9%	90.4%	90.6%	91.1%
3000	91.2%	90.7%	91.0%	91.5%
3300	91.3%	90.8%	91.2%	91.6%
3600	91.3%	90.9%	91.2%	91.5%

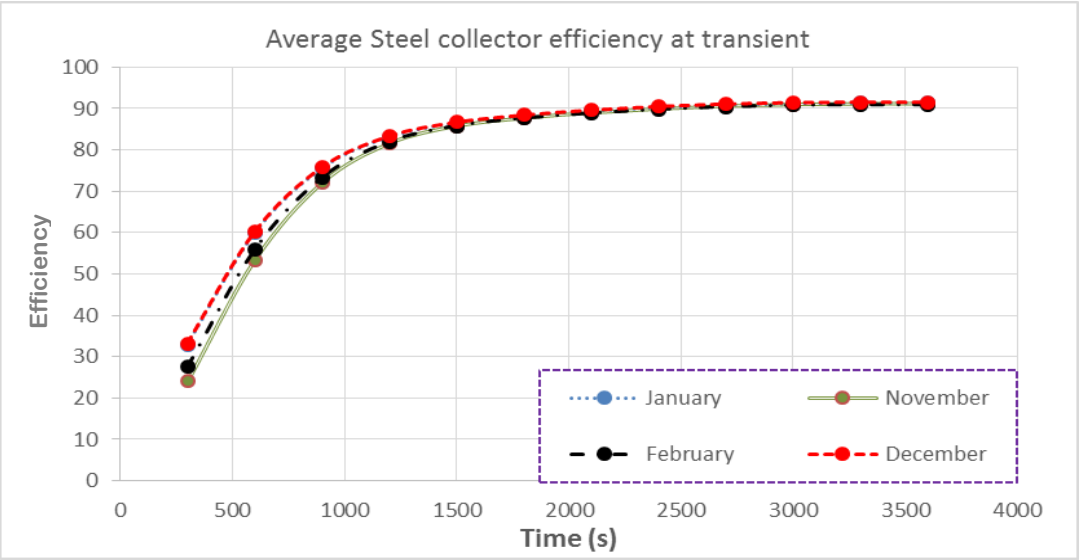

Figure (4.18): Average efficiency for six water mass flow rates using steel collector.

Comparison between aluminum due to copper and steel efficiency is listed in table 4-10 and cleared that aluminum collector has better efficiency than copper at transient time only while it is better than steel collector at transient time and at steady state conditions. Aluminum has the less volumetric specific heat (table 4-3) so accumulated heat in material is less than other materials while less thermal conductivity for steel keeps its efficiency less always.

Table 4-10: Efficiency difference between different materials at transient time.

Time (s)	Efficiency difference between aluminum and copper				Efficiency difference between aluminum and steel			
	Jan.	Feb.	Nov.	Dec.	Jan.	Feb.	Nov.	Dec.
300	2.0%	3.3%	4.3%	1.9%	3.7%	4.8%	5.6%	3.7%
600	2.5%	3.6%	4.5%	2.5%	5.2%	6.3%	6.9%	5.2%
900	2.1%	2.7%	3.2%	2.1%	4.4%	5.3%	5.7%	4.6%
1200	1.4%	1.7%	1.9%	1.6%	3.6%	4.0%	4.1%	3.6%
1500	0.8%	1.0%	1.3%	0.9%	2.9%	3.2%	3.3%	3.0%
1800	0.6%	0.7%	0.8%	0.7%	2.3%	2.5%	2.5%	2.3%
2100	0.5%	0.5%	0.6%	0.5%	1.8%	2.0%	2.0%	1.9%
2400	0.4%	0.4%	0.5%	0.4%	1.5%	1.7%	1.7%	1.6%
2700	0.2%	0.3%	0.4%	0.3%	1.3%	1.5%	1.5%	1.4%
3000	0.2%	0.2%	0.2%	0.2%	1.2%	1.3%	1.3%	1.3%
3300	0.0%	0.1%	0.1%	0.1%	1.2%	1.3%	1.3%	1.3%
3600	0.0%	0.0%	0.0%	0.0%	1.2%	1.3%	1.2%	1.3%

Tables 4-7, 4-8, and 4-9 listed efficiencies for copper, aluminum, and steel solar collectors. It is clear that these efficiencies are higher than real ranges; the reason is while results are calculated due to computer simulation and all losses due to radiation or frame fitting are neglected. Losses due to convection are the only losses, which are calculated in the simulation so efficiency of collector may be so high comparing with real situation.

Tables 4-7, 4-8, 4-9, and table 4-10 show that aluminum has a higher efficiency at transient time while steel has the less efficiency.

The less efficiency, the higher heat losses. Steel and aluminum collectors have higher average temperature at surface of collector as shown in Figures (4.10 A-F) which lead to higher convection losses and so steel and aluminum should have less efficiency than copper. If heat accumulated in collector martial considered as lost heat while it is not sucked by water that means the higher specific heat capacity is the less efficient material.

Table 4-3 shows that copper is less specific heat capacity, which may give idea that copper, is the best efficiency. Collector is having constant volume (not constant mass), so it is important to consider specific heat due to volume (J/m^3. °C) not specific heat due to mass (J/kg.°C). Table 4-2 shows that Aluminum has the less value of specific heat due to volume and that means the less accumulated heat.

Considering surface temperature and accumulated heat at material, it is found that aluminum collector is more efficient than copper and steel at transient time. At steady state condition, no more heat accumulated inside materials and so the leading factor will be surface temperature (led by thermal conductivity) that is less for copper and so it is the higher efficiency.

4.5 Collector behavior at different water mass flow

Six water mass flow rates are used started from (0.005) up to (0.03) kg/s. This range is most suitable for water heater solar collector and may differ due to the use of more than one collector and connection type between collectors (series, parallel).

Next figure show the increment of water temperature with time for each water mass flow rate. Figures are sorted for each month using copper, aluminum, and steel solar collector.

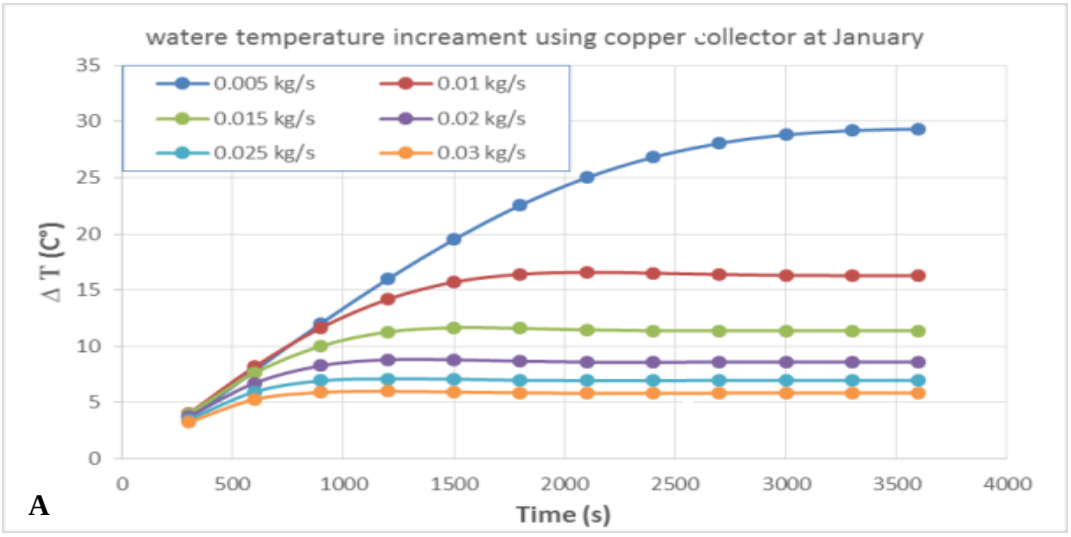
watere temperature increament using copper collector at January
0.005 kg/s
0.01 kg/s
0.015 kg/s
0.02 kg/s
0.025 kg/s
0.03 kg/s
Δ T (C°)
Time (s)

A

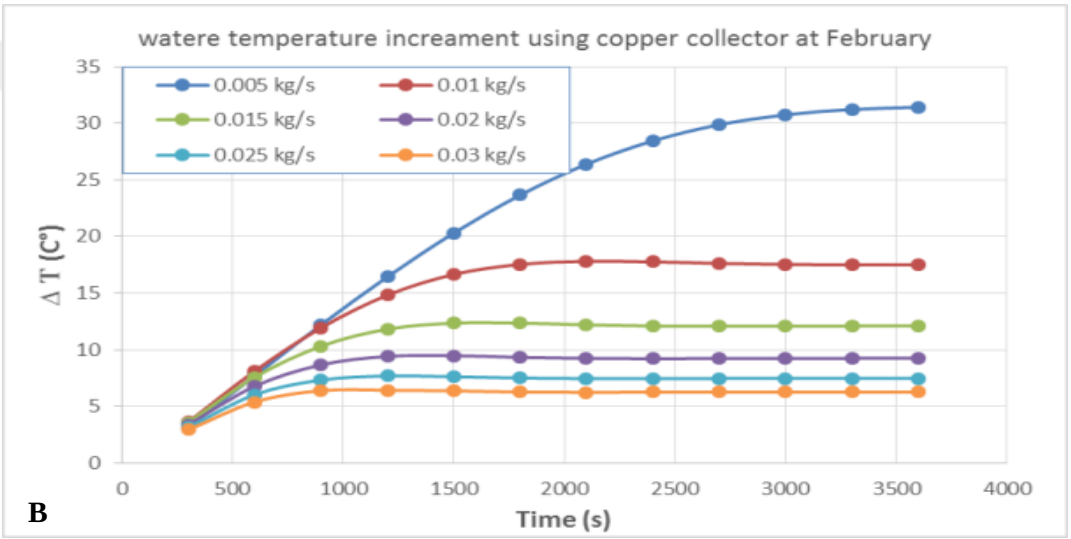
watere temperature increament using copper collector at February
0.005 kg/s
0.01 kg/s
0.015 kg/s
0.02 kg/s
0.025 kg/s
0.03 kg/s
Δ T (C°)
Time (s)

B

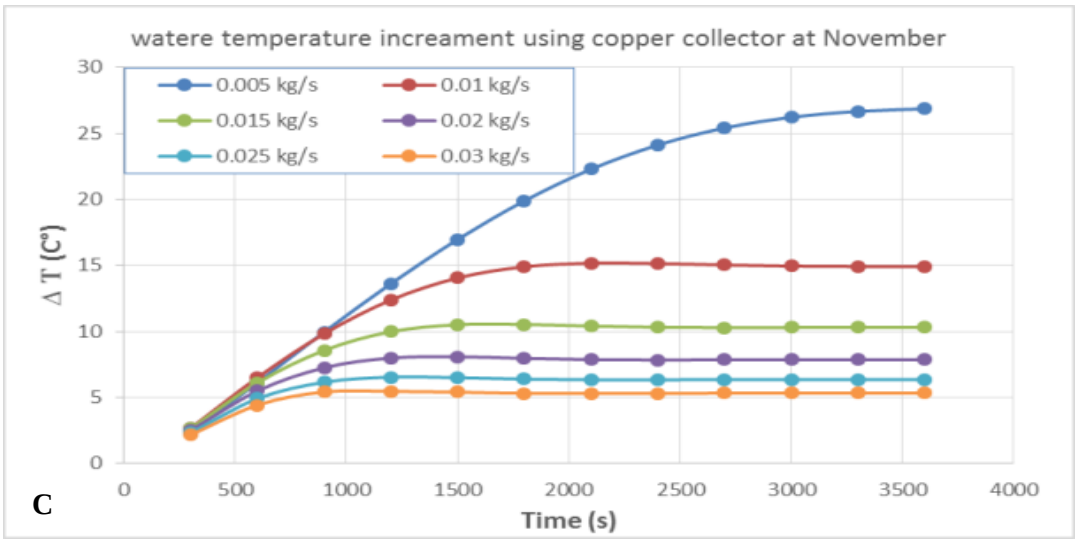
watere temperature increament using copper collector at November
0.005 kg/s
0.01 kg/s
0.015 kg/s
0.02 kg/s
0.025 kg/s
0.03 kg/s
Δ T (C°)
Time (s)

C

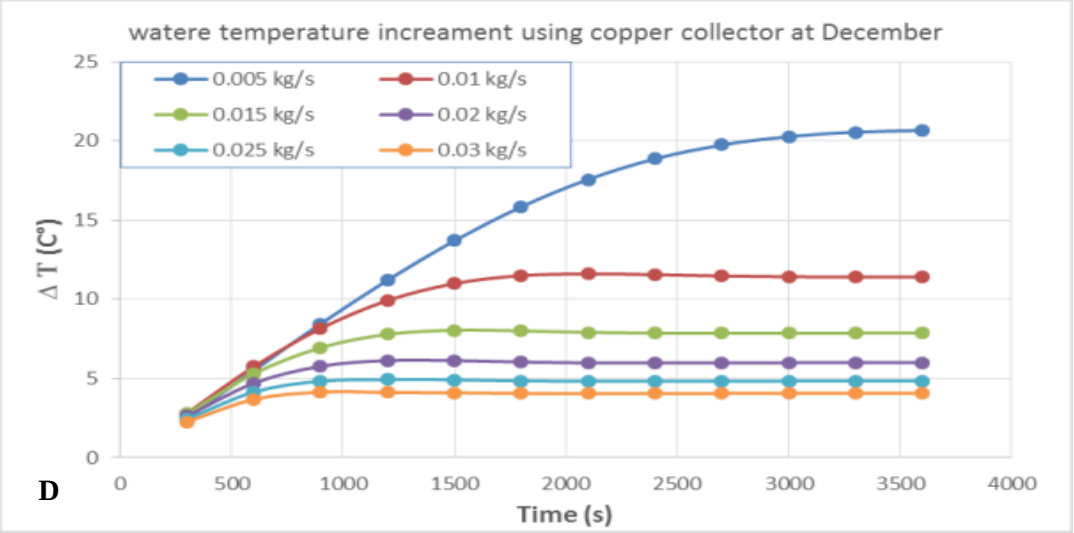

Figure (4.19 A-D): Water temperature increments at transient time for different water mass flow rates using copper collector.

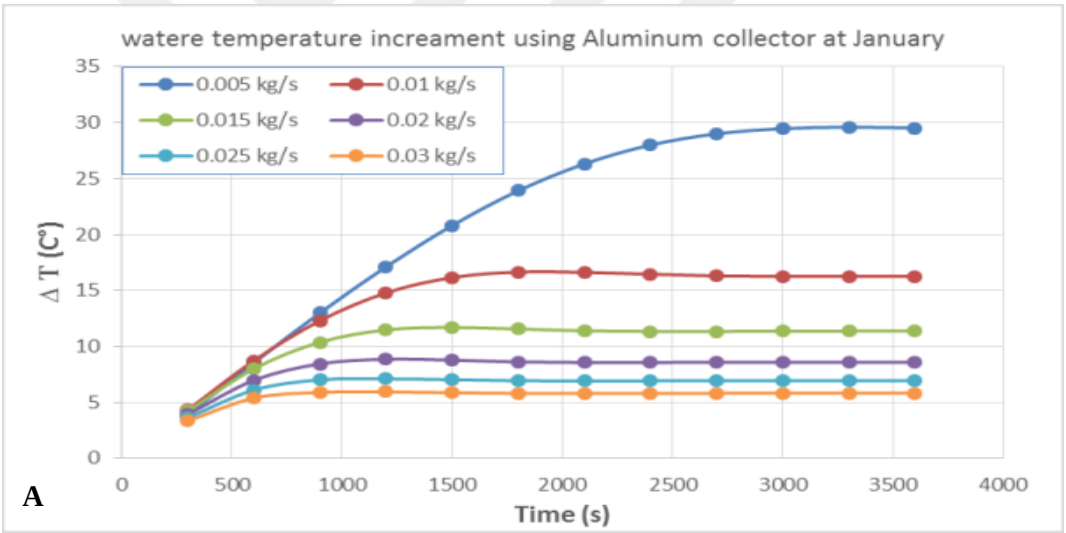

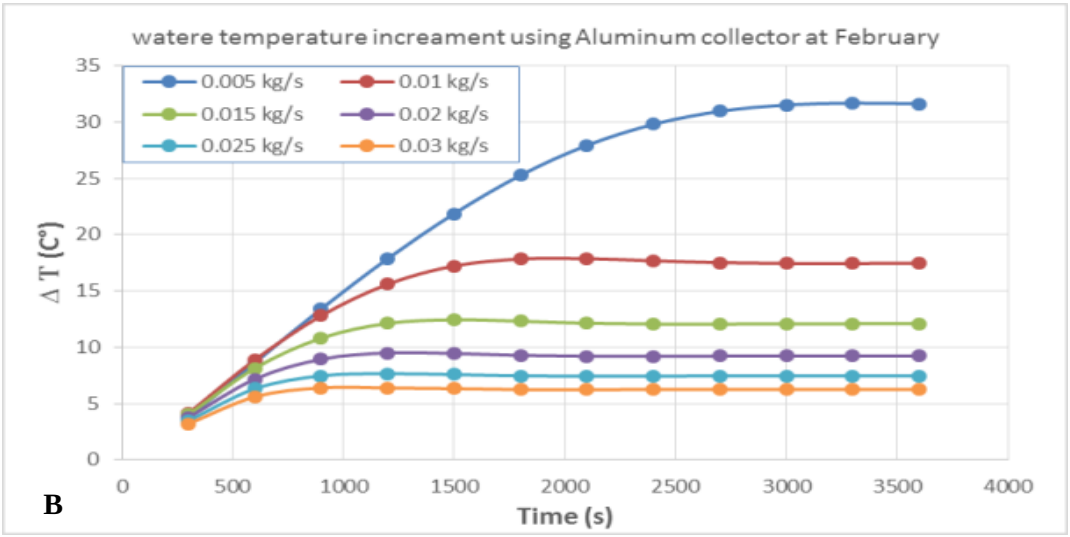

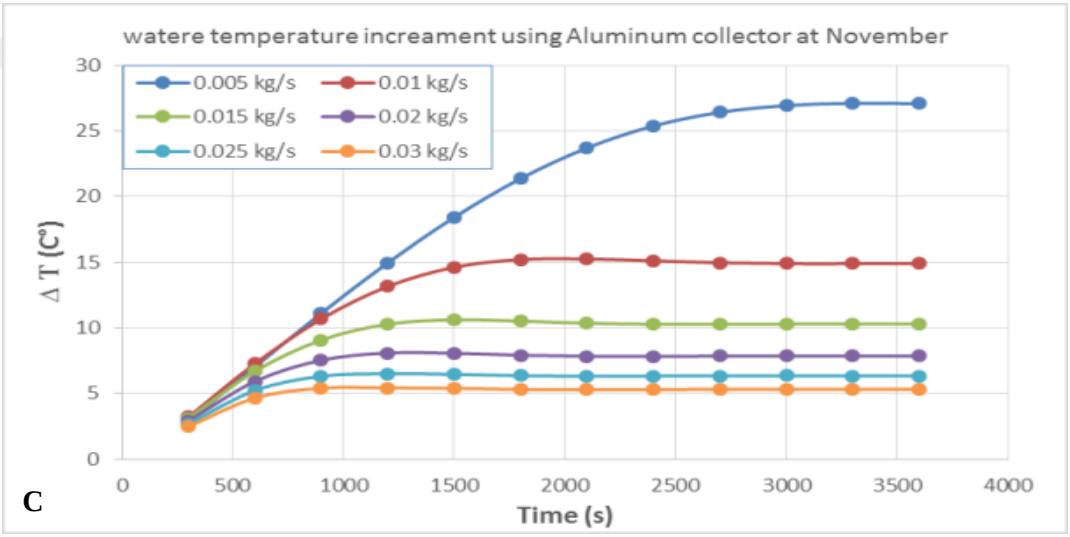

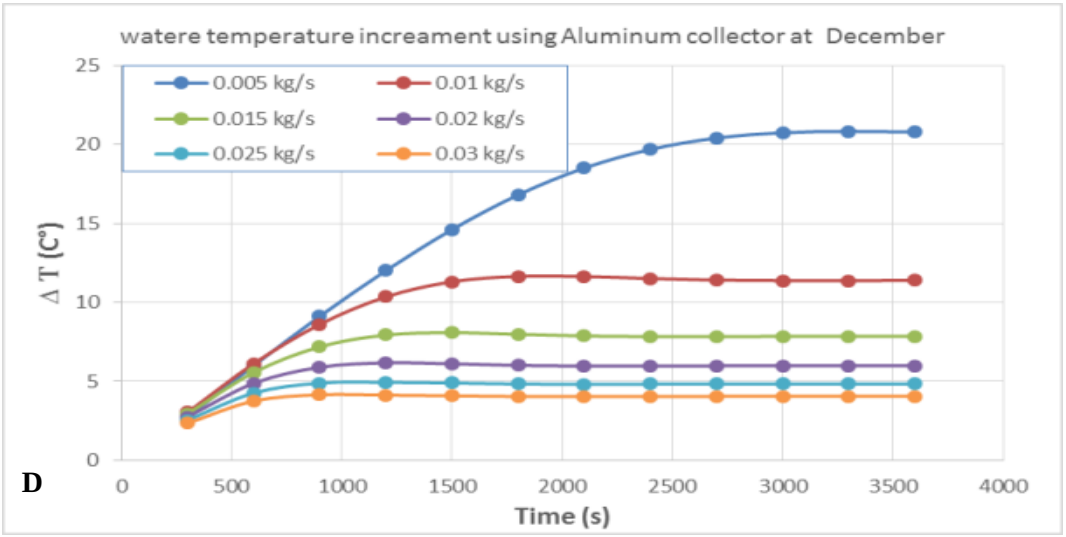

Figure (4.20 A-D): Water temperature increments at transient time for different water mass flow rates using aluminum collector.

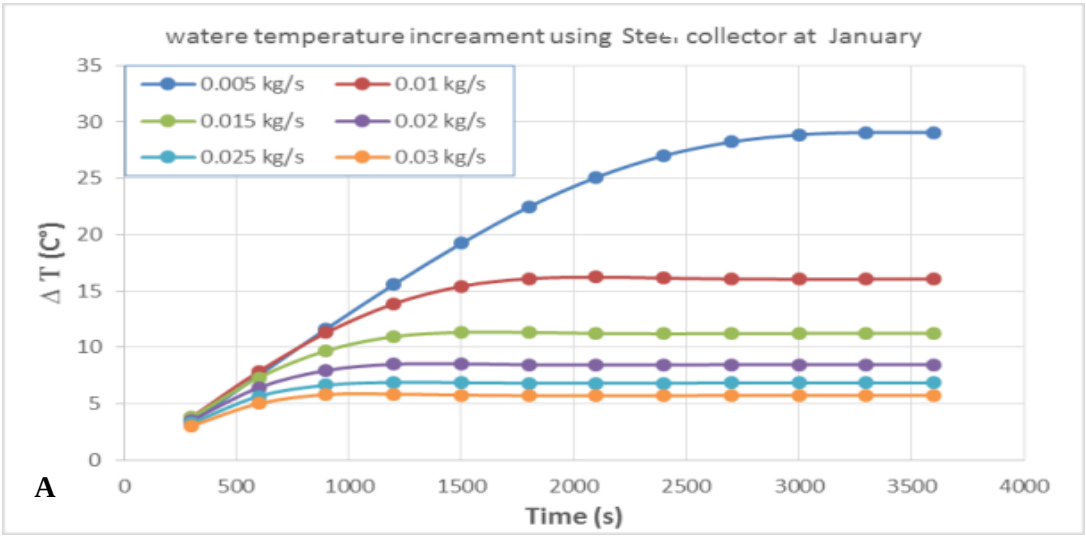
watere temperature increament using Steel collector at January
0.005 kg/s
0.01 kg/s
0.015 kg/s
0.02 kg/s
0.025 kg/s
0.03 kg/s
Δ T (C°)
Time (s)
0
5
10
15
20
25
30
35
0
500
1000
1500
2000
2500
3000
3500
4000

A

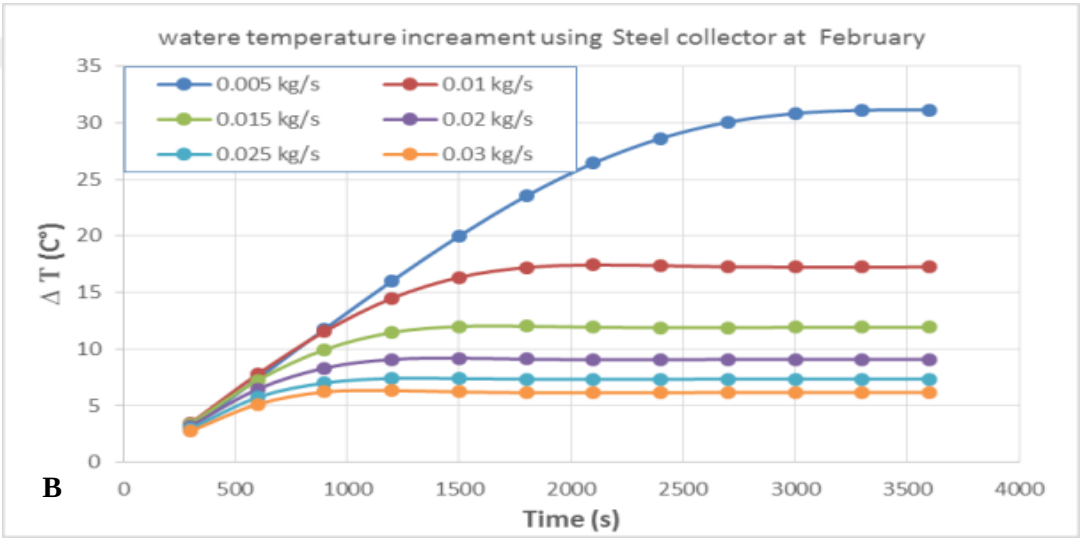
watere temperature increament using Steel collector at February
0.005 kg/s
0.01 kg/s
0.015 kg/s
0.02 kg/s
0.025 kg/s
0.03 kg/s
Δ T (C°)
Time (s)
0
5
10
15
20
25
30
35
0
500
1000
1500
2000
2500
3000
3500
4000

B

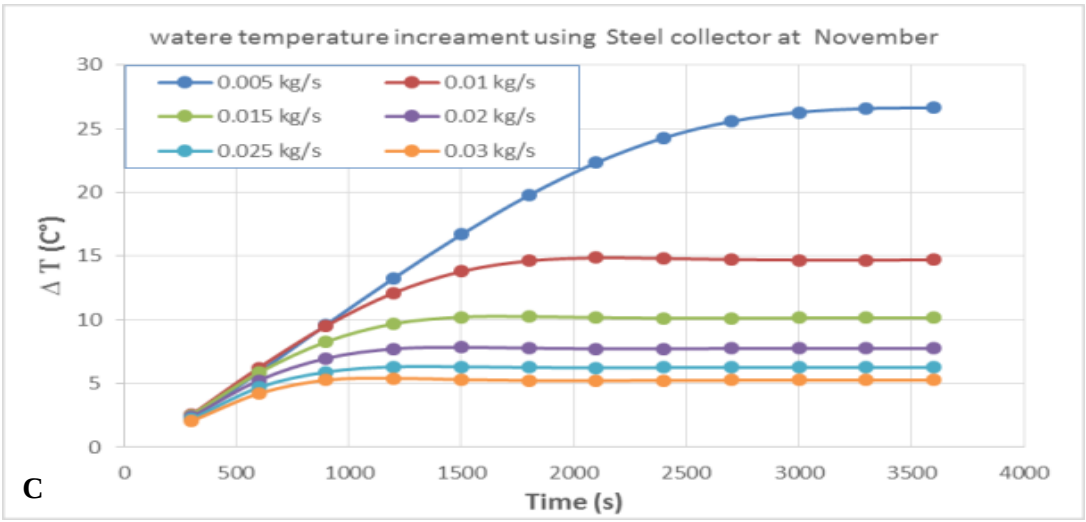
watere temperature increament using Steel collector at November
0.005 kg/s
0.01 kg/s
0.015 kg/s
0.02 kg/s
0.025 kg/s
0.03 kg/s
Δ T (C°)
Time (s)
0
5
10
15
20
25
30
0
500
1000
1500
2000
2500
3000
3500
4000

C

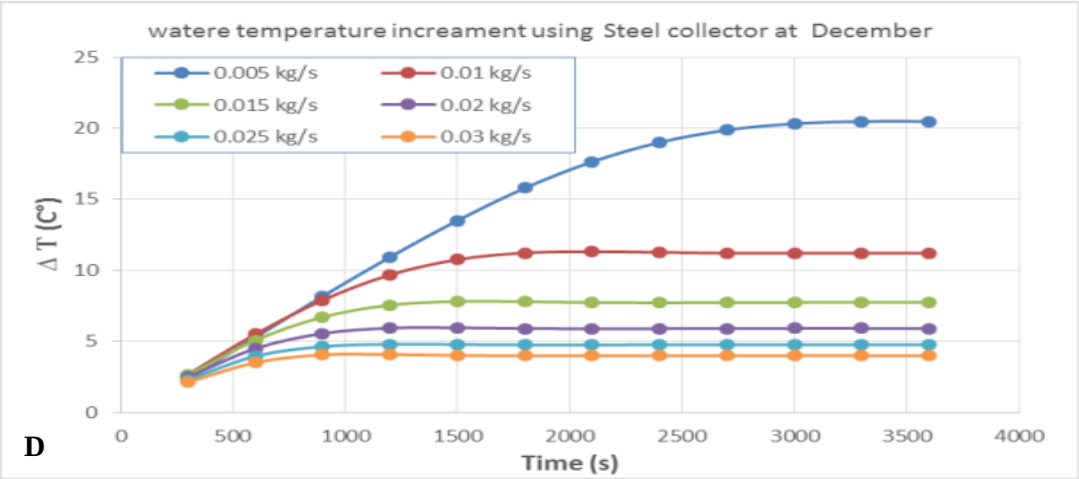

Figure (4.21 A-D): Water temperature increments at transient time for different water mass flow rates using Steel collector.

Table 4-11: Water temperature increments for different materials and different water mass flow rate.

mass flow rate kg/s			0.005	0.01	0.015	0.02	0.025	0.03
Material	month	Time	ΔT_w (°C)					
Copper	Jan.	3600	29.34	16.29	11.39	8.607	6.957	5.833
	Feb.	3600	31.42	17.5	12.11	9.241	7.469	6.264
	Nov.	3600	26.86	14.91	10.32	7.869	6.358	5.333
	Dec.	3600	20.65	11.4	7.867	5.995	4.84	4.058
Aluminum	Jan.	3600	29.52	16.28	11.38	8.591	6.944	5.822
	Feb.	3600	31.63	17.47	12.09	9.225	7.456	6.254
	Nov.	3600	27.07	14.9	10.3	7.859	6.348	5.324
	Dec.	3600	20.79	11.39	7.858	5.987	4.834	4.051
Steel	Jan.	3600	29.07	16.08	11.25	8.477	6.854	5.747
	Feb.	3600	31.14	17.26	11.92	9.095	7.351	6.168
	Nov.	3600	26.64	14.71	10.16	7.753	6.264	5.258
	Dec.	3600	20.48	11.21	7.748	5.914	4.771	4

Figures (4.19, 4.20, and 4.21) clear that water temperature at outlet keep increasing at transient time until reaches to steady state condition and while water mass flow rate increases, the water temperature at outlet decreases.

Increment of water temperature at outlet means increasing of useful power and so increasing collector efficiency. Figures show that using less water mass flow rate required more time to reach up to steady state conditions.

Figure (4.22 A-D) show the average temperature at surface of collector, which is important to calculate heat losses due to convection and radiation.

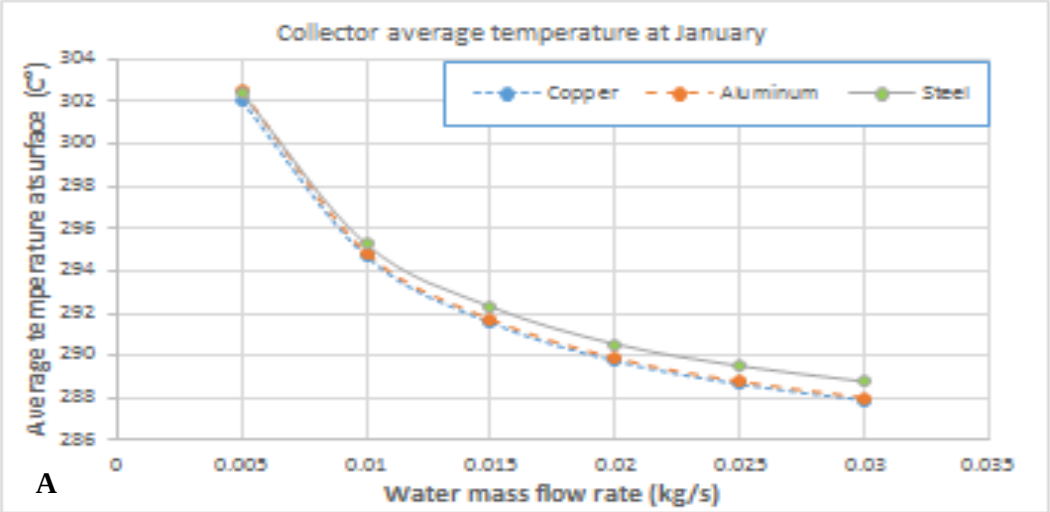
Collector average temperature at January
Copper
Aluminum
Steel
Average temperature at surface (C°)
304
302
300
298
296
294
292
290
288
286
0
0.005
0.01
0.015
0.02
0.025
0.03
0.035
Water mass flow rate (kg/s)

A

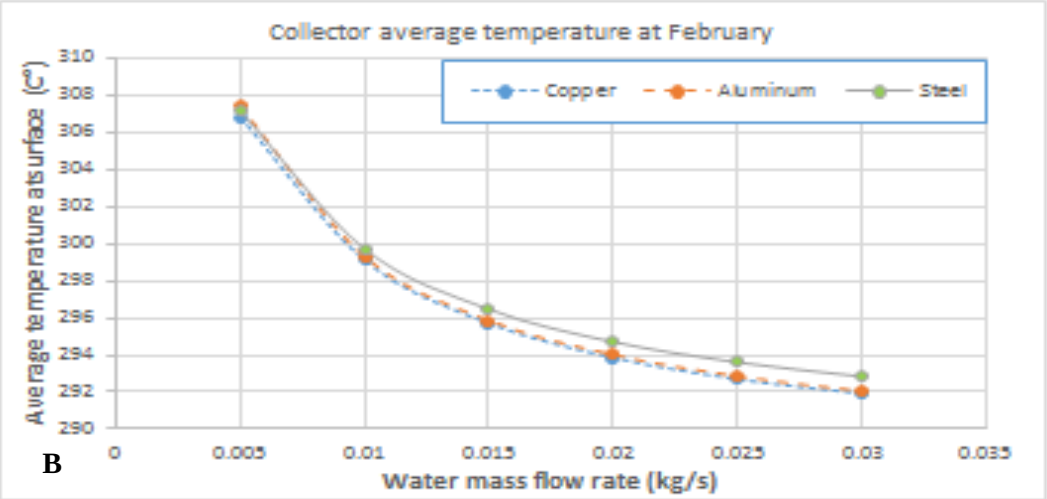
Collector average temperature at February
Copper
Aluminum
Steel
Average temperature at surface (C°)
310
308
306
304
302
300
298
296
294
292
290
0
0.005
0.01
0.015
0.02
0.025
0.03
0.035
Water mass flow rate (kg/s)

B

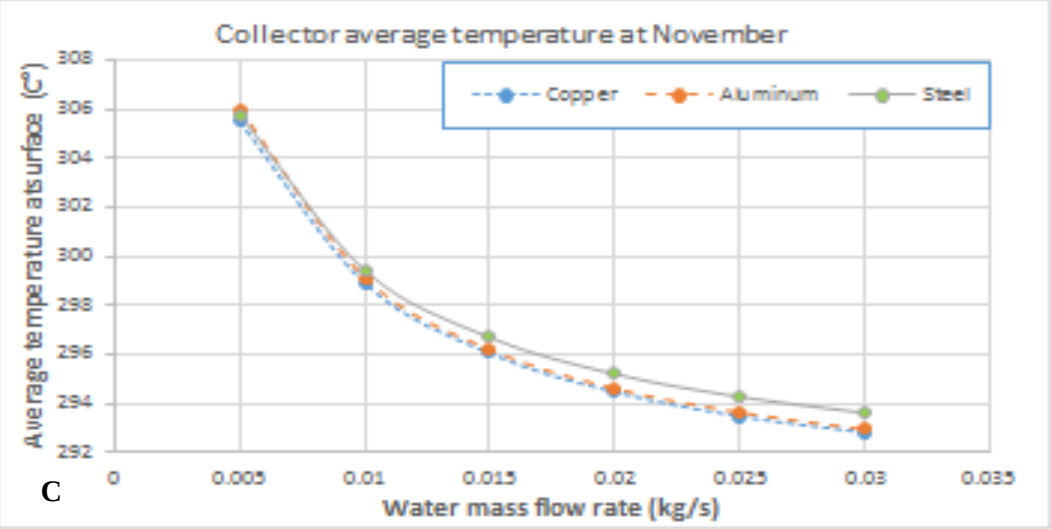
Collector average temperature at November
Copper
Aluminum
Steel
Average temperature at surface (C°)
308
306
304
302
300
298
296
294
292
0
0.005
0.01
0.015
0.02
0.025
0.03
0.035
Water mass flow rate (kg/s)

C

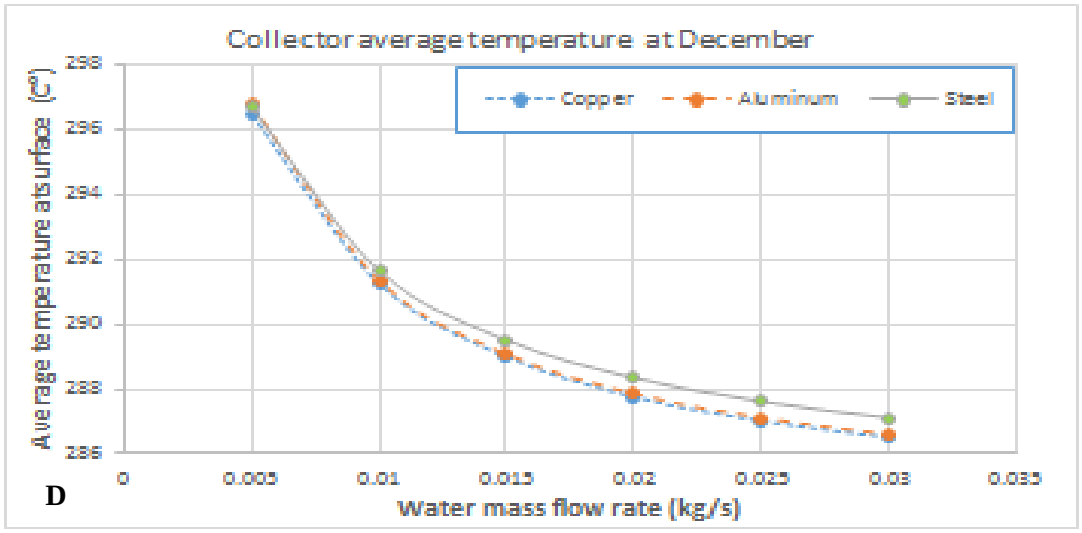

Figure (4.22 A-D) Average temperature at surface of collectors.

Clearly, above figures show that average temperature at surface of collector is decreasing when water mass flow increasing and so decreasing surface collector temperature leads to decrease heat losses to environment finally leads to better collector efficiency.

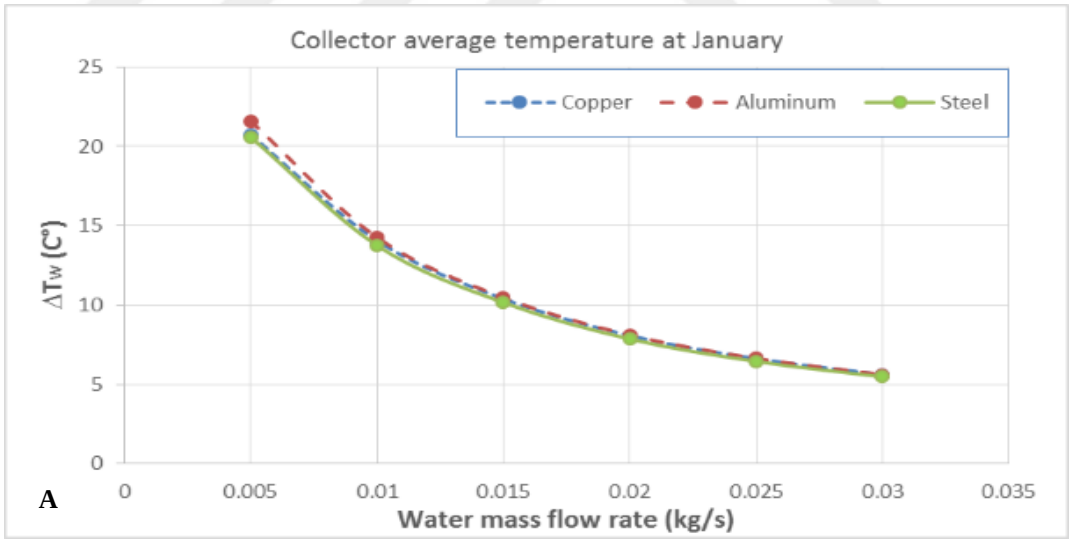

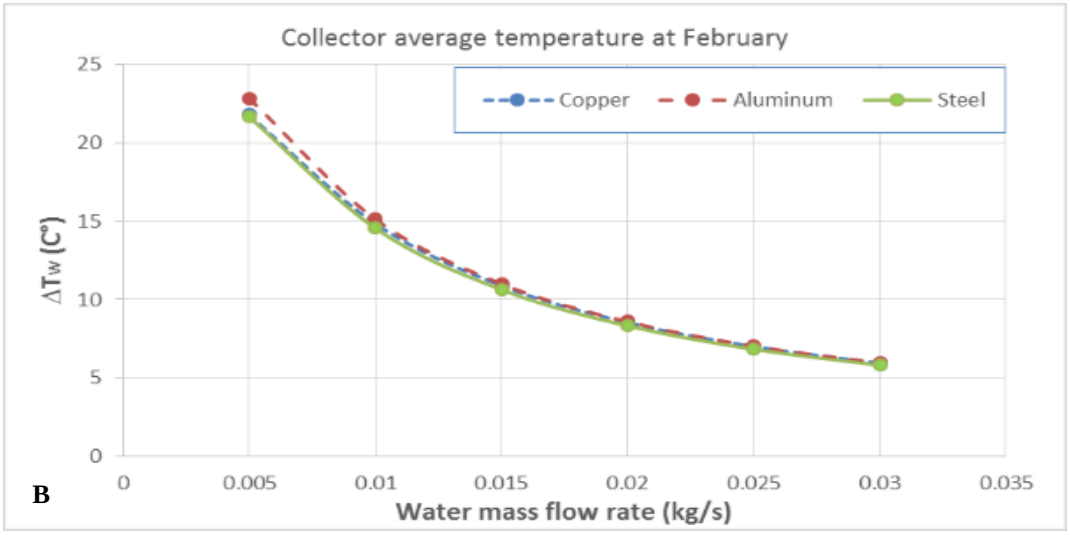

B

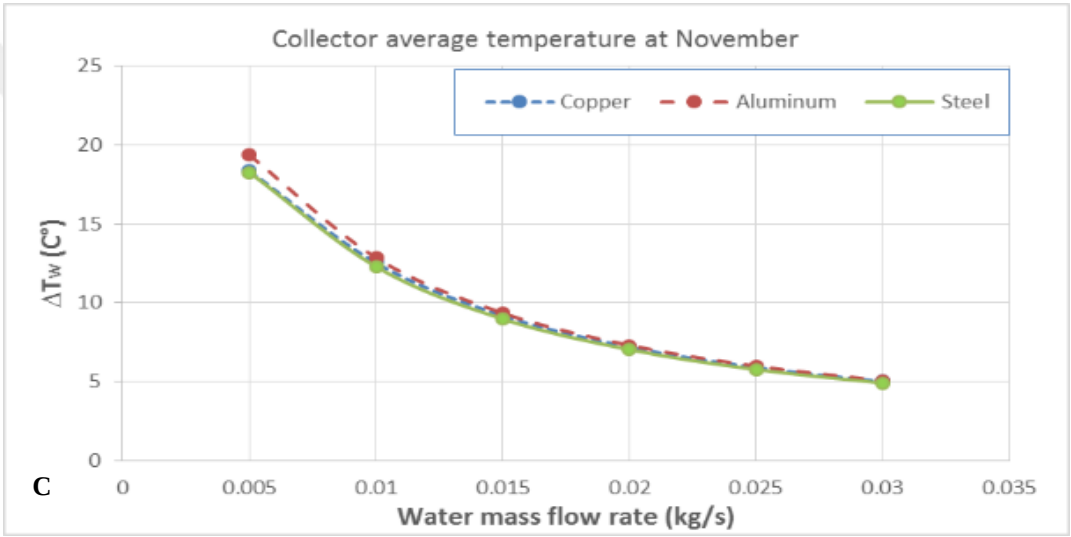

C

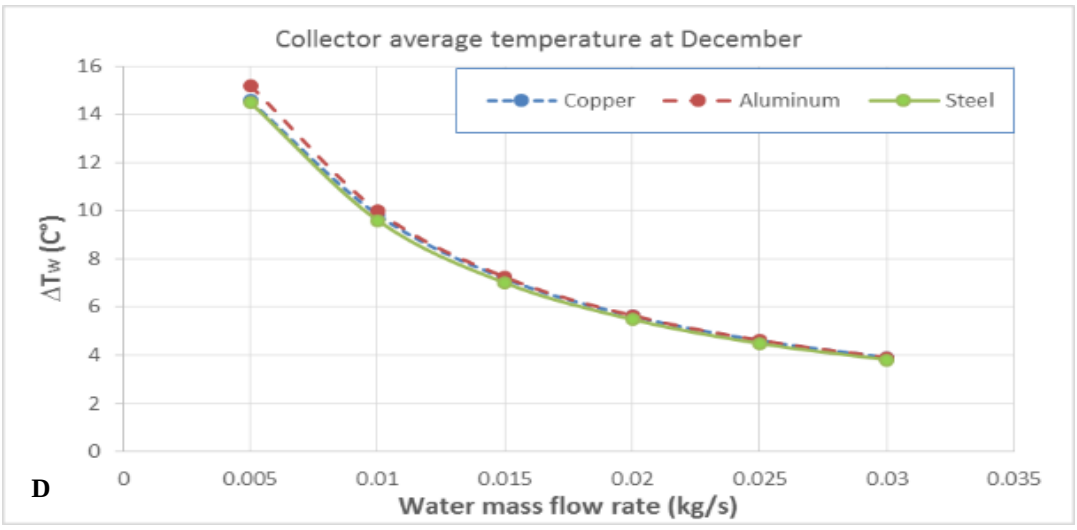

D

Figure (4.23 A-D): Relation between increasing water mass flow rate and its temperature gain.

Figures show that while water mass flow rate increasing, the temperature difference between inlet and outlet is decreasing. Therefore, if collector used to reach up to higher temperature, water mass flow rate should be decreased and vise-versa.

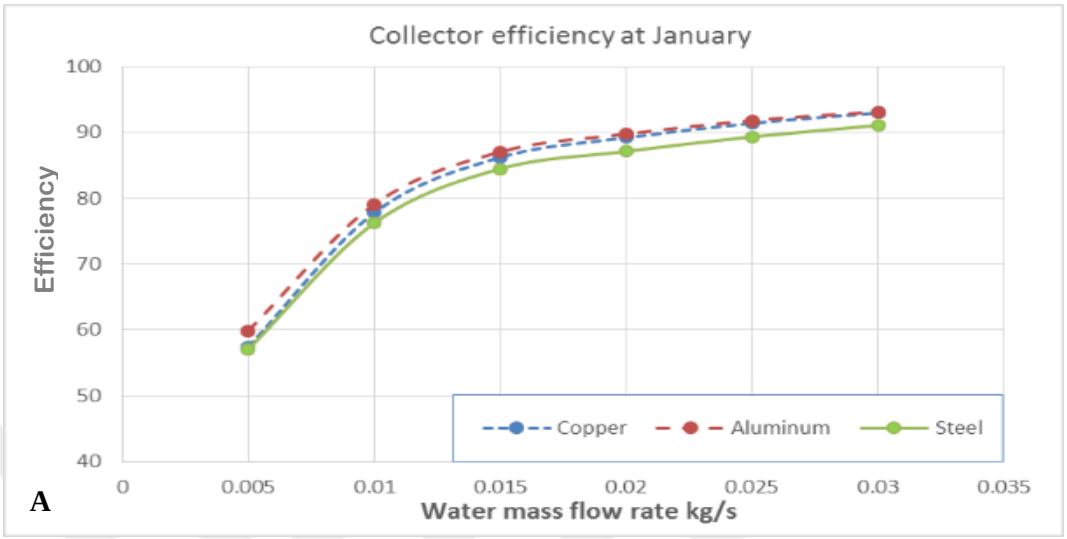

A

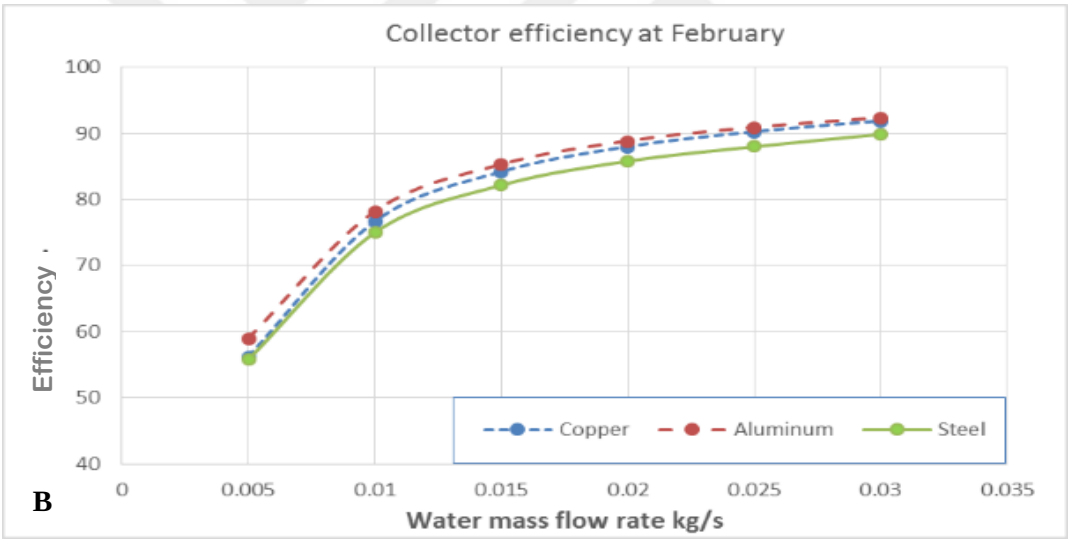

B

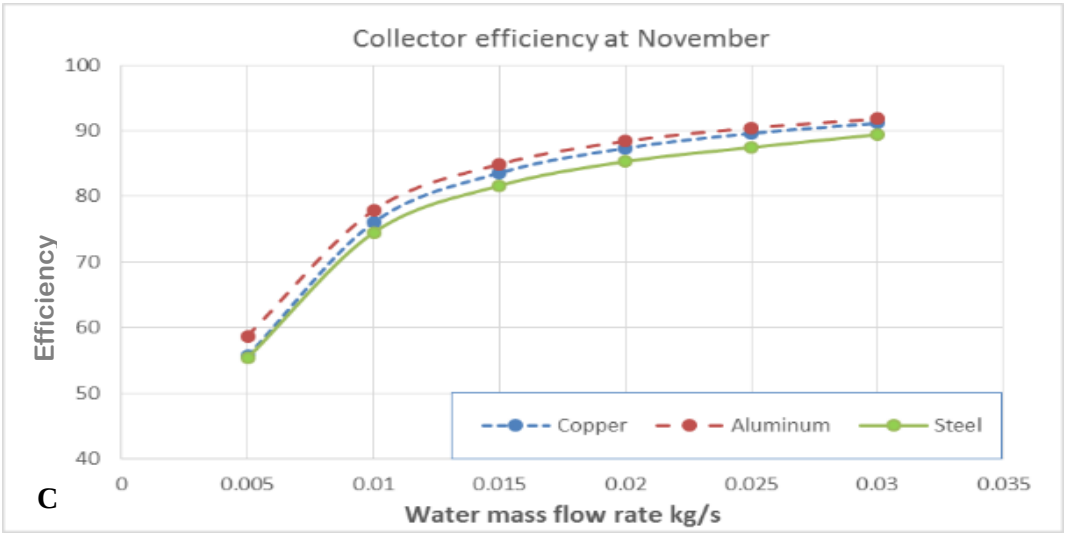

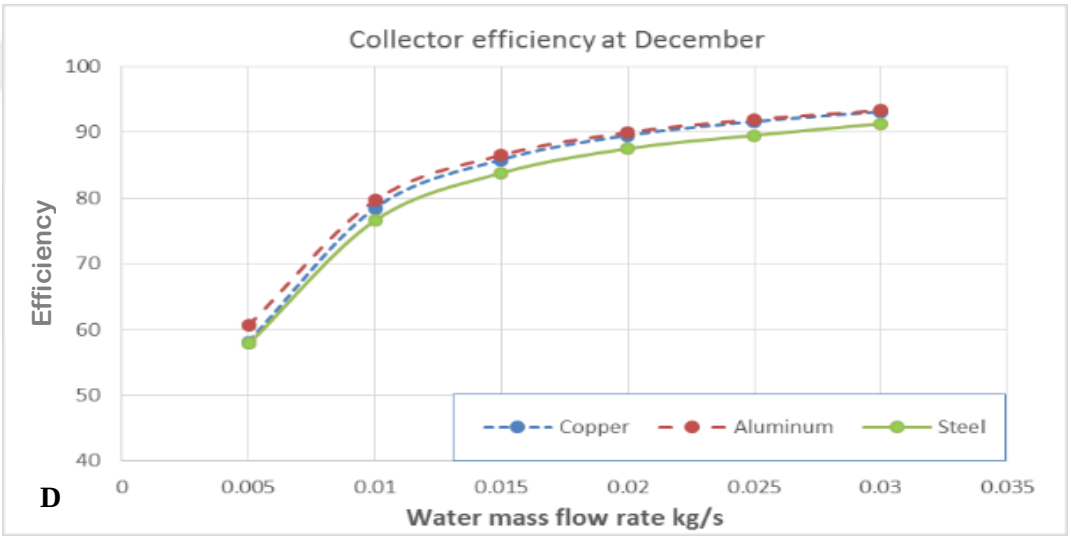

Figure (4.24 A-D) Collector efficiency at transient time for different water mass flow rates.

Above figures, show collector efficiency at different months due to increasing water mass flow rate. Figures clear that collector efficiency is increasing when water mass flow is increased.

Figure (4.24 A-D) show that aluminum has a higher efficiency at transient time while steel has the less efficiency.

4.6 Increasing solar intensity

Comparison for different material are driven at different months (different solar intensity) to show the effect of solar intensity on collector performance.

Figures (4.25 to 4.27) show the average water temperature increasing when solar radiation increasing (average is calculated for six different water mass flow rates).

Table (4-1) shows that solar radiation is higher at February and less at December. Figures clear that higher water temperature increment at month of February while the less at December so heat gain by water increases when solar intensity increases.

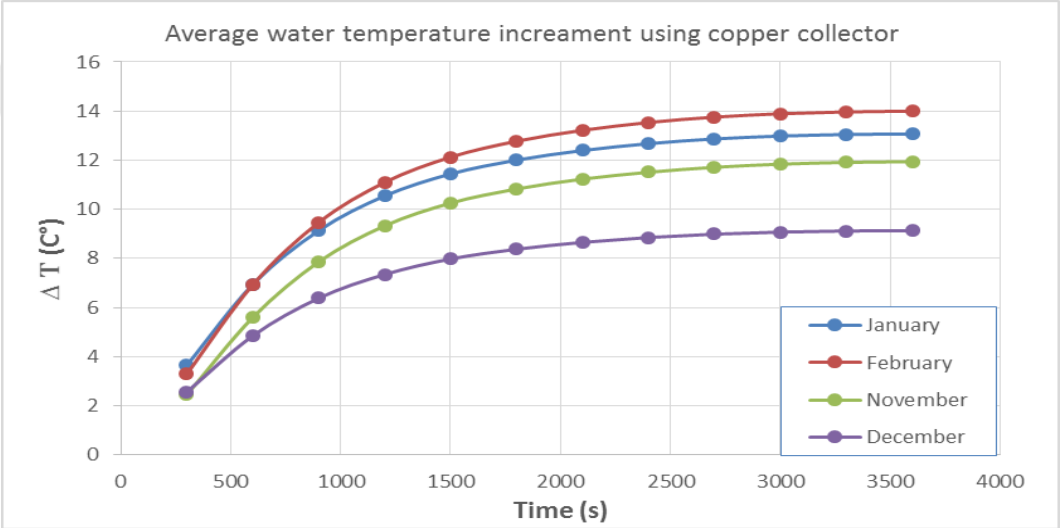

Figure (4.25): Water temperature increment at four months using copper collector.

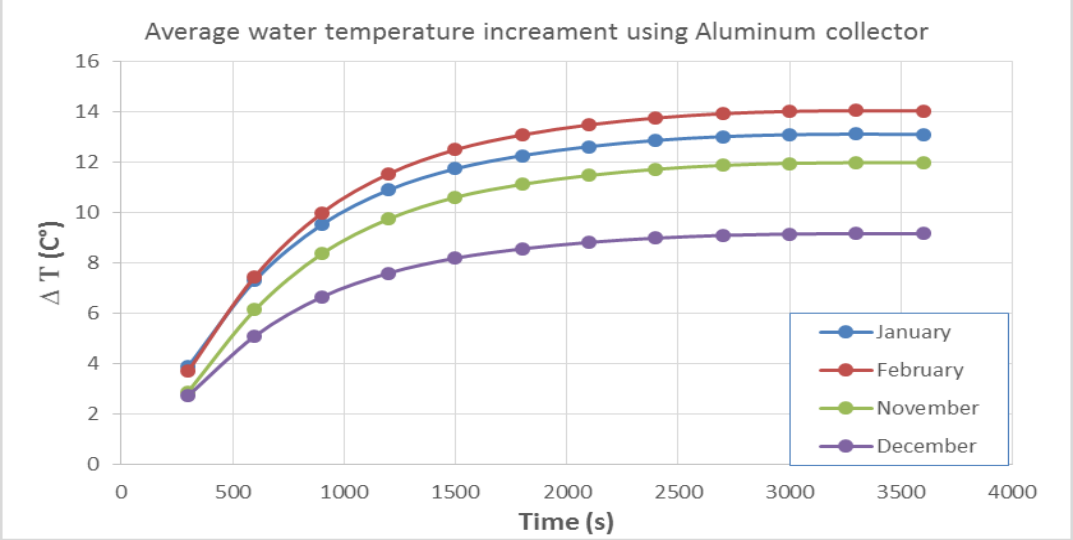

Figure 4.26 show water temperature increment using aluminum collector at four months.

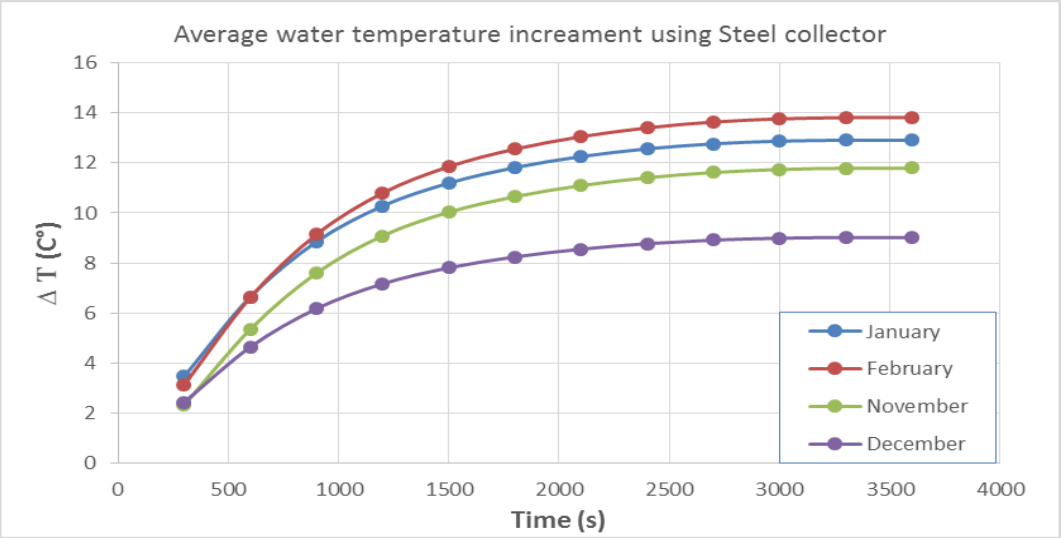

Figure (4.27): Water temperature increment at four months using steel collector.

Total average or copper, aluminum, and steel can be shown in Figure (4.28) to clear useful power different months. Drawing results due different factors clarify that the effect of solar radiation.

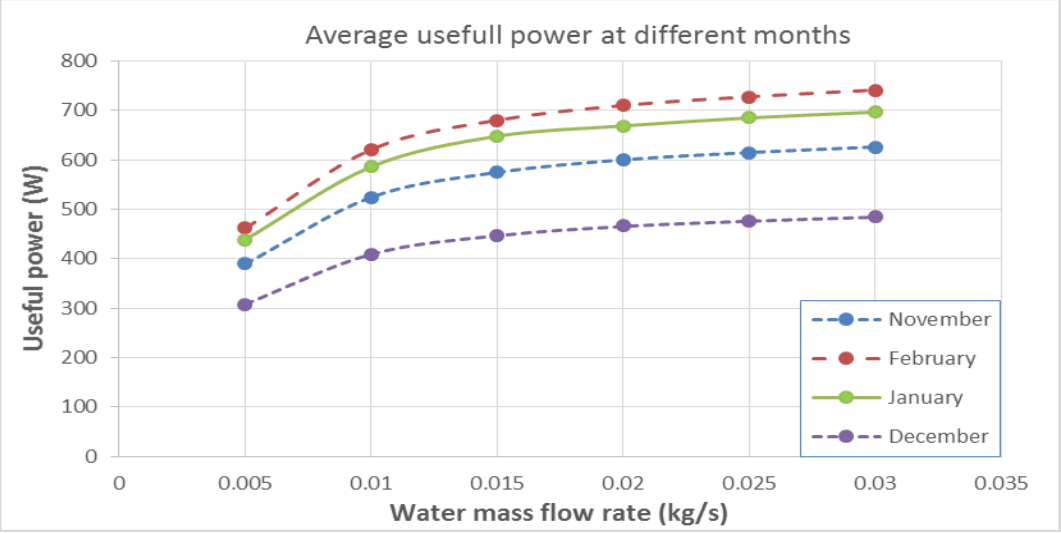

Figure (4.28) Average useful power at four months using steel collector (average is calculated for three different materials.

4.7 Materials Comparison

Three different materials are used in this simulation for water heater solar collector namely, aluminum, copper, and steel. Different materials are used to study the effect of physical properties of these materials (table 4-3) and find the best one of them.

Figures 4.10 show that steel which has the less thermal conductivity required more time to transfer heat from material to water and so will have highest maximum temperature. Comparing Figures (4.10A), (water mass flow rate is 0.005 kg/s) and 4.10F (water mass flow rate is 0.03 kg/s) it found that when water mass flow increases, materials reached steady state conditions faster. Less thermal conductivity keeps materials at higher temperature instead of transfer heat to water which increase losses due to convection and radiation. Due to this feature, copper is the best.

Less specific heat capacity means less heat accumulated at material (accumulated heat in material is lost heat because it is not sucked by water), and this feature in the side of copper also.

Density in the side of aluminum due to the use of less quantity of mass to make collector than copper or steel.

Specific heat and density enhanced aluminum properties over copper and steel and because of that, it is clear from table 4.10 that aluminum collector has higher efficiency than copper and steel at transient time while the difference is vanished with copper collector at steady state conditions.

Table 4-11 show that copper collector is the best at all water mass flow rates while aluminum collector gives higher water temperature at outlet using 0.005 kg/s as a water mass flow rate only. The higher (T_{pave}) at copper than aluminum at water mass flow rate of 0.005 kg/s may be the reason behind this behavior (as shown in table 4-5). This means that copper may be better than aluminum for some ranges of water mass flow rates and solar intensity while aluminum is better at others. Less weight, easy to use, low price makes aluminum used more widely in collectors.

As a computer simulation, results have to compare with real results to validate them. Firstly of all results are compared with equations and they are fully matched with maximum error of 1.18%.

Secondly, due to the use of real environment temperature, wind speed, solar radiation and other factors with a computer simulation so the behavior of solar collectors compared with the behavior of real situation behavior.

Efficiency of collector due to materials changing solar radiation intensity ,water mass flow variation compared with results of [42].

For comparison of metals cost. The prices of copper, aluminum, and steel are 6970$, 2149.5$ and 510$ per ton respectively [43].

Table 4-12 cost of the materials used in collectors

Item	**Heater collector made of**	**Qty**	**Price per kg**	**Total price**
		(Kg)	**US$**	**US$**
1	Aluminum	7.98	2.149	17.15
2	Copper	26.51	6.97	184.77
3	Steel	23.29	0.51	11.87

From Table (4-12) has been gotten results for the heater collector made of steel is the cheapest and the heater collector made of copper is the most expensive, but the efficiency copper is highest.

CHAPTER FIVE

CONCLUSION AND RECOMMENDATIONS

5.1 Conclusion

A solar collector heater is investigated using different three materials namely copper, aluminum, and steel. Investigations included six water mass flow rate at four different months at Al-Najaf weather conditions and it is found that:

- Temperature distribution at solar collector surface depends on material thermal conductivity and water temperature. The higher thermal conductivity, the lower maximum temperature at surface.
- Water temperature distribution at outlet also effected by material used. The higher thermal conductivity lead to distribute heat at all circumference material while lower thermal conductivity focus heat on one side only.
- Efficiency of water solar collector increasing at transient time and reached maximum at steady state conditions.
- At transient time, higher specific heat capacity (J/kg.°C) is considered when same material mass is used while using same volume of material required considering specific heat due to volume (J/m3.°C). The lower specific heat, the lower accumulated heat inside material and so far the lower efficiency. Aluminum shows better efficiency than copper and steel at transient time by 4.5% and 6.9% maximum.
- No more effect for specific heat at steady state condition, so copper efficiency is higher due to better thermal conductivity while steel is the lower.
- Increasing water mass flow decreasing water temperature deference. Table 4.10 list all results for different material at different months.
- Increasing solar radiation, increases useful power and water temperature difference at outlet.

5.2 Recommendations

After completion of this project and during the project steps, it is found that another project may discuss some parts with some expanding like:

1- Use another shape of pipe net at collector surface.
2- Expand solar radiation range with wider range of environment temperature.
3- Using different tilting angle for collector.
4- Using more than one collector in different connections to reach up to required water temperature at outlet.

REFERENCES

[1] S. A. Kalogirou, Solar Energy Engineering Processes and Systems. 2009.

[2] Y. Chu, "Review and Comparison of Different Solar Energy Technologies, annual report," Glob. Energy Netw. Inst., no. August, p. 56, 2011.

[3] A. S. • A. Sharma, "Energy security and sustainability." 2016.

[4] R. K. Gopal Nath ; Mishra, "Advanced Renewable Energy Sources Tiwari." 2011.

[5] T. G.N., "Solar Energy. Fundamentals, Design, Modeling and Applications," New Dehli Alpha Sci. Int. Ltd, p. 25, 2006.

[6] T. A. T. C. Weiss W., "Solar Water Heating. Latvia – Baltic States.," Helsinki Solpros AY, p. 55, 1996.

[7] A. M. A. Alasady, "Solar energy the suitable energy alternative for Iraq beyond oil," 2011 Int. Conf. Pet. Sustain. Dev., vol. 26, pp. 11–15, 2011.

[8] H. A. Kazem and M. T. Chaichan, "Status and future prospects of renewable energy in Iraq," Renew. Sustain. Energy Rev., vol. 16, no. 8, pp. 6007–6012, 2012.

[9] Hadi JM, "Experimental & Theoretical Study to Enhance Solar Air Heater by Using Vortex Generator." Thesis, University of technology, Iraq, 2005.

[10] G. Iordanou, "Flat-Plate Solar Collectors for Water Heating with Improved Heat Transfer for Application in Climatic Conditions of the Mediterranean Region." 2009.

[11] "http://www.moelc.gov.iq/index.php?name=Pages&op=page&pid=230." Ministry of Electricity.Retrieved 9/9/2017.

[12] A. A. Kazem, M. T. Chaichan, and H. A. Kazem, "Dust effect on photovoltaic utilization in Iraq : Review article," Renew. Sustain. Energy Rev., vol. 37, pp. 734–749, 2014.

[13] Y. Al-Douri and F. M. Abed, "Solar energy status in Iraq: Abundant or not—Steps forward," J. Renew. Sustain. Energy, vol. 8, no. 2, p. 25905, 2016.

[14] "Solargiscom. (2017). Solargiscom. Retrieved 9/9/2017, from http://solargis.com/products/maps-and-gis-data/free/download/Iraq." .

[15] "Charles Smith, History of Solar Energy Revisiting, Past Solar Power Technology Review,1995."

[16] “http://www.1001-home-efficiency-tips.com/solar_energy_history1.html Retrieved 5/9/2017.”

[17] “Dr. Mohamed Salem Elmnefi, Lecture3 of Solar Energy Systems, Department of Aeronautical EngineeringFaculty of Aeronautics and Astronautics EngineeringUniversity of Turkish Aeronautical Association (UTAA).”

[18] “S. Kalogirou, Solar thermal collectors and applications, Progress in Energy and Combustion,” Sci. 30, 231–295, 2004.

[19] J. Duffie and W. Beckman, Solar Engineering of Thermal Processes, 4th ed., vol. 116. 2013.

[20] V. Quaschning, “Solar thermal water heating.” . Retrieved 4/10/2017 from ,https://www.volker-quaschning.de/articles/fundamentals4/index.php,.

[21] U. S. D. of Energy, “Energy Efficiency and Renewable Energy Solar Energy Technologies Program.” http://www1.eere.energy.gov/solar/.

[22] S. I. Sadaq, S. N. Mehdi, M. M. Ishrath, and A. Mehar, “Performance analysis of solar flat plate collector 1,” 2015.

[23] E. Azad, “Assessment of three types of heat pipe solar collectors,” Renew. Sustain. Energy Rev., vol. 16, no. 5, pp. 2833–2838, 2012.

[24] A. Patel, H. Parmar, and S. Namjoshi, “Comparative Thermal Performance Studies of Serpentine Tube Solar Water Heater with Straight Tube Solar Water Heater,” IOSR J. Mech. Civ. Eng. Ver. III, vol. 13, no. 4, pp. 2278–1684, 2016.

[25] Billy, “Effect of Absorber Plate Material on Flat Plate Collector Efficiency,” 2010.

[26] C. L. editor-F. Jackson-editor, “Solar domestic water heating,” 2010.

[27] N. V. K.-V. M. Khartchenko, Advanced Energy System, Second edu. 2010.

[28] D. Chwieduk, Solar energy in building, 1st Editio. 2014.

[29] P. K. Richman R, “Quantifying and predicting performance of the solardynamic buffer zone (SDBZ) curtain wall through experimentation and numer-ical modeling. Energy and Buildings.” 2010.

[30] “https://caeai.com/courses/introduction-ansys-mechanical-workbench. Last ,Retrieved 20.09.2017.” .

[31] R. 7. 10. 2017 Najaf Governorate / Abbasiyah, “http://agromet.gov.iq/index.php?name=News&file=article&sid=46.” .

[32] “http://www.maplandia.com/iraq/an-najaf/an-najaf/ Retrieved 7.10. 2017.” .

[33] R. 7. 10. 2017 Encyclopædia Britannica, “https://www.britannica.com/place/Al-Najaf.”

[34] I. A. network. R. 4. 7. 2017, “http://agromet.gov.iq/index.php?name=Pages&op=page&pid=206.”

[35] 2007 ASHRAE, “Source. Solar Energy Engineering Processes and Systems,” vol. book.

[36] D. M. S. Elmnefi, “Lectures Solar Energy Systems Lec.2,Department of Aeronautical EngineeringFaculty of Aeronautics and Astronautics EngineeringUniversity of Turkish Aeronautical Association (UTAA).”

[37] Dr. Mohamed Salem Elmnefi, “Lectures7of Solar Energy Systems ,Department of Aeronautical EngineeringFaculty of Aeronautics and Astronautics EngineeringUniversity of Turkish Aeronautical Association (UTAA).”

[38] T. Yousefi, E. Shojaeizadeh, F. Veysi, and S. Zinadini, “An experimental investigation on the effect of pH variation of MWCNT–H 2 O nanofluid on the efficiency of a flat-plate solar collector,” Sol. Energy, vol. 86, no. 2, pp. 771–779, 2012.

[39] F. Struckmann, “Analysis of a Flat-plate Solar Collector,” 2008.

[40] I. Journal and O. F. Chemtech, “Effect Of Dust On The Performance Of Solar PV Panel,” vol. 5, no. July, pp. 65–72, 2015.

[41] R. 7. 10. 2017 Buildings.HeatTransfer.Data.Solids, “https://simulationresearch.lbl.gov/modelica/releases/latest/help/Buildings_HeatTransfer_Data_Solids.htm.”

[42] Z. Chen, S. Furbo, B. Perers, J. Fan, and E. Andersen, “Efficiencies of flat plate solar collectors at different flow rates,” Energy Procedia, vol. 30, pp. 65–72, 2012.

[43] Steelnetwork, “http://steel-network.com/index.php?go=metal.”

APPENDIX A DATA SOURCES

APPENDIX A1

Najaf Governorate - Abbasiyah / February 2016									
Date	TM C°	Tm C°	T C°	HM %	Hm %	SRt Mj/m2/m	WS_avg m/s	WS_max m/s	Et_o _avg mm/day
2/1/2016	20.01	1.69	9.91	83.23	27.59	14.76	0.98	4.85	2.10
2/2/2016	20.78	2.28	10.87	99.98	19.98	15.07	0.79	4.49	2.00
2/3/2016	19.85	3.67	11.06	97.65	26.10	15.14	1.49	5.79	2.50
2/4/2016	18.92	5.05	11.25	95.32	32.21	15.21	2.18	7.09	2.70
2/5/2016	20.49	0.91	11.07	99.98	30.25	3.20	1.00	5.00	1.50
2/6/2016	16.19	7.04	11.64	99.97	39.39	2.41	1.92	7.66	1.50
2/7/2016	18.01	4.78	11.33	99.98	49.74	10.39	1.46	8.06	1.80
2/8/2016	17.31	6.26	11.73	99.77	35.97	16.55	2.76	8.81	2.70
2/9/2016	18.03	4.16	10.58	99.24	28.52	16.63	1.81	6.61	2.60
2/10/2016	18.94	2.80	11.38	99.98	33.10	15.38	1.30	5.00	2.30
2/11/2016	17.86	7.48	12.17	99.97	33.29	15.93	2.74	9.15	2.90
2/12/2016	19.91	6.54	12.89	93.80	31.57	16.21	2.22	8.15	3.00
2/13/2016	21.96	5.60	13.60	87.62	29.84	16.48	1.70	7.15	3.00
2/14/2016	24.26	6.58	14.81	99.97	22.79	15.87	0.73	4.24	2.40
2/15/2016	25.60	7.83	16.07	99.81	21.22	16.04	1.02	4.60	2.80
2/16/2016	25.33	11.37	17.38	72.32	23.41	16.95	3.50	11.24	5.00
2/17/2016	27.16	9.50	17.21	75.80	15.05	16.93	1.39	5.41	3.50
2/18/2016	26.89	10.20	17.18	60.79	15.95	17.38	1.83	6.25	4.10
2/19/2016	27.59	8.53	17.66	73.18	11.47	17.02	1.45	6.93	3.80
2/20/2016	24.96	10.26	17.49	76.72	29.80	15.98	2.23	8.39	3.80
2/21/2016	23.96	12.22	17.24	88.34	24.63	8.91	2.51	10.14	3.50
2/22/2016	22.96	14.17	16.99	99.95	19.46	1.83	2.79	11.88	2.80
2/23/2016	22.30	12.72	16.75	99.96	40.30	16.70	1.95	9.46	3.10
2/24/2016	22.23	11.22	15.63	99.96	40.76	18.15	1.59	6.73	3.00
2/25/2016	22.87	10.47	16.12	99.97	41.80	17.89	1.27	5.57	2.90
2/26/2016	23.20	9.75	16.62	99.97	40.81	15.84	1.10	4.94	2.70
2/27/2016	20.68	13.81	16.50	99.96	68.12	7.27	1.97	8.49	1.70
2/28/2016	21.65	12.41	17.05	99.97	69.71	12.81	1.95	6.90	2.20
2/29/2016	25.04	13.36	18.23	99.97	36.23	18.75	3.13	10.31	4.20

APPENDIX A2

Najaf Governorate - Abbasiyah / November 2016									
Date	TM C°	Tm C°	T C°	HM %	Hm %	SRt Mj/m2/m	WS_avg m/s	WS_max m/s	Et_o _avg mm/day
11/1/2016	33.28	17.14	24.53	61.62	19.10	12.76	1.00	6.38	3.10
11/2/2016	27.44	16.61	22.53	59.29	26.84	11.29	3.33	10.74	4.90
11/3/2016	27.44	16.61	22.53	59.29	26.84	11.29	3.33	10.74	4.90
11/4/2016	24.43	11.40	17.65	49.69	14.57	11.08	1.08	4.77	2.70
11/5/2016	25.71	12.46	18.23	47.86	18.07	11.93	2.00	8.95	3.80
11/6/2016	25.39	9.83	16.48	61.26	11.84	14.29	2.02	8.62	3.90
11/7/2016	26.03	7.83	16.31	65.51	13.48	13.89	1.58	7.48	3.40
11/8/2016	26.83	6.52	16.88	63.77	15.70	13.20	1.45	8.49	3.20
11/9/2016	27.34	8.37	17.27	68.05	15.44	12.44	1.24	6.68	2.90
11/10/2016	27.85	10.21	17.66	72.32	15.18	11.67	1.03	4.86	2.70
11/11/2016	29.01	7.84	17.43	75.97	14.96	12.90	0.72	4.02	2.30
11/12/2016	27.96	13.13	19.50	48.99	16.38	12.52	1.68	6.35	3.60
11/13/2016	29.40	12.61	20.01	51.59	17.93	12.23	1.34	4.64	3.20
11/14/2016	30.77	10.38	18.79	75.43	13.52	12.16	0.59	2.90	2.10
11/15/2016	30.61	10.94	19.97	74.84	13.20	10.24	0.80	3.33	2.40
11/16/2016	28.96	11.46	18.74	87.88	17.09	11.31	0.97	3.83	2.50
11/17/2016	24.59	13.57	18.19	64.06	34.68	8.22	1.77	6.36	2.80
11/18/2016	23.11	11.81	16.75	60.44	26.23	9.39	2.04	7.12	3.10
11/19/2016	21.62	10.04	15.31	56.81	17.77	10.55	2.31	7.88	3.40
11/20/2016	24.19	7.70	15.41	41.26	14.44	12.28	2.86	7.95	4.50
11/21/2016	22.13	8.91	14.77	46.43	17.85	8.57	1.91	6.40	3.20
11/22/2016	20.85	7.57	13.19	44.17	13.84	12.13	3.23	9.60	4.30
11/23/2016	20.00	6.00	11.54	36.35	11.85	10.78	2.01	5.37	3.20
11/24/2016	18.40	2.85	9.06	50.14	9.66	12.23	2.07	6.03	3.00
11/25/2016	19.63	0.76	8.74	40.41	12.39	11.31	1.19	4.12	2.30
11/26/2016	21.06	2.85	9.19	57.55	9.93	11.06	1.15	3.68	2.30
11/27/2016	19.94	2.47	9.13	53.82	11.85	11.08	1.33	4.48	2.40
11/28/2016	18.82	2.08	9.06	50.09	13.77	11.10	1.51	5.28	2.50
11/29/2016	21.39	2.14	11.06	59.50	13.58	9.71	0.89	4.10	1.90
11/30/2016	21.45	11.41	15.99	65.50	22.22	6.60	1.64	7.40	2.50

APPENDIX A3

Najaf Governorate - Abbasiyah / December 2016									
Date	TM C°	Tm C°	T C°	HM %	Hm %	SRt Mj/m2/m	WS_avg m/s	WS_max m/s	Et_o _avg mm/day
12/1/2016	21.03	15.66	18.35	-	-	5.70	2.70	8.31	1.90
12/2/2016	20.96	12.16	16.56	-	-	6.83	2.20	9.05	2.10
12/3/2016	20.61	7.66	14.14	-	-	10.69	1.14	5.89	1.80
12/4/2016	19.41	6.43	12.92	-	-	8.79	1.37	5.84	1.80
12/5/2016	19.82	11.15	15.49	-	-	5.41	1.28	4.50	1.50
12/6/2016	20.73	6.90	13.82	-	-	9.97	2.41	7.88	2.60
12/7/2016	16.34	2.47	9.41	-	-	11.05	2.23	6.88	2.10
12/8/2016	18.10	0.93	9.52	-	-	9.60	1.39	4.97	1.90
12/9/2016	14.20	3.48	8.84	-	-	10.99	2.22	7.33	1.80
12/10/2016	16.49	-0.79	7.85	-	-	11.13	1.43	6.21	1.80
12/11/2016	17.68	-2.23	7.73	-	-	10.56	0.85	4.43	1.50
12/12/2016	18.31	1.16	9.74	-	-	9.97	0.75	3.83	1.40
12/13/2016	19.27	1.38	10.33	-	-	8.79	1.57	7.19	2.10
12/14/2016	20.23	5.43	12.83	-	-	9.83	2.26	7.02	2.50
12/15/2016	15.73	0.70	8.22	-	-	9.53	1.91	8.86	2.00
12/16/2016	17.09	-0.99	8.05	-	-	9.21	0.85	5.13	1.40
12/17/2016	18.41	-0.67	8.87	-	-	9.14	1.13	4.65	1.70
12/18/2016	15.10	3.27	9.19	-	-	7.53	1.47	5.13	1.60
12/19/2016	13.09	3.63	8.36	-	-	5.87	1.56	6.00	1.40
12/20/2016	10.20	-0.36	4.92	-	-	5.17	1.87	8.83	1.40
12/21/2016	13.00	-3.74	4.63	-	-	8.72	0.65	4.63	1.10
12/22/2016	16.29	-2.82	6.74	-	-	8.30	0.62	3.41	1.20
12/23/2016	19.07	1.96	10.52	-	-	6.31	0.73	2.93	1.40
12/24/2016	15.08	8.71	11.90	-	-	5.41	1.14	9.63	1.20
12/25/2016	15.49	8.33	11.91	-	-	6.14	0.88	6.40	1.10
12/26/2016	15.90	7.95	11.93	-	-	6.88	0.62	3.16	1.10
12/27/2016	11.94	7.17	9.56	-	-	5.98	0.53	2.96	0.90
12/28/2016	16.18	4.55	10.37	-	-	11.60	1.45	7.53	1.70
12/29/2016	10.89	4.55	7.72	-	-	5.12	0.76	3.61	0.90
12/30/2016	17.63	5.98	11.81	-	-	8.31	1.19	4.57	1.50
12/31/2016	20.20	10.02	15.11	-	-	5.89	1.25	4.57	1.60

APPENDIX B TOTAL SOLAR RADIATION AND DAYLENGTH

APPENDIX B1

Total Solar Radiation and Day length of January

DATE	Declination, =δ	Day length	SRT$\left(Mj/m^2/m\right)$	SRT$\left(W/m^2\right)$
1/1/2016	-23.0116	9.78	2.65	75.30414002
1/2/2016	-22.9305	9.78	13.71	389.2424941
1/3/2016	-22.8427	9.79	12.84	364.1842733
1/4/2016	-22.748	9.80	13.31	377.1131129
1/5/2016	-22.6466	9.82	10.14	286.9680263
1/6/2016	-22.5385	9.83	12.51	353.6062731
1/7/2016	-22.4237	9.84	11.82	333.5256037
1/8/2016	-22.3023	9.85	11.12	313.4724424
1/9/2016	-22.1742	9.87	10.35	291.3406146
1/10/2016	-22.0396	9.88	14.04	394.6040533
1/11/2016	-21.8985	9.90	13.95	391.4449949
1/12/2016	-21.7509	9.92	11.35	317.9534747
1/13/2016	-21.5968	9.93	13.66	381.996522
1/14/2016	-21.4363	9.95	13.90	388.0030028
1/15/2016	-21.2695	9.97	13.34	371.6713229
1/16/2016	-21.0963	9.99	13.94	387.4942731
1/17/2016	-20.917	10.01	14.53	403.2292057
1/18/2016	-20.7314	10.03	10.38	287.4653773
1/19/2016	-20.5397	10.05	11.94	329.9658104
1/20/2016	-20.3419	10.07	12.87	354.8910234
1/21/2016	-20.138	10.10	12.87	354.0977178
1/22/2016	-19.9282	10.12	3.93	107.8803487
1/23/2016	-19.7125	10.14	6.37	174.4505596
1/24/2016	-19.491	10.17	12.27	335.2273227
1/25/2016	-19.2636	10.19	13.39	364.9361901
1/26/2016	-19.0306	10.22	14.51	394.4806516
1/27/2016	-18.7919	10.24	10.26	278.2331297
1/28/2016	-18.5477	10.27	14.59	394.6408335
1/29/2016	-18.2979	10.30	15.05	406.0236605
1/30/2016	-18.0428	10.32	15.31	411.9474412
1/31/2016	-17.7823	10.35	14.26	382.6681945
aver		10.02	12.10	335.4213578

APPENDIX B2

Total Solar Radiation and Day length of February

DATE	Declination, =δ	Day length	SRT$\left(Mj/m^2/m\right)$	SRT$\left(W/m^2\right)$
2/1/2016	-17.5165	10.36	14.76	329.176933
2/2/2016	-17.2455	10.39	15.07	338.4160527
2/3/2016	-16.9695	10.42	15.14	357.1727847
2/4/2016	-16.6883	10.44	15.21	364.9304797
2/5/2016	-16.4023	10.47	3.20	381.1006568
2/6/2016	-16.1114	10.50	2.41	176.5476566
2/7/2016	-15.8157	10.53	10.39	199.7219524
2/8/2016	-15.5153	10.56	16.55	335.5776112
2/9/2016	-15.2104	10.59	16.63	367.8214315
2/10/2016	-14.9009	10.62	15.38	385.5200068
2/11/2016	-14.587	10.65	15.93	287.8942568
2/12/2016	-14.2688	10.68	16.21	366.3811729
2/13/2016	-13.9463	10.71	16.48	372.2651468
2/14/2016	-13.6198	10.75	15.87	356.9705685
2/15/2016	-13.2892	10.78	16.04	363.7304502
2/16/2016	-12.9546	10.81	16.95	370.4419408
2/17/2016	-12.6162	10.84	16.93	414.5222817
2/18/2016	-12.2741	10.87	17.38	392.6333246
2/19/2016	-11.9283	10.91	17.02	378.2325235
2/20/2016	-11.579	10.94	15.98	367.7095296
2/21/2016	-11.2263	10.97	8.91	374.9056971
2/22/2016	-10.8703	11.01	1.83	87.27590862
2/23/2016	-10.511	11.04	16.70	219.1473034
2/24/2016	-10.1486	11.08	18.15	390.9486823
2/25/2016	-9.78319	11.11	17.89	384.5086602
2/26/2016	-9.41489	11.14	15.84	388.2894778
2/27/2016	-9.04381	11.18	7.27	184.2576888
2/28/2016	-8.67004	11.21	12.81	130.3594666
2/29/2016	-8.29371	11.25	18.75	406.8531863
aver		10.79	14.06	360.8129039

APPENDIX B3

Total Solar Radiation and Day length of November

DATE	Declination, =δ	Day length	SRT$\left(Mj/m^2/m\right)$	SRT$\left(W/m^2\right)$
11/1/2016	-15.6661	10.64854	12.76	332.5194822
11/2/2016	-15.9641	10.62117	11.29	295.0728796
11/3/2016	-16.2574	10.59413	11.29	295.9309142
11/4/2016	-16.5459	10.56745	11.08	291.2652633
11/5/2016	-16.8295	10.54112	11.93	314.508788
11/6/2016	-17.1081	10.51516	14.29	377.796737
11/7/2016	-17.3817	10.48957	13.89	368.2573407
11/8/2016	-17.65	10.46438	13.20	350.9418587
11/9/2016	-17.9132	10.43959	12.44	331.5181333
11/10/2016	-18.171	10.41522	11.67	311.9752092
11/11/2016	-18.4235	10.39126	12.90	345.790783
11/12/2016	-18.6705	10.36775	12.52	336.5026645
11/13/2016	-18.912	10.34467	12.23	329.5765907
11/14/2016	-19.1478	10.32205	12.16	328.5440997
11/15/2016	-19.378	10.2999	10.24	277.3792346
11/16/2016	-19.6025	10.27823	11.31	307.1378834
11/17/2016	-19.8211	10.25705	8.22	223.7801145
11/18/2016	-20.0339	10.23636	9.39	256.1203758
11/19/2016	-20.2407	10.21619	10.55	288.6044081
11/20/2016	-20.4415	10.19654	12.28	336.7201894
11/21/2016	-20.6363	10.17742	8.57	235.5324308
11/22/2016	-20.8249	10.15884	12.13	334.1240787
11/23/2016	-21.0074	10.14082	10.78	297.5911144
11/24/2016	-21.1837	10.12335	12.23	338.3437753
11/25/2016	-21.3537	10.10647	11.31	313.5453403
11/26/2016	-21.5173	10.09016	11.06	307.2370126
11/27/2016	-21.6746	10.07445	11.08	308.398781
11/28/2016	-21.8255	10.05933	11.10	309.5446962
11/29/2016	-21.9699	10.04483	9.71	271.2809633
11/30/2016	-22.1077	10.03095	6.60	184.7205174
aver		10.31	11.34	306.6753887

APPENDIX B4

Total Solar Radiation and Day length of December

DATE	Declination, =δ	Day length	SRT$\left(Mj/m^2/m\right)$	SRT$\left(W/m^2\right)$
12/1/2016	-22.2391	9.87	5.70	150.9324084
12/2/2016	-22.3638	9.85	6.83	212.3218082
12/3/2016	-22.4819	9.84	10.69	353.3695078
12/4/2016	-22.5934	9.83	8.79	255.586485
12/5/2016	-22.6981	9.82	5.41	254.0245627
12/6/2016	-22.7962	9.80	9.97	252.4385134
12/7/2016	-22.8874	9.79	11.05	328.9103775
12/8/2016	-22.9719	9.78	9.60	372.3044018
12/9/2016	-23.0496	9.78	10.99	332.5713603
12/10/2016	-23.1205	9.77	11.13	202.6443335
12/11/2016	-23.1845	9.76	10.56	150.9324084
12/12/2016	-23.2416	9.75	9.97	212.3218082
12/13/2016	-23.2919	9.75	8.79	288.9800807
12/14/2016	-23.3352	9.74	9.83	255.586485
12/15/2016	-23.3717	9.74	9.53	254.0245627
12/16/2016	-23.4012	9.74	9.21	252.4385134
12/17/2016	-23.4237	9.73	9.14	206.9103775
12/18/2016	-23.4394	9.73	7.53	221.3044018
12/19/2016	-23.448	9.73	5.87	305.5713603
12/20/2016	-23.4498	9.73	5.17	302.6913084
12/21/2016	-23.4446	9.73	8.72	210.3218082
12/22/2016	-23.4324	9.73	8.30	199.3695078
12/23/2016	-23.4133	9.74	6.31	185.586485
12/24/2016	-23.3873	9.74	5.41	164.0245627
12/25/2016	-23.3543	9.74	6.14	249.4385134
12/26/2016	-23.3144	9.75	6.88	150.9324084
12/27/2016	-23.2676	9.75	5.98	212.3218082
12/28/2016	-23.2139	9.76	11.60	153.3695078
12/29/2016	-23.1533	9.76	5.12	168.586485
12/30/2016	-23.0859	9.77	8.31	150.9324084
12/31/2016	-23.0116	9.78	5.89	213.0082434
ave		9.77	8.21	233.024413

APPENDIX C Reynolds Number and Nusselt Number

$$\mathrm{Re} = \frac{\rho v D_i}{\mu}$$

Where

Re = Reynolds number Re < 2300 laminar

ρ =Density (kg/m^3)

v =Fluid velocity (m/s)

D_i = Tube inside diameter (m)

μ =Viscosity (kg/m-s)

$$\mathrm{Nu} = \frac{\mathrm{h\,D_i}}{\mathrm{k}}$$

Where

Nu= Nusselt Number

h = Convection heat transfer coefficient (W/ m^2 - °C).

k= Thermal conductivity (W/m- °C).

$$\mathrm{h} = \frac{\mathrm{Q_u}}{\pi\,\mathrm{D_i L}(\mathrm{T_p} - \mathrm{T_{av}})}$$

Table (AC.1) Reynolds and Nusselt numbers of water mass flow rate January using copper collector.

Mass flow rate	v (m/s)	$T_{av.}$ (k)	Re	Nu
0.005	0.01	298.36	281.5	22.99
0.03	0.061	286.6	1270	14.8

CURRICULUM VITAE (C.V.)

PERSONAL INFORMATION:

Full Names: Azhar Shamkhi Jabbar JABBAR

Gender: Male

Nationality: Iraqi

City and Date of Birth: Baghdad – 21.12.1976

Mobile Number: 00905378737743

E-mail address: azhr_1976@yahoo.com

EDUCATION:

High School: Nebuchadnezzar Secondary School

Bachelor: University of Baghdad / College of Engineering / Mechanical Engineering Department, 1999.

WORK EXPERIENCES:

Year : 2002- Present

Place : Iraqi Ministry of Electricity/

Directorate General for Energy Production Projects.

First Project : Baiji Power Plant.

Second Project : Al-Musayyib Power Plant.

Third Project : East-Karbala Diesel Power Plant.

Fourth Project : North-Diwaniyah Diesel Power Plant.

Fifth Project : Al-Najaf Power Plant**.**